KU Leuven

Biomedical Sciences Group

Faculty of Medicine

Department of Cardiovascular Sciences

Center for Molecular and Vascular Biology

ADAMTS13 DEFICIENCY AND OBESITY AS RISK FACTORS FOR THROMBOTIC THROMBOCYTOPENIC PURPURA

Lotte GEYS

Promoter:	Prof. Dr. H. Roger Lijnen
Co-promoter:	Prof. Dr. Ilse Scroyen
Chair:	Prof. Dr. Paul Herijgers
Jury members:	Prof. Dr. Peter Lenting, Université Paris-Sud
	Prof. Dr. Johann Wojta, Medical University of Vienna
	Prof. Dr. Kathelijne Peerlinck, KU Leuven
	Prof. Dr. Hans Deckmyn, KU Leuven Campus KULAK Kortrijk

Dissertation presented in partial fulfillment of the requirements for the degree of Doctor in Biomedical Sciences

June 2017

Center for Molecular
and Vascular Biology

Out of clutter, find simplicity. From discord, find harmony.

In the middle of difficulty lies opportunity.

Albert Einstein (1879 – 1955)

Acknowledgements/Dankwoord

Beste juryleden, collega's, lieve vrienden en familie

Hier sta ik dan: helemaal alleen vooraan in de aula met een uiteraard buitengewoon geïnteresseerd publiek voor mij ;-) Vier jaar geleden leek deze dag nog ver verwijderd (wat ook zo was). Ik heb ondertussen een lange weg afgelegd, maar gelukkig stond ik er tijdens dit doctoraatsavontuur niet helemaal alleen voor. Een groot aantal mensen zou ik dan ook graag willen bedanken om mij, op welke manier dan ook, te vergezellen, helpen en bij te staan.

Allereerst zou ik mijn promotor, professor Lijnen, willen bedanken. Roger, bedankt voor het vertrouwen de afgelopen jaren. In 2012 stapte ik voor het eerst binnen in uw labo voor wat men de "labrotatie" van de masterstudenten noemt. Het was de eerste kennismaking met hoe het er in een academisch labo aan toegaat. Ik heb toen de smaak te pakken gekregen en ben in het CMVB blijven hangen voor zowel mijn masterthesis als mijn doctoraat. Bedankt voor deze mooie kansen, voor de deur die (bijna) altijd openstond, de goede raad en het bewaren van de focus wanneer ik het noorden kwijt was (en mensen die mij kennen, weten dat mijn gevoel voor oriëntatie niet altijd opperbest is)! Mijn copromotor verdient ook een woordje van dank. Ilse, dankzij jou voelde ik mij meteen thuis in het CMVB. Je hebt me gedurende mijn labrotatie en thesisjaar de basistechnieken getoond en aangeleerd, waardoor ik tijdens mijn doctoraat in staat was zelfstandig te werken. Je vertrek (voor 90% dan toch) naar de hogeschool viel me in eerste instantie zwaar, maar bij nader inzien ben ik ervan overtuigd dat het mij zeker ook positief beïnvloed heeft.

A special thanks to my external jury members, professor Johann Wojta and professor Peter Lenting, for your time to read and evaluate my work, your enthusiasm, encouraging annotations, quick responses to emails and to come to Leuven.
Professor Hans Deckmyn, professor Kathelijne Peerlinck, jullie hebben mijn werk sinds het begin opgevolgd en ik zou jullie graag bedanken voor het nalezen van deze thesis en jullie aanwezigheid bij voorafgaande doctoraat gerelateerde aangelegenheden. Bedankt voor jullie tijd, commentaren en aanmoedigende woorden.
Professor Herijgers, bedankt om, ondanks uw drukke agenda, mijn doctoraatsverdediging voor te zitten.

Dit doctoraat is mede tot stand gekomen door de samenwerking met onze vrienden van de KULAK in het verre Kortrijk. Bedankt professor Karen Vanhoorelbeke, Elien Roose en Claudia Tersteeg voor de samenwerking, de verhelderende vergaderingen, vlotte mailconversaties, de

muizen en de vele analyses die in het Laboratorium voor Trombose-Onderzoek uitgevoerd zijn.

Vervolgens zou ik graag de Lijnen-groep bedanken. Ilse (hoewel je nu tot de Scroyen-groep behoort?), Bianca, Liesbeth, Inge, Christine, Annemie en ½ Marleen ;-), bedankt voor alle geboden hulp. Ik kon steeds op jullie rekenen als ik vragen had over bepaalde technieken, beroep moest doen op jullie ervaring of handen tekort schoot bij massadissecties. Kylie, although you are not working in the Lijnen group anymore, I want to thank you for the short time we were colleagues and even thereafter. Thank you for your kindness. It was always nice talking to you. Ellen, sinds maart maak je (opnieuw) deel uit van onze bureau en jouw jeugdig enthousiasme heeft me werkelijk plezier gedaan de laatste maanden. Sorry als ik met momenten te veel aan het zeuren was, maar in mijn verdediging: je kwam toe tijdens mijn laatste loodjes en die schijnen het zwaarst te zijn ;-)
Dan rest er mij van de Lijnen-groep nog maar één iemand om te bedanken en dat is Dries. Het zal voor niemand een openbaring zijn als ik zeg dat je mijn favoriete collega was. Ik kon altijd op je rekenen als dat nodig was en ook wanneer het tijd was om te ventileren, stond je klaar om naar mijn gezaag en geklaag te luisteren (of dat altijd volledig naar je zin was, is een andere kwestie). Voor computerproblemen, het aanpassen van figuren (vooral bij de submissie van mijn eerste artikel), lay-out van documenten of zelfs het kaartlezen op congres in Praag kon ik altijd op jou terugvallen (je was dan ook de enige met een Y-chromosoom en volgens sommige niet nader genoemde personen is dat gelinkt met elkaar).

Naast de mensen van onze groep zijn er ook anderen verbonden aan het CMVB die mij vooruit geholpen hebben. Soetkin, bedankt voor de hulp en raad over histologie en de antibodies waarop ik steeds weer beroep mocht doen wanneer ik ze dringend nodig had en jullie ze in voorraad hadden. Professor Hoylaerts, Marc, ook u zou ik willen bedanken voor de interesse die u toonde in mijn doctoraat, het nodige advies, de goede raad, kritische ingesteldheid en de verschillende uren die we gespendeerd hebben om nieuwe inzichten te verwerven en mogelijke toekomstige studies te beramen.

Bedankt ook aan de andere doctoraatsstudenten van het CMVB voor jullie wetenschappelijke hulp en raad, occasionele babbeltjes, begrip bij een kapot real-time toestel, het tonen van de plaatjesisolatie, hulp bij de opkuis van histologie… In het bijzonder ook een dankjewel aan Dries, Jorien en Anouck. Bedankt voor de gezellige middagpauzes en tussentijdse babbeltjes. Het waren altijd weer gezellige (en af en toe ook wat bizarre) gesprekken ;-) Na al deze jaren van gedeelde vreugde en smart ben ik blij dat ik jullie naast collega's ook tot mijn vrienden kan rekenen. We moeten zeker nog eens sushi gaan eten! ;-)

Doctoreren vulde het grootste deel van mijn dagen de afgelopen vier jaar, maar daarbuiten had ik gelukkig ook nog een relatief uitgebreid sociaal leven en de mensen die hier deel van uitmaken, verdienen zeker ook een woordje van dank, want ook al hebben ze niets te maken met mijn onderzoek, zonder hen zou het leven minder mooi zijn en had ik het minder ver geschopt…

Klarinet spelen doe ik al sinds ik nog een ukkie was met handjes zo klein dat de lage sol bijna onmogelijk te spelen was. Het maakt een significant (beroepsmisvorming om dergelijke woorden te gebruiken) deel uit van mijn leven en heeft er ook voor gezorgd dat ik uitgegroeid ben tot de persoon die ik nu ben. In de muziekwereld geldt zeker ook: samen is leuker dan alleen en graag zou ik dan ook de mensen bedanken die ervoor gezorgd hebben dat het musiceren telkens weer een plezier was om te doen. Bijna 15 jaar geleden (bij deze weet ik ook weer dat er een jubileum zit aan te komen) werd ik lid van de Nieuwe Harmonie Lommel. Eerst bij het jeugdorkest en niet veel later ook bij het harmonie-orkest (bij de “grote” zoals dat ook wel (verkeerdelijk) genoemd wordt). Iedere vrijdagavond ga ik graag repeteren. De meer dan twee uur durende reis van Leuven naar Lommel (anno 2008) was niet altijd even aangenaam, maar de vrijdagavond werd door de harmonie toch altijd in schoonheid afgesloten en het weekend werd steevast goed ingezet met een rondje (of 2 of 3 of 8…) aan de toog tijdens de “après-repetitie”. De vaste kern “kroegtijgers” (of “tooggiraffen” voor zij die dat verkiezen) hebben een plaatsje in mijn hart en ik wil hen dan ook graag bedanken voor al die jaren sfeer en gezelligheid met een score van minstens 10 ;-)

Ook de vrienden van het Universitair HarmonieOrkest verdienen een plaats in dit dankwoord. Acht jaar geleden had ik niet gedacht dat ik in 2017 nog altijd mijn dinsdagavonden in het STUK zou doorbrengen waar warme klanken en wat riet, maar ook mensen samen gebracht worden tot een mooier geheel. “Wij zijn het UHO, wij zijn één!” Ik heb gedurende mijn studententijd bevestigd zien worden dat muzikanten allesbehalve saai zijn. Mooie momenten heb ik beleefd door deel uit te maken van het “het grootste orkest van Leuven én met de beste sfeer” met muzikale hoogtepunten zoals de jaarlijkse aulaconcerten en Leffe-recepties achteraf met bijhorende party hits en als absolute summum de concertreizen naar diverse Europese steden. Naast muzikale climaxen, stond het UHO ook daarbuiten vaak ingepland in de agenda waardoor verveling tijdens mijn studententijd een ongekend begrip was. Ik zou nog thesismanuscripten vol kunnen schrijven over het UHO, maar dan zouden de drukkosten te hoog oplopen en sommige dingen kunnen misschien beter niet zwart op wit vermeld worden ;-) Kortom, bedankt UHO en vooral bedankt aan de UHO-fossielen (de één al verder versteend dan de ander).

Na deze lofzang voor mijn medemuzikanten zijn mijn woorden nog lang niet op. De Meisjes (groepsnamen moeten niet altijd ingewikkeld zijn), meer bepaald Anne, Charlotte, Evelien,

Lotte en Sofie, zou ik zeker nooit vergeten te vermelden. De laatste jaren zien we elkaar niet meer op regelmatige basis, maar het delen van vorderingen in de bouw, vakantiekiekjes, examenresultaten of zelfgemaakte kunstwerken zorgen er telkens weer voor dat we op de hoogte blijven en elkaar niet uit het oog verliezen. Gelukkig zijn er toch ook momenten dat we elkaar nog eens in real-life zien om de belangrijkste heuglijke gebeurtenissen aan te kondigen en te vieren. Ze zeggen dat als je zeven jaar bevriend bent met iemand dat het dan voor het leven is. De berekening is snel gemaakt: vanaf de kleuterschool/de eerste jaren van het middelbaar tot nu → we zitten safe ;-)

De vriendengroep van Lommel bestaat echter niet alleen uit meisjes en vandaar dat ik toch ook graag een woordje van dank uitbreng aan het mannelijke deel, want het mag al eens gezegd worden: af en toe wat mannelijke nuchterheid en relativering kan geen kwaad en verrijkt het leven ;-) Ik ben blij al sinds het middelbaar deel uit te maken van de vriendengroep en dat ik samen met jullie Social Deals kan kopen om gezellig te tafelen, op café kan gaan en indien het jaar het toelaat een WK of EK van onze Rode Duivels mee te volgen!

Na het middelbaar begon ik aan mijn studies Biomedische Wetenschappen in de parel van Vlaams-Brabant (zo wist de conducteur me laatst te vertellen): Leuven. Zondagavond 21 september 2008 begon het grote Leuvenavontuur. Dankzij Lotte had ik na de eerste treinrit Lommel-Leuven mijn kot weten te vinden in de Minderbroedersstraat (nog steeds grote dankbaarheid daarvoor; waar zou ik anders beland zijn?) en wat ben ik blij dat ik daar terecht gekomen ben. Gedurende onze studententijd is de B1-gang van residentie Cruysberghs tot een hechte vriendengroep uitgegroeid die tot op de dag van vandaag erin slaagt zo nu en dan nog samen te komen. Bedankt Jelle, Peter, Cathérine, Céline, Lette, Dorien, Nele en Kim voor de mooie jaren. Zoals bij elk weerzien hebben we ook tijdens de academiejaren altijd heel wat afgelachen en zelfs de blok- en examenperiodes werden door jullie aangename tijden. Middag- of avondpauzes liepen soms uit de hand, maar we hebben het desondanks toch allemaal met vlag en wimpel gehaald en de bunzing zal mijn geheugen nooit meer verlaten ;-)

Naast het centrum van Leuven, heb ik ook menig broek en kleedje versleten op Gasthuisberg waar het merendeel van onze lessen en practica doorgingen. We zijn gestart met meer dan 300 en op één of andere manier is het gelukt de leukste dames eruit te kiezen als vriendinnen voor het leven die ik voor geen geld van de wereld zou willen missen. Ze gaan niet graag hebben dat ik onze groepsnaam hier vermeld, maar ik doe het toch: bedankt, Hot Scientists! :-D We hebben veel mooie momenten beleefd tijdens de lestijden en practica. “Gaat daar mee naar den oorlog!” of “Da’s uw DNA!” (gevolgd door het doorzoeken van de vuilbak) of “Waarom ziet da bij ullie blauw?!” of “Ons membraan!” of “ik heb da ook in da dopke gepipetteerd!!” al dan niet gepaard gaande met al dan niet terechte paniek of het uitbarsten in lachen, zijn maar

enkele uitspraken gerelateerd aan ons talent voor wetenschappelijk onderzoek (haha). Ook al hebben we er ondanks wat beweerd werd als mogelijk te zijn, geen “twientieg op twientieg” op gehaald en hebben we wat af geklungeld van tijd, we zijn er allemaal geraakt en verre van met hakken over de sloot. Ook buitenschools hebben we elkaar gevonden. Naar het einde toe van onze studies zaten we in mijn herinnering meer avonden bij elkaar dan gescheiden van elkaar (sorry buren voor de overmatig geproduceerde decibels). We organiseerden Sinterklaas-, Kerst- en Paasfeestjes, want dat waren telkens weer mooie excuses om buitensporig veel suiker en vet op te nemen (gelukkig werd het gecompenseerd door Cola Light te drinken), gingen samen op reis, kweelden mee met de Backstreet Boys en stonden klaar voor elkaar wanneer dat nodig was. Ook nu nog zijn we een hechte vriendinnengroep die nog verder naar elkaar toegegroeid is. Naast chocolade, suiker en vet hebben we een gemeenschappelijke liefde voor sushi ontdekt en naast Turkije, hebben we onze sporen ondertussen ook achtergelaten in Londen en Kreta. We kennen nagenoeg geen gêne en kunnen volledig onszelf zijn bij elkaar. Ine, Kelly, Marjolijn en Caroline, bedankt voor alles de afgelopen jaren en alvast bedankt voor alles wat we nog samen gaan beleven.

Naast deze vriendengroepen maak ik ook deel uit van een grote familie. Hiervan ben ik een selectie zeker een woord van dank verschuldigd. Bedankt moeke en pa om steeds in mij te geloven en te vragen hoe het was met de muizen. Ik ben blij dat jullie hier vandaag aanwezig kunnen zijn! Ook aan alle tantes, nonkels, nichten, neven en vriendjes en vriendinnetjes, bedankt om op tijd en stond interesse te tonen in mijn doctoraat. Hopelijk hebben jullie ook iets van mijn uitleg begrepen.

Hanne, je was mijn groot voorbeeld toen ik klein was. Ondanks dat ik de Bert en Ernie brooddoos mooier vond, koos ik toch ook die van de Lion King, want als jij die gekozen had, zouden mijn boterhammen daar toch zeker het beste in smaken. Mijn vertrouwen in jou was (en is nog steeds) groot. Ik was jouw kleine zusje en ik ben er zeker van dat je voor mij je hand in het vuur zou hebben gestoken. We bellen elkaar niet elke dag en zien elkaar misschien niet elke week, maar toch heb ik veel aan jou en zie ik je nog steeds als mijn grote zus die me ten alle tijden zal beschermen en er is wanneer dat nodig blijkt.

Ben, ook bedankt voor de persoon die je bent en de toevoeging van je humoristische noot en jeugdig enthousiasme aan ons gezin. Wanneer we spelletjes spelen, ligt in 98% van de gevallen de winnaar al vast, ook al spant iedereen samen tegen jou. Het blijft desondanks toch nog altijd spannend en leuk en ik zeg het niet graag, maar doorgaans ben je de verdiende winnaar ;-)

Mama en papa, de grootste dankjewel is voor jullie. Zonder jullie was er van dit dankwoord geen sprake geweest. Jullie hebben me onnoemelijk veel kansen gegeven gedurende mijn

hele leven en geleerd ergens voor te gaan en niet te snel op te geven. Ik mocht een muziekinstrument kiezen dat ik wou doen (het zou kunnen dat jullie mij bewust uit de buurt van het slagwerk gehouden hebben, maar mijn interesse daarvoor was toen toch niet zo groot), ik mocht een andere richting dan Latijn kiezen (want die woordjes leren iedere dag zei me niet veel), gaan studeren en op kot gaan in een zelf gekozen studentenstad. Jullie hebben mijn leven hierdoor gemakkelijker gemaakt en waren er wanneer ik daar behoefte aan had. Tot voor kort werd de was en de plas nog voor mij gedaan, tijdens de blok- en examenperiodes kwamen jullie mij bezoeken en bevoorraden en zelfs nu nog kan ik in het weekend of wanneer dan ook gebruik maken van het liefdevolle Hotel Mama en Papa en terecht onder moeders en vaders vleugels. Ik ben verwend!

Ongeveer twee jaar geleden heb ik er ook nog een extra familie bij gekregen. Bedankt Marc, Hilde en Matthias. Bedankt voor de deur die altijd open staat, het overvloedige en lekkere eten als we op bezoek zijn en vooral de warme welkom die ik vanaf het begin heb mogen ervaren!

Dat brengt mij tot de laatste persoon, mijn grote steun en toeverlaat die altijd voor mij klaarstaat: Christophe :-) Ondanks dat je zelf geen wetenschappelijke achtergrond hebt (we zullen die discussie over humane wetenschappen later verderzetten), is het toch dankzij de wetenschap dat we samengekomen zijn. Hierbij ben ik genoodzaakt Dries nogmaals te bedanken, want zonder hem had ik jou nooit leren kennen (of was de kans toch grenzend aan het onwaarschijnlijke geweest, gezien mijn beperkte interesse in het voetbal).
Christophe, ik weet dat ik niet altijd de gemakkelijkste ben en soms om onverklaarbare redenen mijn frustraties op jou uitwerk (een kort lontje zoals je dat dan noemt). De manier waarop je hiermee omgaat, is bewonderingswaardig. Je laat me lachen, voelt aan wanneer er een haar in de boter zit, durft je te excuseren, maar af en toe gelukkig ook kwaad te maken en tegen mij in te gaan. Verder maakt onze gedeelde liefde voor eten en vooral zoetigheden dat we voor elkaar bestemd zijn (het sporten dat we gingen doen vanaf dat we samenwoonden, komt er wie weet zelfs ook nog ooit van om te compenseren voor die overdosis aan calorieën). Liefde zit in kleine dingen zoals een lief briefje bij mijn boterhammen (die je zo goed als iedere ochtend voor mij maakt), een onverwacht minicadeautje, het naar buiten leiden van meikevers, de afwas die gedaan is wanneer ik thuiskom van het werk, een paar lieve woordjes of gewoon je ondeugende lach (al dan niet gepaard gaande met een bijpassend dansje). Bedankt, lieve Christophe, voor de persoon die je bent en om er steeds voor mij te zijn. Ik zie je graag :-)

En u, beste lezer, bedankt om al tot het einde van mijn dankwoord te geraken. Ik wens u nog veel plezier met al het resterende ;-)

Lotte

Table of Contents

List of Abbreviations

α2-AP	α2-antiplasmin
ADAMTS13	a disintegrin and metalloproteinase with thrombospondin-1 repeat, member 13
Adamts13$^{-/-}$	ADAMTS13 deficient
ADP	adenosine diphosphate
ALT	alanine aminotransferase
AMR	Ashwell-Morell Receptor
AST	aspartate aminotrasferase
AT	adipose tissue
ATP	adenosine triphosphate
Bcl-2	B-cell lymphoma 2
BMI	body mass index
C8	cysteine 8
CD	cluster of differentiation
Clodronate	dichloromethylene bisphosphonate
CLS	crown-like structures
CMFDA	5-chloromethylfluorescein diacetate
CMTMR	5-(and-6)-(((4-chloromethyl)benzoyl)amino)tetramethylrhodamine
Col1a1	α-1 type I collagen
CRP	C reactive protein
CUB	Complement component C1r/C1s, Urinary epidermal growth factor (Uegf), and Bone morphogenic protein-1
Cys	cystein
DMEM	Dulbecco′s Modified Eagle′s Medium
DNA	desoxyribonucleic acid
ER	endoplasmatic reticulum
FAS	fatty acid synthase
FATP	fatty acid transport protein
FBS	fetal bovine serum
FFA	free fatty acids
GlcNac	N-acetyl D-glucosamine
GLUT	glucose transporter
GN	gonadal
GP	glycoprotein
GPX1	glutathione peroxidase-1
HDL	high density lipoprotein
HFD	high fat diet
HIV	human immunodeficiency virus
HMW	high molecular weight

HOMA-IR	homeostasis model assessment of insulin resistance
HSC	hematopoietic stem cell
HUS	hemolytic uremic syndrome
IL	interleukin
ITP	immune thrombocytopenia
LDH	lactate dehydrogenase
LDL	low densitly lipoprotein
LMW	low molecular weight
LRP-1	low density lipoprotein receptor-related protein 1
MCAD	medium chain acyl-CoA dehydrogenase
MCC	methionine choline control diet
MCD	methionine choline deficient diet
MCP-1	monocyte chemotactic protein-1
Met	methionine
mRNA	messenger RNA
mVWF	mouse von Willebrand Factor
NAFLD	non-alcoholic fatty liver disease
NASH	non-alcoholic steatohepatitis
PAI	plasminogen activator inhibitor
PAP	plasmin-α2-antiplasmin complex
PPAR	peroxisome proliferator-activated receptor
PSGL-1	P-selectin glycoprotein ligand-1
RBC	red blood cell
ROS	reactive oxygen species
rADAMTS13	recombinant ADAMTS13
rVWF	recombinant von Willebrand Factor
SC	subcutaneous
SEM	standard error of the mean
SFA	saturated fatty acid
SFD	standard fat diet
α-SMA	α-smooth muscle actin
SOD1	superoxide dismutase 1
SREBP-1	sterol regulatory element-binding protein 1
Stx	Shiga toxin
SVF	stromal vascular fraction
TAFI	thrombin activatable fibrinolysis inhibitor
TAT	thrombin-antithrombin complex
TF	tissue factor
TGF	transforming growth factor
TIL	trypsin-inhibitor-like
TIMP	tissue inhibitor of metalloproteinases

TLR	Toll-like receptor
TMA	thrombotic microangiopathy
TNF	tumor necrosis factor
tPA	tissue-type plasminogen activator
TPO	thrombopoietin
TSP-1	trombospondin-1
TTP	thrombotic thrombocytopenic purpura
Tyr	tyrosine
UL-VWF	ultra-large von Willebrand Factor
uPA	urokinase
VE-cadherin	vascular endothelial cadherin
VEGF	vascular endothelial growth factor
VEGFR	vascular endothelial growth factor receptor
VWD	von Willebrand disesase
VWF	von Willebrand Factor
WAT	white adipose tissue
WBC	white blood cell
WC	waist circumference
WHO	World Health Organization
WP	Weibel Palade
WT	wild-type
XDH1	xanthine dehydrogenase 1

Chapter 1

General Introduction

1. Thrombotic Thrombocytopenic Purpura

Thrombotic thrombocytopenic purpura (TTP) is a very rare disease with an incidence of 4-11 cases/10^6 per year, according to the OKLAHOMA TTP-HUS registry (1). When left untreated, it is a life-threatening thrombotic microangiopathic disorder (TMA), characterized by severe thrombocytopenia and microangiopathic hemolytic anemia, with symptoms including microthrombosis in capillaries and arterioles, presence of fragmented red blood cells (RBC) (schistocytes) and low hematocrit levels. Other less specific symptoms are fever, neurological dysfunction and renal impairment (2). To understand the pathophysiology of TTP, basic principles of blood, platelets, hemostasis and von Willebrand Factor (VWF) will be discussed in the following paragraphs.

1.1. Blood

The human body contains approximately 5 liters of blood of which the main component is plasma (55%), consisting mainly of water, but also of nutrients, oxygen, waste products, salts and proteins. The remaining 45% of the blood is formed by the blood cells, including red blood cells (RBC) or erythrocytes, white blood cells (WBC) or leukocytes and blood platelets or thrombocytes. These cells have various specific functions and are the final product of hematopoiesis, a highly regulated process originating in the bone marrow. RBC bind oxygen via hemoglobin and transport it from the lungs to the tissues (3). The volume of RBC in whole blood, expressed in percentage, is termed hematocrit and is normally around 45% in both men and mice (Table 1). It is a measure for the effectiveness of oxygen delivery to the tissues and low hematocrit levels are related to anemia (4).

WBC consist of neutrophils, eosinophils, basophils, monocytes, macrophages and lymphocytes. These cells protect the body from infectious diseases and foreign invaders, and thus are important in innate and acquired immunity (5).

The primary function of platelets is coagulation or blood clotting, but they are also involved in other processes such as tissue repair, host defense and production of inflammatory cytokines (6).

1.1.1. Platelets

Every day, 10^{11} blood platelets are produced in and removed from the human body to maintain a steady state with an average platelet count of 150-400 x 10^3 platelets per microliter of blood. Human platelets are anuclear, very small (1.5-3 µm) cells, with a discoid shape (lens shaped) because of the highly specialized cytoskeleton (7, 8). Two-thirds of the platelets circulate through the body whereas the rest is stored in the spleen. Platelets have a plasma membrane rich in specific glycoprotein (GP) surface receptors regulating platelet adhesion, activation and aggregation (9). The most abundant surface receptor is the αIIbβ3 integrin of which there are 40-80 x 10^3 per platelet, even further increasing after platelet activation (10). Furthermore, platelets contain secretory α- and dense granules storing biologically active molecules. Especially the α-granules, which contain proteins involved in platelet adhesion such as von Willebrand factor (VWF) and αIIbβ3, are well represented (40-80/platelet) (11, 12). Factors released after platelet activation such as serotonin, adenosine diphosphate (ADP), adenosine triphosphate (ATP) and calcium are stored in the dense granules (13).

The average survival time of blood platelets in humans is between 8 and 10 days. When platelet counts are lower than 150 x 10^3 platelets per microliter of blood, this condition is called thrombocytopenia and is associated with bleeding at platelet

numbers below 30 x 10^3 platelets per microliter. There are significant differences between human and murine platelets (Table 1). In mice, normal platelet counts are 4 to 6 times higher than in humans and can reach levels up to 1600 x 10^3 platelets per microliter of blood. Additionally, platelets in mice are much smaller than in humans and their survival time is 2 to 3 times shorter. Moreover, the α-granules in murine platelets are more heterogeneous in size and shape (circular or elongated) and there are fewer dense granules than in human platelets (14).

Table 1: Normal values for the blood cell count and platelet characteristics of male human and murine (C57BL/6; age 8-10 weeks) blood and platelets.

	Human	Murine
Red blood cell count (x10^6/µL)	4.0 - 6.0	9.5
Hematocrit (%)	47	47
Hemoglobin (g/dL)	13.5 - 16.5	14.2
White blood cell count (x10^3/µL)	4.8 - 10.8	8.9
Platelet count (x10^3/µL)	150 - 400	900 - 1600
Mean platelet volume (fL)	9.7 - 12.8	5.0
Platelet diameter (µm)	1.5 - 3.0	0.50
Platelet lifespan (days)	± 10	± 4.0

Source: Charles River Mouse Hematology; Anatomy and Philology (15, 16).

Platelet production and clearance are strictly regulated processes, in both physiological and pathological conditions, monitoring constant numbers of platelets in order to prevent spontaneous bleeding or thrombus formation and subsequent organ damage (7).

The most prominent player in regulation of platelet production is thrombopoietin (TPO), which is produced mainly by hepatocytes, bone marrow and kidneys. Platelet precursors in the bone marrow, the megakaryocytes, mature under influence of diverse chemokines and cytokines (e.g. TPO, interleukin (IL)-6, IL-3, IL-11, colony-stimulating factor) and become polynuclear during a process called endomitosis. While

megakaryocytes mature, their cytoplasm increases in size and is filled with platelet-specific α- and dense granules (8). In a next step, polynuclear megakaryocytes develop extensions and form proplatelets that extend through or between sinusoidal cells into the blood circulation. These proplatelets fragment into anuclear, sialylated platelets, which are released into the blood stream (Figure 1) (17).

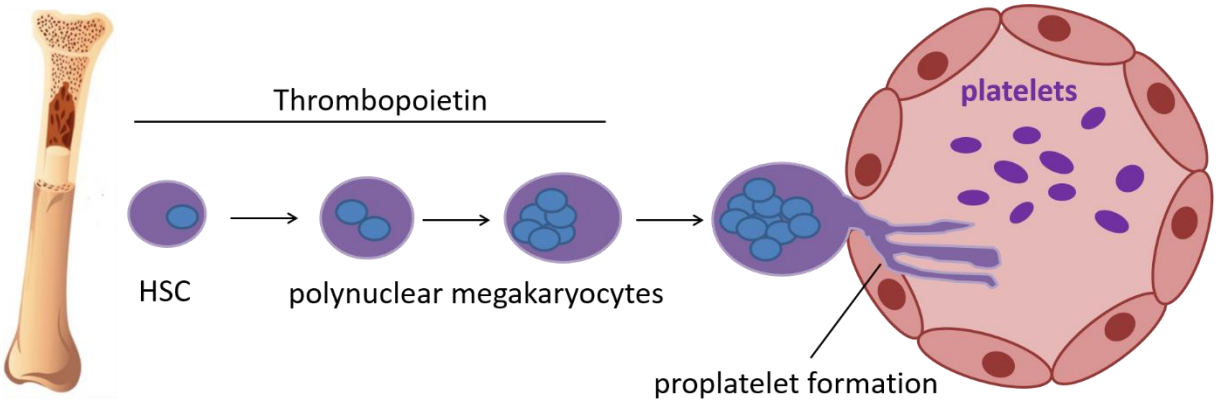

Figure 1: Platelet production from megakaryocytes in the bone marrow.
From hematopoietic stem cells (HSC) in the bone marrow, megakaryocytes are formed regulated by thrombopoietin (megakaryopoiesis). Megakaryocytes mature and become polynuclear, form long extensions (proplatelets) and release sialylated platelets into the circulation. *Figure based on (7).*

After being split off from the megakaryocytes and released into the blood stream, platelets will eventually be consumed in a hematopoietic process or cleared from the circulation. Platelet clearance occurs through the liver and the spleen, and is regulated by different mechanisms: intrinsic apoptosis (a), clearance by antibodies (b), ageing-induced (senescence) (c) or cold-induced (d) (by storage for platelet transfusion) clearance (7).

a) Although platelets are anuclear, the intrinsic apoptotis pathway is involved in platelet clearance. B-cell lymphoma 2 (Bcl-2) family members are present in human platelets, driving clearance through apoptosis. Pro-survival proteins of the Bcl-2 family protect healthy platelets from apoptosis. However, these

proteins can be inhibited leading to mitochondrial damage, cytochrome C release and ultimately caspase activation resulting in apoptosis and clearance via scavenger receptors (Figure 2.1). It was shown that *ex vivo* inhibition of the Bcl-2 family member Bcl-xL in platelets resulted in mitochondrial damage, caspase activation and externalization of phosphatidylserine, which is typical for dying nucleated cells (18, 19). Furthermore, thrombocytopenia was caused in mice and dogs within 2 hours after administration of a Bcl-xL inhibitor (20). The triggering event leading to activation of the apoptotic pathway remains unclear (18). Moreover, it is unknown whether Bcl-2 family members influence sialic acid content on the platelet surface. It is possible that sialic acid loss could trigger intrinsic apoptosis, thereby affecting platelet survival (7).

b) In immune thrombocytopenic purpura, also known as immune thrombocytopenia (ITP), autoantibodies directed against different surface receptors on platelets e.g. αIIbβ3 or GPIb-IX-V are produced by B cells after interaction of reactive T cells with memory B cells (21). It is thought that the first antigenic response occurs in the spleen and is followed by stimulation of other antibody-producing tissues, particularly the bone marrow (22). When passing through the sinusoids of the spleen, macrophages will recognize and phagocytose auto-antibody-coated platelets, leading to destruction (23) (Figure 2.2).

c) Platelet surface glycoproteins, e.g. GPIb, are important in glycan-lectin mediated platelet clearance. In ageing (senescent) circulating platelets, the VWF-binding GPIbα subunit is desialylated by platelet sialidases. Due to the removal of the sialic acids, galactose residues become exposed, which leads to recognition of the platelets by specific liver lectins called the Ashwell-Morell

receptors (AMR), resulting in clearance of the senescent platelets (24) (Figure 2.3). Recently, it became clear that elimination of senescent platelets by the hepatic AMR drives TPO production in the liver followed by increased megakaryocyte and platelet production, assuring an equilibrium between production and clearance (25).

d) Refrigerated platelets used for platelet transfusion are cleared more rapidly from the circulation than room temperature stored platelets, because cooled platelets lose, apart from the sialic acids groups, also the underlying galactose residues, whereby N-acetyl D-glucosamine (GlcNac) groups become exposed. After transfusion of cooled platelets, these monosaccharides cluster and are recognized as foreign by the αMβ2 integrin on the hepatic Kupffer cells, followed by phagocytosis and removal of the transfused platelets (26) (Figure 2.3). Consequently, platelets for transfusion are stored at room temperature risking bacterial contamination and loss of platelet functionality, limiting the storage time to maximum 5 days (27).

Hence, platelet counts are regulated in a complex way. Production and clearance of platelets seem interrelated as shown by the regulation of TPO after senescent platelet clearance by the hepatic AMR. Under pathological conditions, platelets are cleared via spleen macrophages, while senescent platelets are removed from the circulation by liver cells or apoptosis, regulated partly by desialylation of platelet surface glycoproteins.

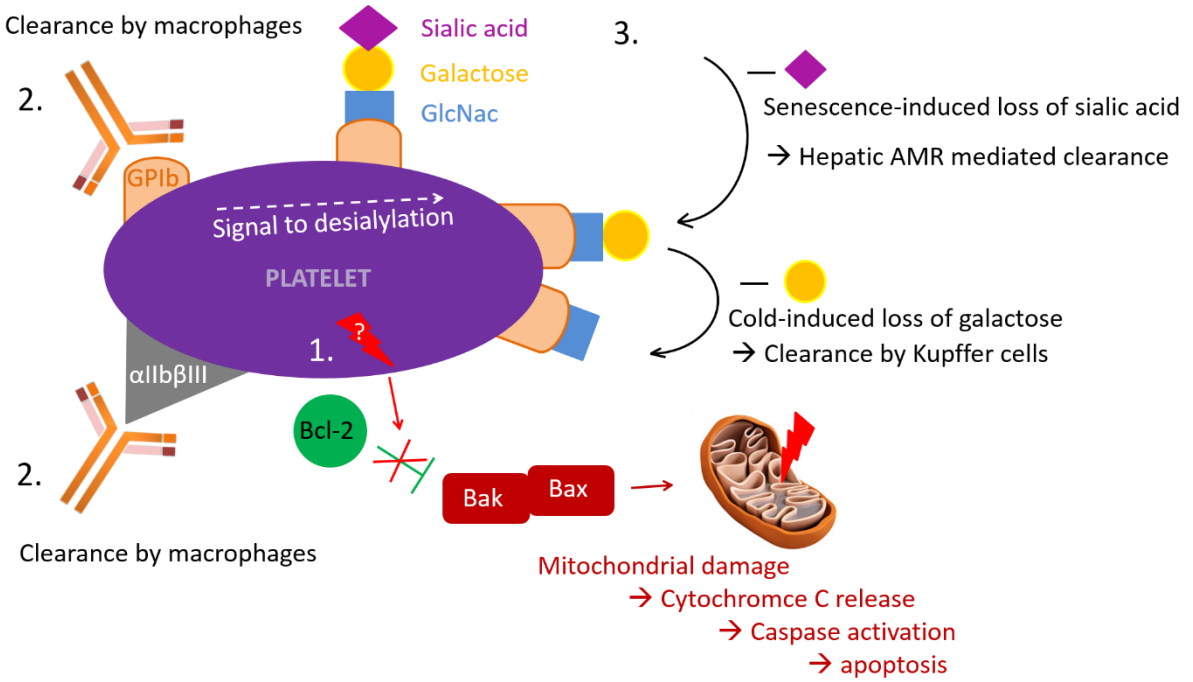

Figure 2: Mechanisms of platelet clearance in the liver and spleen.
1) Clearance mediated by programmed cell death (apoptosis) via the intrinsic apoptotic pathway: the balance between pro- and anti-apoptotic Bcl-2 family members is disturbed leading to discontinuation of the inhibition of Bak and Bax resulting in apoptosis. The triggering factor is still unknown. 2) Auto-antibody mediated clearance: antibodies against αIIbβ3 or GPIb leading to phagocytosis or platelet desialylation, respectively. 3) Glycan-lectin mediated clearance: due to ageing, desialylation results in recognition and clearance of the platelet by the AMR on hepatocytes. In addition, stored platelets can lose galactose thereby exposing GlcNAc that will be recognized by the Kupffer cell αMβ2 integrin in the liver leading to phagocytosis of the platelet. *Figure based on (7).*
Abbreviations: GPIb: glycoprotein I b; Bcl-2: B-cell lymphoma 2; AMR: Ashwell-Morell receptor; GlcNac: N-acetyl D-glucosamine.

1.1.2. Circulatory system and shear stress

Blood is pumped from the heart through the body by a network of arteries, arterioles, capillaries, venules and veins. These blood vessels are built of three distinct layers: tunica intima, tunica media and tunica adventitia. The tunica intima contains endothelial cells surrounded by a basal membrane: the subendothelium that is surrounded by the internal elastic lamina. The tunica media is formed by a layer of smooth muscle cells together with connective tissue. Beneath the smooth muscle cells,

a second elastic layer, the external elastic lamina, is located. The outer layer is the tunica adventitia built of connective tissue that consists of collagen and fibroblasts. The vessel size and type determines the thickness and composition of these three layers. Arteries and arterioles have a thicker layer of smooth muscle cells than veins and venules and can therefore resist higher pressures. The pressure in veins and venules is much lower than in arteries and arterioles. Veins and venules also lack the elastic laminas. Nevertheless, because of the presence of valves in the central venous circulation, it is possible to bring the blood back to the heart. The capillaries form the connection between arterioles and venules and are located in the tissues. These consist only of a thin layer of endothelial cells to facilitate diffusion and supply the tissues with oxygen and nutrients (3).

Blood is a viscous fluid and can flow because of a pressure gradient resulting in tangential forces generated at the vessel wall in the direction of the flow, which is called shear stress (28). The blood flow is laminar in a cylindrical vessel and therefore the velocity of the blood stream is highest in the middle of a blood vessel and decreases towards zero at the blood vessel wall. In contrast, the shear stress is highest at the vessel wall and in small vessels such as arterioles and capillaries (29, 30).

1.1.3. Hemostasis

Hemostasis is the resting condition in which pro-coagulant and anti-coagulant processes are balanced. Disturbed hemostasis will lead to thrombosis or bleeding, which can be life-threatening. When a vessel is damaged, platelets react immediately by binding to the injured vessel wall, leading to the formation of a blood clot preventing excessive blood loss. To form and dissolve a clot, three mechanisms are important: primary and secondary hemostasis and fibrinolysis.

Primary hemostasis comprises three phases in which platelets play a prominent role, namely adhesion, activation and aggregation (Figure 3) (31-33).

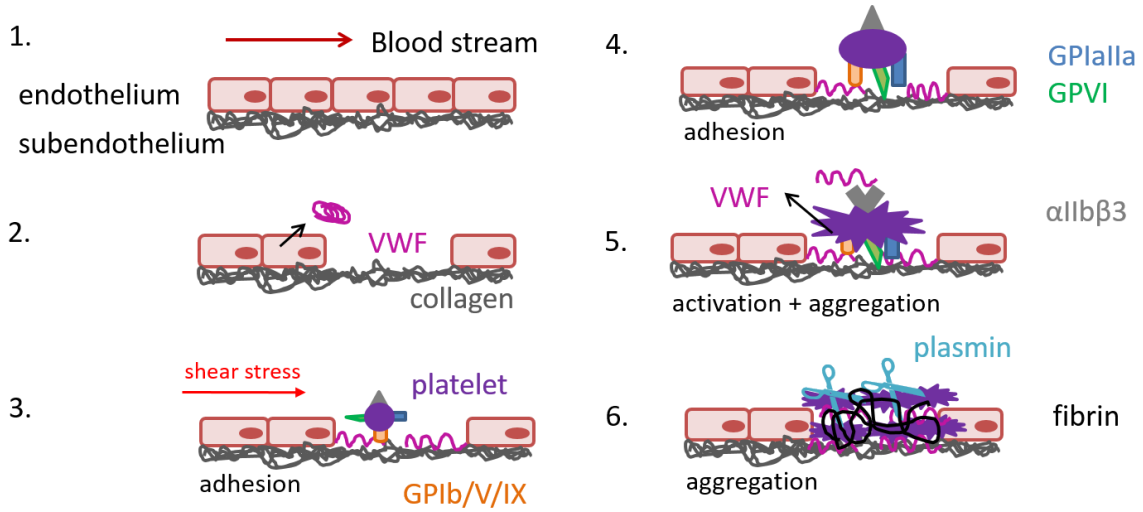

Figure 3: (Primary) hemostasis after vessel injury.
1. The intact blood stream. 2. Blood vessel damage leading to VWF release from the Weibel Palade bodies in the endothelial cells. 3. VWF can bind with its A3 domain to the exposed collagen of the subendothelium and will unfold due to shear stress. Platelets are now able to bind to VWF with their GPIb receptor. This binding is reversible and the platelets start to roll over VWF. 4. During the rolling phase, platelets bind with the GPIaIIa and GPVI receptors to collagen and platelets become activated. Step 3 and 4 are called adhesion. 5. In the next step, the activation phase, the conformation of αIIbβ3 receptor on platelets changes, 6. allowing fibrinogen binding and thus crosslinking αIIbβ3 on adjacent platelets resulting in aggregation and blood clot formation. The platelet clot formed during primary hemostasis can be stabilized further in the secondary hemostasis by fibrin and thrombin. Ultimately, in wound healing the blood clot is removed by plasmin during fibrinolysis.
Abbreviations: VWF: von Willebrand Factor; GP: glycoprotein.

During the adhesion phase (Figure 3.3 and 3.4), platelets will adhere to the vessel wall by binding with their GPIb receptor to VWF that in a previous step already bound to the naked collagen of the subendothelium of the injured vessel and consequently unfolded due to shear stress (Figure 3.2 and 3.3) (31). This platelet-VWF binding is transient and therefore, platelets will roll over the damaged vessel wall, which slows down the platelets allowing them to interact with collagen via integrin α2β1 (GPIaIIa)

and GPVI (34). Subsequently, platelets become activated, characterized by a conformational change and spreading of platelets (Figure 3.5). In addition, the content of the α- and dense granules is secreted resulting in further activation of rolling platelets. Activated platelets express the activated αIIbβ3 receptor, which makes it possible to form platelet aggregates (clots) in the aggregation phase (Figure 3.6) (33).

This platelet aggregate would, however, quickly dissolve and only postpone bleeding. Therefore, the clot is simultaneously stabilized by a fibrin network involving the coagulation cascade or **secondary hemostasis** cascade in which thrombin plays a major role (35) (Figure 4). Tissue factor (TF), the key initiator of the coagulation cascade, circulates in blood at low concentrations (100-150 pg/mL plasma) and is active or can be activated. Furthermore, TF is expressed by cells surrounding blood vessels. When a blood vessel is damaged, blood will leak into the extravascular tissues and will be exposed to TF. This will initiate the extrinsic coagulation cascade in which thrombin is formed after a number of enzymatic reactions. Apart from the extrinsic pathway, the coagulation cascade can be amplified by activating coagulation factor XII, but especially factor XI by negatively charged surfaces such as glass (*in vitro*) or negatively charged phosphatidylserine (*in vivo*); this is called intrinsic coagulation. Thrombin formed in the early extrinsic pathway can also activate factor XI. Ultimately, both the extrinsic and intrinsic coagulation share a common pathway in which prothrombin is converted into thrombin that will convert fibrinogen into insoluble fibrin and can further activate platelets. In addition, thrombin will interact with the GPIb receptor on platelets, thereby activating factor IX, factor VIII and factor V, resulting in high levels of thrombin. During primary hemostasis, luminal (inside the vessel) activated platelets and endothelial cells will release P-selectin that will bind to P-selectin glycoprotein ligand-1 (PSGL-1) on monocytes. This results in induction of TF-

rich microvesicles transported to the thrombus ultimately leading to generation of thrombin (36, 37).

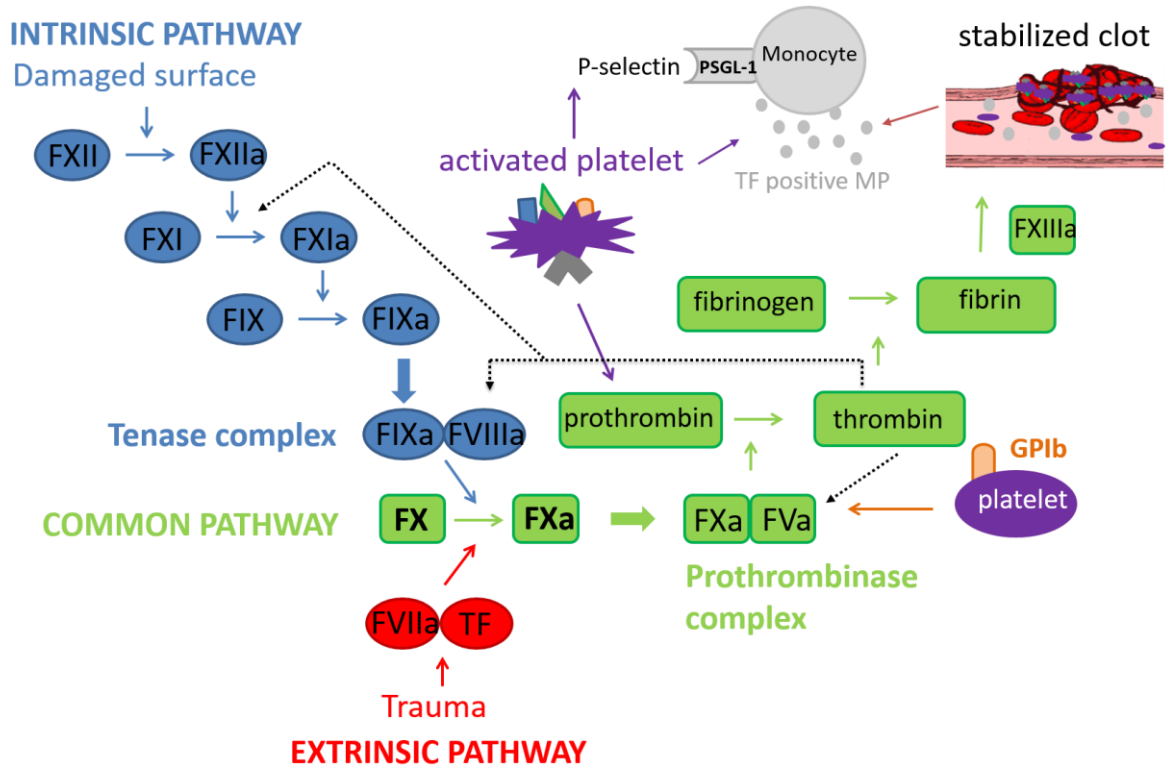

Figure 4: The secondary hemostasis or coagulation cascade.
In the extrinsic pathway (red), trauma leads to exposure of tissue factor (TF) and activated factor VII (FVIIa). Together, this complex activates factor X (FX). The intrinsic pathway (blue), after a cascade of enzymatic reactions, also leads to activation of FX by the tenase complex. Subsequently, the common pathway (green) results in formation of thrombin from prothrombin, which will also bind to the GPIb receptor on platelets, activate FVIII and FV leading to a thrombin burst. Thrombin converts fibrinogen to insoluble fibrin that will stabilize the platelet plug formed during primary hemostasis. In addition, thrombin is able to activate platelets leading to further secretion of coagulation cascade factors (e.g. prothrombin). At the inside of the vessel, P-selectin secreted from activated platelets and endothelial cells will bind to PSGL-1 on monocytes resulting in TF positive MP generation and increased thrombin generation. MP can also be formed by platelets and endothelial cells.
Abbreviations: F: factor; a: activated; TF: tissue factor; GP: glycoprotein; PSGL-1: P-selectin glycoprotein ligand-1; MP: microparticles.

When activated, platelets also secrete several factors of the coagulation cascade (e.g. prothrombin) and negatively charged phosphatidylserine becomes exteriorized (38),

forming a surface on which coagulation can proceed. Moreover, VWF is the carrier protein of coagulation factor VIII. Thus, primary and secondary hemostasis collaborate to form a stable thrombus, which happens very rapidly after vessel injury (32, 35).

The traditional classification into extrinsic and intrinsic pathway of the coagulation cascade is still valid, but nowadays coagulation is often subdivided into initiation, amplification, propagation and stabilization. During the initiation phase, thrombin is generated, which further activates factor V and VIII to activate the prothrombinase complex leading to a thrombin burst in several positive feedback loops during the amplification phase. In the propagation phase, the tenase and prothrombinase complexes assure continuous generation of thrombin and fibrin to form a large clot. Thrombin generation results in factor XIII activation covalently linking fibrin polymers resulting in a stable platelet clot during the stabilization phase (39).

In the third process, i.e. **fibrinolysis** (Figure 5), plasmin breaks down fibrin in order to dissolve the blood clot. Furthermore, the fibrinolytic system is important in protecting the body from thrombus formation in healthy vessels (32). The fibrinolytic system contains several cofactors, receptors and inhibitors, and is therefore highly regulated and controlled. The precursor of plasmin, plasminogen, is produced by the liver and activated by tissue-type plasminogen activator (tPA) or urokinase (uPA) that are secreted by endothelial cells or urinary epithelium. Inhibitors of the fibrinolytic system are important to prevent hyperactivity of plasmin. Plasminogen activator inhibitor (PAI)-1 and -2 can inhibit tPA and uPA, whereas α2-antiplasmin (α2-AP) inhibits plasmin in a 1:1 ratio. However, plasmin generated at the fibrin surface is protected from rapid inhibition by α2-AP. In addition, α2-AP can also bind to fibrin protecting it from cleavage by plasmin and protecting the clot from fibrinolysis. Thrombin activatable fibrinolysis inhibitor (TAFI) exerts anti-fibrinolytic activity by eliminating C-terminal lysines on fibrin,

leading to a strongly decreased binding of plasminogen to fibrin (40). Thus, fibrinolysis is a regulated enzymatic process preventing unneeded fibrin clot formation, assuring balanced hemostasis and breakdown of platelet-fibrin plugs when necessary (41, 42).

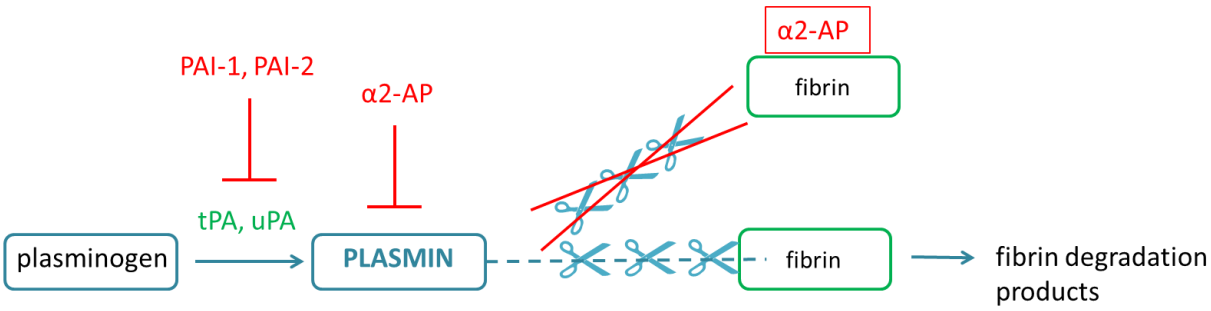

Figure 5: The fibrinolytic system.
Plasmin can cleave fibrin into fibrin degradation products leading to clot breakdown, thus dissolving a blood clot. The precursor plasminogen is activated to plasmin by tPA or uPA, which can be inhibited by PAI-1 and PAI-2. Furthermore, α2-AP can inhibit plasmin or bind to fibrin to delay its cleavage.
Abbreviations: tPA: tissue-type plasminogen activator; uPA: urokinase; PAI: plasminogen activator inhibitor; α2-AP: α2-antiplasmin.

1.2. von Willebrand Factor

VWF is a multimeric plasma glycoprotein that plays a major role in primary hemostasis (as described above). VWF is produced by endothelial cells and megakaryocytes and can be stored in Weibel Palade bodies or α-granules in either endothelial cells or platelets, respectively. The blood VWF concentration is 5-15 µg/mL blood (43).

1.2.1. Synthesis, release and clearance

The VWF encoding gene is located at chromosome 12. After transcription, the VWF mRNA is translocated to the cytoplasm where it is translated to the pre-pro-VWF precursor consisting of a signal peptide, propeptide and the mature VWF subunit. Thereafter, the signal peptide is responsible for the translocation of pre-pro-VWF to the endoplasmatic reticulum where the pre-peptide is cleaved and VWF dimers, also known as protomers, are formed by a disulfide bond between two pro-VWF moieties.

Further multimerization occurs in the Golgi complex via additional disulfide bridges resulting in multimers consisting of 2 to 60 subunits (44). The pro-peptides are released by furin after glycosylation and the mature ultra-large VWF (UL-VWF) is transported to the α-granules of megakaryocytes or platelets, to Weibel Palade bodies of endothelial cells, or is secreted directly into the blood stream (Figure 6) (45, 46). The formation of Weibel Palade bodies in the endothelial cells is VWF dependent, whereas α-granules in platelets will be generated regardless of VWF.

Release of VWF from endothelial cells into the blood stream can be either constitutively or in a regulated process, whereas VWF secretion from α-granules requires platelet activation (45). Consequently, all the VWF in circulation comes from the endothelium. Most of the VWF secreted by endothelial cells arises from the constitutive secretory pathway. Endothelial stimulation (as upon vascular injury) leads to massive release of Weibel Palade bodies and the production of longer hyperactive VWF multimers that anchor to endothelial cells and induce spontaneous microaggregate formation. Consequently, platelets will be recruited and primary hemostasis occurs (47).

The half-life of therapeutic VWF antigen in humans is approximately 16 hours, but the half-life of endogenous VWF is very variable depending on its glycosylation pattern. Since VWF is a carrier protein of the coagulation cascade factor VIII, also the half-life of the latter will depend on the individual half-life of VWF (48).

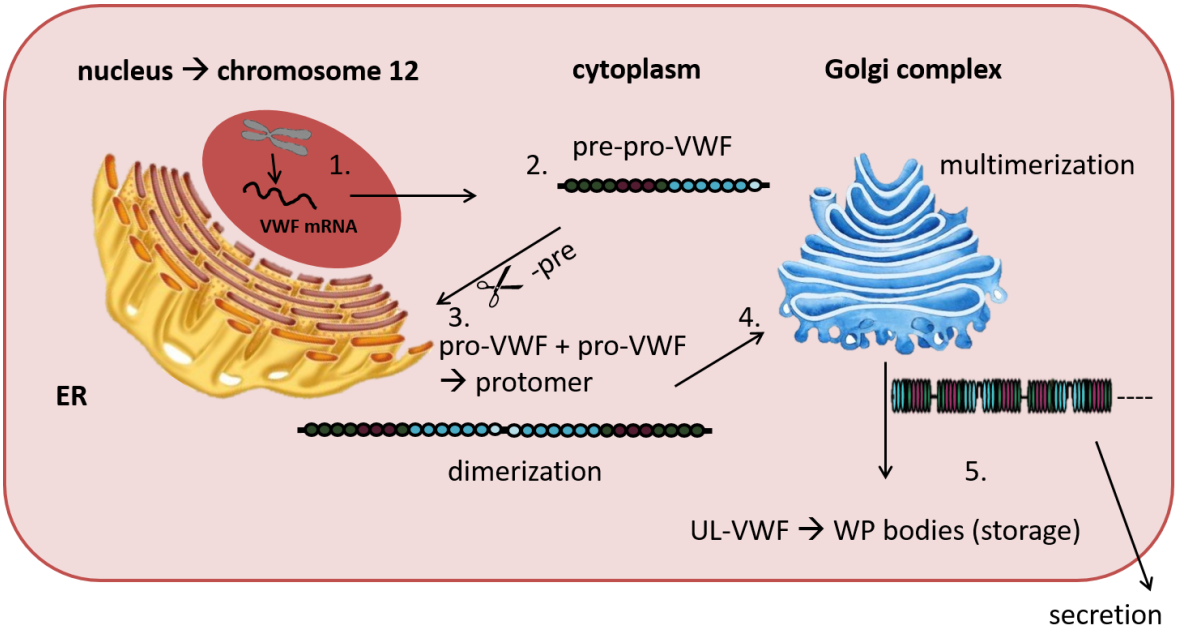

Figure 6: Synthesis of VWF in endothelial cells.

1. The gene that encodes VWF is located on chromosome 12. 2. The VWF mRNA is translocated to the cytoplasm where it is translated to the pre-pro-VWF protein, which is translocated to the endoplasmatic reticulum (ER) via its signal peptide. 3. The pre-peptide is cleaved in the ER, VWF dimers (protomers) are formed by a disulfide bond between two pro-VWF moieties. 4. Further multimerization occurs in the Golgi complex. 5. The propeptides are released and the mature ultra-large VWF is transported to the Weibel Palade bodies of the endothelial cell or secreted into the blood stream. *Figure based on (48).*

Abbreviations: ER: endoplasmatic reticulum; VWF: von Willebrand Factor; mRNA: messenger RNA; UL-VWF: ultra-large VWF; WB: Weibel Palade.

Since VWF and macrophages generally co-localize and after depletion of macrophages endogenous VWF levels increase strikingly, the major elimination route of VWF is via macrophages in the liver and spleen (49). It is believed that VWF is cleared by receptor-mediated endocytosis, possibly involving the Ashwell receptor, low density lipoprotein receptor-related protein 1 (LRP1), sialic acid binding Ig like lectin 5 (Siglec-5) or C-type lectin domain family 4 member M (CLEC4M) receptors; in particular the LRP1 receptor appears to be important in VWF clearance. However, since deficiency of this receptor leads to only a twofold increase of the VWF half-life it is plausible that other, up until now unknown, receptors could also play a role (50).

1.2.2. Structure, function and activity

VWF multimers consist of monomers of 250 kDa built of 2050 amino acids that form different domains, more specifically D1-D2-D'-D3-A1-A2-A3-D4-C1-C2-C3-C4-C5-C6-CK (Figure 7).

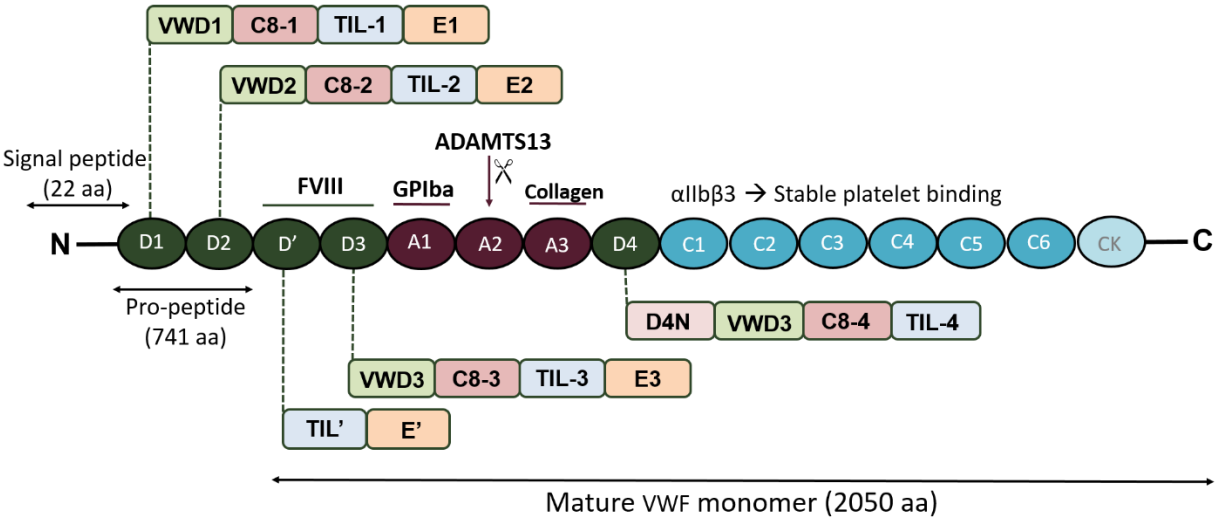

Figure 7: Domain structure of VWF.

The pre-pro-VWF protein contains the signal peptide of 22 amino acids (aa), the pro-peptide of 741 aa that contains the D1 and D2 domain, and the mature monomer of 2050 aa. The mature monomer contains different domains. *Figure based on (48) and (50).* Abbreviations: aa: amino acids; VWD: von Willebrand Factor D; C8: cysteine 8; TIL: trypsin-inhibitor-like; E: E module; FVIII: factor 8; GP: glycoprotein; ADAMTS13: a disintegrin and metalloproteinase with thrombospondin-1 repeat, member 13; VWF: von Willebrand Factor.

Recently it has been discovered that the D1, D2 and D3 domains contain von Willebrand Factor D (VWD), cysteine 8 (C8), trypsin-inhibitor-like (TIL) structures and an E module. D4 domains lack E modules, but enclose a unique D4N domain. The D' domains do not contain VWD or C8 domains (Figure 7) (50, 51). The D1-D2 domains form the pro-peptide and the remaining protein is the mature VWF subunit. Each mature monomer contains 12 N-linked and 10 O-linked glycosylation sites essential for the secretion, clearance and folding of VWF. The A1 domain is able to bind platelets via the GPIb receptor, the A2 domain contains the cleavage site where ADAMTS13 (a

disintegrin and metalloproteinase with thrombospondin-1 repeat, member 13) can bind and the A3 domain contains the major physiological binding site for fibrillar collagens I and III, whereas the A1 domain can bind to collagen VI (52). The platelet receptor αIIbβ3 interacts with the C1 domain of VWF, resulting in a stable platelet binding.

In normal physiologic conditions, VWF is in its folded, inactive globular form in order to prevent spontaneous platelet binding to circulating VWF. While circulating, the A3 domain is constitutively accessible and able to bind to exposed collagen at sites of vascular injury. Subsequently, mechanical shear forces will induce the conformational change of VWF, uncovering the A1 and A2 domains leading to binding with platelets and/or cleavage by ADAMTS13, respectively (45, 53) (Figure 8).

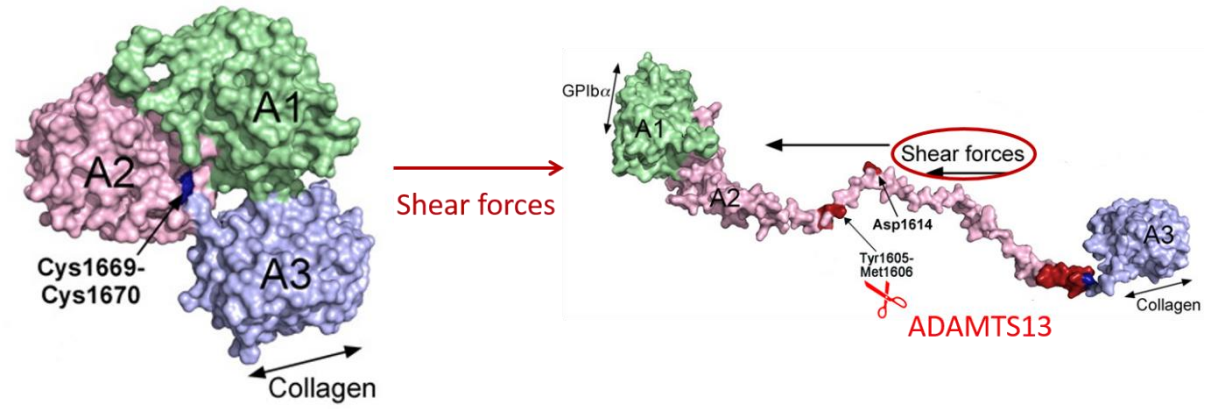

Figure 8: Unfolding and activation of VWF.

In normal physiologic conditions, VWF is in its globular, folded conformation. Shear stress leads to unfolding, thereby exposing the A1 and A2 domains of VWF. Platelets can bind to the A1 domain; ADAMTS13 can bind and cleave VWF in its A2 domain decreasing the activity of VWF. ***Figure adapted from (45).***

Abbreviations: VWF: von Willebrand Factor; ADAMTS13: a disintegrin and metalloproteinase with thrombospondin-1 repeat, member 13.

The activity of VWF is determined by its multimeric composition. The largest VWF multimers, ultra-large (UL)-VWF, are the most hemostatically active in binding with blood platelets. These UL-VWF multimers unfold better under high shear rates as

present in arterioles and capillaries and can spontaneously interact with platelets, resulting in intravascular platelet plugs. However, normally ADAMTS13 will cleave, fragment and thereby inactivate VWF to prevent unwanted platelet plug formation (45, 46, 50). The domain structure and functions of ADAMTS13 are described in section 2 of this general introduction.

Besides ADAMTS13, VWF can be cleaved *in vitro* by thrombin, plasmin, proteinase 3, cathepsin G, elastase and granzyme B. However, the significance of these factors for proteolysis of VWF *in vivo* is still questionable (47, 54).

1.3. Types of TTP

TTP is caused by a deficiency or total absence of the VWF cleaving proteinase ADAMTS13 resulting in uncleaved UL-VWF multimers leading to platelet aggregation and microthrombosis, especially in arterioles and capillaries (the microcirculation) (Figure 9). Most TTP patients develop their first TTP episode during adolescence or even later in life. Therefore, it is thought that besides a lack or absence of ADAMTS13, a secondary triggering factor generating shear stress or endothelial activation is needed to evoke acute TTP. Known triggers are pregnancy, alcohol abuse, HIV, surgery, etc. (55). However, in most cases the trigger remains undiscovered, and therefore the exact etiology of TTP is still unknown.

The two main types of TTP are the congenital and acquired form. Congenital TTP, also known as Upshaw-Schulman Syndrome, is provoked by a recessively inherited mutation in the ADAMTS13 gene resulting in disturbed synthesis, secretion or activation of the proteinase. Consequently, ADAMTS13 activity is severely reduced. Notwithstanding that there are more than 140 different mutations in the ADAMTS13 gene described, congenital TTP is extremely rare and represents less than 5% of all TTP cases (56). Patients with congenital TTP generally develop their first attack in

early childhood and tend to relapse, but in uncommon cases the disease state remains undetected until adolescence. Acquired TTP, on the other hand, is the most common form of TTP and is caused by autoantibodies directed against ADAMTS13, thereby clearing it from the circulation or inhibiting its function. Thus, acquired TTP is an autoimmune disease. The predominant binding sites for the antibodies are the spacer and cysteine-rich domains of ADAMTS13 (45). Acquired TTP may be secondary to specific conditions such as pregnancy, infections, certain pharmacological therapies, autoimmune diseases and alcohol abuse, but is usually idiopathic (55).

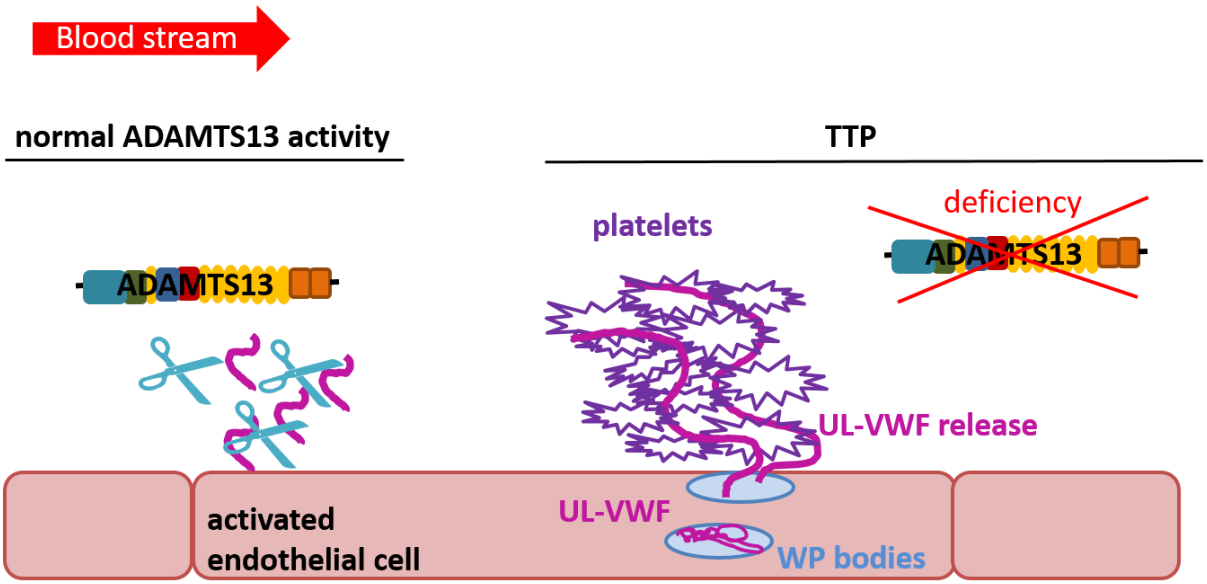

Figure 9: Pathophysiology of TTP.

Triggering factors may activate the endothelium, resulting in release of platelet activating factors and UL-VWF from the WP bodies. When ADAMTS13 activity is normal, the UL-VWF multimers will be cleaved and inactivated. However, in TTP, ADAMTS13 is deficient or absent. Consequently, the UL-VWF multimers will not be cleaved and remain hyperactive leading to platelet binding and activation, which results in the formation of VWF/platelet-rich blood clots especially in the microcirculation where the shear stress is highest. *Figure based on (56).* Abbreviations: UL-VWF: ultra-large von Willebrand Factor multimers; WP: Weibel Palade; ADAMTS13: a disintegrin and metalloproteinase with thrombospondin-1 repeat, member 13; TTP: thrombotic thrombocytopenic purpura.

1.4. Diagnosis and treatment of TTP

As already mentioned above, TTP is originally characterized by a pentad of symptoms, more specifically: severe thrombocytopenia (< 50 000 platelets/µL of blood), microangiopathic hemolytic anemia (formation of microthrombi, schistocytes in blood smears and a low hematocrit), fever, neurological signs and kidney failure. These five symptoms are not always present altogether, and TTP also shows overlap with other TMA's. However, the sooner the treatment is started, the better the prognosis will be (55). Therefore, when a patient presents with severe thrombocytopenia and signs of hemolytic anemia, the patient should be diagnosed for TTP and treatment should be started immediately without unnecessary delay. Plasma, serum and blood cells are to be checked for ADAMTS13 and VWF levels. Since TTP is a rare disease, it is not always easy to recognize and is therefore a challenging hematological emergency. Nowadays, the overall survival rate of a TTP episode is over 80%, but 40% of the patients will relapse with possibly a fatal outcome (57).

Congenital TTP is treated by plasma infusion therapy in which 20-40 mL/kg body weight of fresh frozen donor plasma is infused, thereby administering donor ADAMTS13. Acquired TTP cannot be treated by plasma infusion therapy, because the administered donor ADAMTS13 would be neutralized by the autoantibodies. Consequently, plasma exchange therapy will be used instead in order to remove the autoantibodies. The plasma infusion or exchange therapy for, respectively, congenital or acquired TTP is given on a daily basis until platelet counts and lactate dehydrogenase (LDH) activity levels (marker of organ damage related to microthrombosis) normalize, and signs of hemolysis and organ damage improve (55).

Other options to treat acquired TTP are immunosuppressive therapy to limit further synthesis of autoantibodies, or Rituximab, a monoclonal antibody against the CD20

antigen of B-cells to destroy the antibody producing B-cells. Rituximab is now generally used in patients that do not react well to treatment and occasionally even as first line therapy. For patients with refractory or frequently relapsing TTP, splenectomy could also be helpful (55, 57).

TTP therapy should be improved further to ameliorate the response rate in TTP episodes and prevent relapses. Therefore, international clinical trials are currently performed to evaluate new therapeutics such as Caplacizumab. This nano-body against the A1 domain of VWF (in a phase two clinical trial) prevents binding of platelets to VWF (58). Another very promising treatment is recombinant ADAMTS13 (rADAMTS13) that can substitute the deficient or inhibited proteinase (59).

1.5. Animal models for TTP

As the exact etiology of TTP is still unclear, animal models are of great value to investigate the etiology of this rare disease, and thereby develop new, more specific treatments or strategies to prevent TTP (60).

1.5.1. Mouse models

The first ADAMTS13 deficient (*Adamts13*$^{-/-}$) mouse was generated by Motto *et al*. in 2005 (61). Exons 1-6 of the ADAMTS13 gene were replaced by a neomycin resistant cassette in a mouse on a C57BL/6J and 129X1/SvJ mixed genetic background. Despite complete loss of ADAMTS13 activity, this *Adamts13*$^{-/-}$ mouse was healthy and did not show any signs of TTP. Another research group developed an *Adamts13*$^{-/-}$ mouse on a pure 129/Sv background by eliminating exon 3-6 of the ADAMTS13 gene. Similar to the *Adamts13*$^{-/-}$ mice on the mixed background, ADAMTS13 activity was completely lost, but the mice were healthy (62). Thus, deficiency of ADAMTS13 is not sufficient to develop TTP symptoms in mice.

Interestingly, mice on a CASA/Rk background have 5- to 10-fold higher VWF levels as compared to mice on a mixed C57BL/6J and 129X1/SvJ background (63). In this context, Motto *et al.* tried to improve their *Adamts13*$^{-/-}$ mouse TTP model by backcrossing it into the CASA/Rk background and thereby obtaining higher VWF levels that could induce TTP. However, even though some mice showed a lower platelet count and reduced survival, spontaneous TTP development was exceptional (61).

In a following step, based on the second hit theory for evoking an acute TTP event, several triggering factors were suggested to elicit TTP symptoms in genetically predisposed *Adamts13*$^{-/-}$ mice. For instance, infection with bacterial Shigatoxin (Stx), produced by *Shigella dysenteriae* and *Escherichia coli,* can cause Hemolytic Uremic Syndrome (HUS), which shows similarities with TTP. Injection of Stx in *Adamts13*$^{-/-}$ mice in a CASA/Rk background induced TTP-like symptoms such as severe thrombocytopenia, severe anemia, microangiopathic hemolytic anemia and VWF-rich thrombi in the microcirculation. However, these signs were not present in all mice that were treated with the toxin (61). Another TTP triggering factor in mice is high dose (2000 U/kg) recombinant human VWF (rVWF) containing highly active UL-VWF multimers. Intravascular injection of this rVWF resulted in severe thrombocytopenia in all treated animals, a decreased hematocrit, increased LDH activity indicating organ damage and schistocytes in the blood smears. Nevertheless, none of the animals died since end-stage TTP was not attained (64).

1.5.2. Baboon model

Baboons are non-human primates, and when injected with neutralizing monoclonal ADAMTS13 antibodies (3H9, inhibitory monoclonal anti-ADAMTS13 antibody directed against a metalloproteinase epitope; 5C11 non-inhibitory anti-ADAMTS13 antibody directed against the second thrombospondin-1 (TSP-1) repeat as control antibody) can

serve as model for acquired TTP. Administration of the antibody resulted in ADAMTS13 activity levels below the detection limit (< 5%) and the baboons suffered from severe thrombocytopenia and hemolytic anemia. In addition, they had increased LDH levels, schistocytes in their blood smears and microthrombi in the microvasculature. However, since none of the animals died, it was defined as early stage TTP (65).

2. ADAMTS13

ADAMTS13 is a constitutively active Zn^{2+}- and Ca^{2+}-dependent metalloproteinase (66). It is produced and secreted by the hepatic stellate cells (67) and to a lesser extent by vascular endothelial cells (68). ADAMTS13 is able to cleave VWF, its only known substrate, in the A2 domain, more specifically between amino acid 1605 (Tyr) and 1606 (Met).

2.1. Domain structure

ADAMTS13 is a glycoprotein with a plasma concentration of 1 µg/mL and a half-life of 2-3 days in man. It consists of different domains: the metalloproteinase (MP), disintegrin (D), cysteine-rich (Cys), spacer (S), TSP-1 repeat (TSR) and 2 CUB (Complement component C1r/C1s, Urinary epidermal growth factor (Uegf), and Bone morphogenic protein-1) domains (Figure 10) (69). The interaction of the MP-D-TSP-1-Cys-S domains with VWF is well described, but the role of the C-terminal tail domains (7 TSP-1 and 2 CUB domains) is still largely unknown. The MP domain is the catalytic domain, whereas the D-TSP-1-Cys-S domains are especially involved in the correct positioning of ADAMTS13 on VWF. The MP-D-TSP-1-Cys-S domains as such can degrade VWF multimers *in vitro* and *in vivo* to the same extent as the complete ADAMTS13 proteinase. However, deletion of the Cys or S domain markedly decreases the ADAMTS13 activity (70). In humans, but not in mice, it is believed that the distal

domains inhibit the MP domain until it is bound to unfolded VWF that will support its own destruction by activating ADAMTS13 (71). VWF strings are UL-VWF multimers secreted from the endothelium that remain anchored to the activated endothelial cell surface. These multimers can unravel due to shear stress and bind to platelets, resulting in string-like structures that wave in the direction of the flow (47). The proteolysis of these strings is regulated positively by the TSR2-8-CUB domains, probably because these domains can serve as docking site for VWF multimers (70).

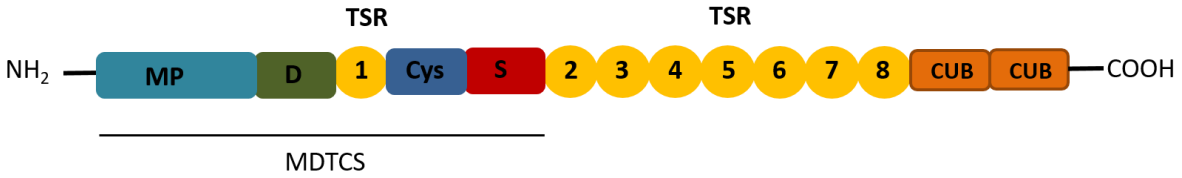

Figure 10: Domain structure of ADAMTS13.
The VWF cleaving proteinase ADAMTS13 is built of different domains: metalloproteinase, disintegrin, cysteine-rich, spacer, TSP-1 repeat and 2 CUB domains.
Abbreviations: MP: metalloproteinase; D: disintegrin; Cys: cysteine-rich; S: spacer; TSR: thrombospondin-1 repeat; CUB: Complement component C1r/C1s, Urinary epidermal growth factor (Uegf), and Bone morphogenic protein-1.

2.2. Functions of ADAMTS13

ADAMTS13 is able to bind to VWF in its globular form, but cannot cleave it because the A2 domain is buried in the globular conformation. Therefore, cleavage is only possible when VWF is in its active, unfolded conformation (72). Moreover, the A2 domains in the middle of a larger VWF multimer are more prone to unfolding due to shear stress and therefore to cleavage by ADAMTS13, as compared to shorter VWF multimers or non-centered A2 domains of the multimers (73). Due to its potential to cleave VWF, ADAMTS13 has anti-thrombotic capacities.

There is no known specific inhibitor of ADAMTS13 and the proteolytic activity is dependent on the availability of the VWF cleavage site. ADAMTS13 cleaves unfolded

VWF in circulation, at sites of platelet clot formation and newly secreted VWF from endothelial cells (45). Thrombin and collagen, both present upon vessel damage and coagulation, counteract cleavage of VWF by ADAMTS13, thereby allowing clot formation. VWF can easily bind to the exposed collagen, unfolds in response to shear stress and activates platelets leading to stable clot formation. Additional platelets will be recruited and activated independently of VWF and can therefore become resistant to the effects of ADAMTS13-regulated cleavage of VWF. The platelet plug grows, but formation occurs more efficiently in presence of collagen and thrombin, which are only present at the site of injury. Therefore, beyond the injury, VWF-platelet binding is less pronounced, probably allowing efficient cleavage of VWF by ADAMTS13. Thus, platelet plug growth remains restricted to the site of vessel damage (45). In contrast, large VWF multimers present in the circulation can unfold naturally. However, since collagen and thrombin are absent in this situation and ADAMTS13 will cleave the unraveled VWF multimer in the A2 domain, the formation of platelet-rich microthrombi is prevented (45).

High VWF/ADAMTS13 ratios are of significant importance in stroke development. Recently it was shown that rADAMTS13 could be administered as pontential pharmacological therapy in stroke, especially in tPA resistant cases. Ischemic stroke thrombi are indeed VWF-rich. Thus, in an *Adamts13*$^{-/-}$ mouse model with VWF-rich thrombotic occlusion, administration of rADAMTS13 led to recanalization of the occluded vessel, implying thrombolytic potential of the proteinase (74).

UL-VWF multimers are important in thrombus formation, but also play a role in inflammation. Thrombosis and inflammation share an analogous first step in which VWF is involved: platelet adhesion. Thus, apart from its antithrombotic role, ADAMTS13 affects inflammatory-related processes: it prevents rolling of leukocytes in

unstimulated veins, and decreases adhesion and extravasation of leukocytes in inflammatory conditions (75, 76).

ADAMTS13 is part of the ADAM/ADAMTS family that consists of 21 ADAM and 19 ADAMTS proteinases. They can regulate cell adhesion and migration (disintegrin domain) and degrade extracellular matrix components (metalloproteinase domain), and consequently play a role in cell proliferation and angiogenesis (77). TSP-1 domains, however, inhibit angiogenesis. *In vitro*, rADAMTS13 as such has pro-angiogenic capacities, but after addition of vascular endothelial growth factor (VEGF), VEGF-induced angiogenesis is inhibited by ADAMTS13 due to the TSP-1 domains that affect VEGF receptor (VEGFR) 2 phosphorylation (78, 79). Thus, the angiogenic capacities of ADAMTS13 depend on its TSP-1 repeats, that can mediate pro- or anti-angiogenic effects on VEGF levels and VEGFR2 phosphorylation (76).

2.3. Plasmin as backup for ADAMTS13

Probably because of oscillating ADAMTS13 levels, TTP is a disease characterized by recurrent acute episodes of microangiopathic hemolytic anemia alternated by periods of remission. Strikingly, human subjects with very low levels or complete absence of ADAMTS13 activity can present without symptoms of microangiopathy, suggesting that other factors can compensate for ADAMTS13 (80). Plasmin, the protagonist of fibrinolysis, is proposed as a candidate for ADAMTS13 substitution to degrade platelet/VWF complexes during thrombotic microangiopathic episodes (81). *In vitro*, plasmin is able to cleave VWF, but in human subjects, the results are less clear. During an acute TTP episode in patients, plasma plasmin-α2-antiplasmin (PAP) complexes, a measure of plasminogen activation, are increased predominantly in patients with severe microangiopathy and undetectable ADAMTS13 activity. This implies that thrombolysis is increased in TTP patients, which is rather counterintuitive. It was

hypothesized that hypoxia, resulting from microthrombi, triggers plasminogen activation on the endothelium of ischemic tissue. Consequently, VWF degradation by plasmin leads to destruction of the microthrombi and clinical symptoms will not develop. Only when microthrombi formation exceeds the endogenous plasmin formation, TTP symptoms will appear due to the inability to clear the obstructions (54, 81).

3. Obesity

3.1. Definition and prevalence of obesity

According to the World Health Organization (WHO), obesity is defined as an excessive accumulation of adipose tissue impairing health. The body mass index (BMI) is calculated as weight (kg) divided by the square of the length (m^2) and is the most used index to classify obesity (Table 2) (82).

Table 2: WHO classification of BMI.

BMI (kg/m^2)	**classification**
<18.5	Underweight
18.5-24.9	Healthy, normal
25-29.9	Overweight
30-34.9	Obese class I
35-39.9	Obese class II
≥ 40	Obese class III or morbidly obese

The BMI does, however, not correspond to the same degree of fatness in different individuals, because it cannot distinguish weight associated with muscle from weight associated with fat (83). Hence, other indices such as waist-to-hip ratio (WHR), waist circumference (WC) and waist-to-height ratio (WHtR) are also used (84-87). The WC is an integral feature to diagnose the metabolic syndrome (88, 89), which is a cluster

of metabolic disorders that enhance the risk of heart disease, impaired glucose tolerance and insulin resistance (90).

Obesity is a multifactorial disease, as both genetic and environmental factors play a role in its etiology (91). However, the WHO reported that dietary and nutritional changes, especially the increased intake of foods rich in fat and sugar, in combination with a sedentary lifestyle are the major causes of the obesity pandemic. The most recent data state that worldwide more than 1.9 billion adults are overweight and 600 million people are obese (June 2016) (82). The obesity problem is not confined to Western societies, but has a global impact, even touching continents threatened by starvation (92).

In 2010, 54% of the Belgian adults were overweight and 15% were obese; in 2014, the mean BMI of a Belgian adult was 25.5 kg/m² and 21% of the Belgian adults were obese. In 2012, 21% of Belgian children between 10 and 12 years old were overweight (93). Obesity has become the second most important cause of early death, after smoking. In the USA 112,000 people die from obesity-related causes every year (94).

As a consequence, the health care costs related to overweight, obesity and comorbidities are substantial (95). In Western European countries, the estimated obesity-related health care costs range from 0.09% to 0.61% of total annual gross domestic product (GDP). The highest annual costs were reported in Germany and corresponded to 10.4 billion Euros in 2002 (96). Similar data were reported in studies from Canada and New Zealand, where obesity-related costs ranged from 0.2% to 0.6% of the GDP (97-99). In the future, further increases are expected.

3.2. (White) adipose tissue

Obesity is characterized by an excessive accumulation of adipose or fat tissue. Adipocytes form 90% of the adipose tissue volume, but only 20-40% of the cellular content (100). In addition to adipocytes, fat tissue consists of the stromal vascular fraction (SVF) containing pre-adipocytes, fibroblasts, vascular smooth muscle cells, endothelial cells, neurons, macrophages and lymphocytes. There are different types of adipose tissue including brown and beige (101), but the white adipose tissue (WAT) is the most abundant.

3.2.1. Unlimited growth potential of white adipose tissue

WAT protects the internal and delicate organs from mechanical stress and functions as insulator against heat loss. However, its most important function is its role in nutritional homeostasis, especially as energy storing organ. When energy intake exceeds expenditure, the excess of energy is stored in white adipocytes in the form of triglycerides. The storing capacity of white adipocytes for lipids has an almost unlimited potential, which is a unique feature in comparison with other organs. Adipocytes have a unilocular morphology and are able to grow. The latter process is called hypertrophy and thereby adipocytes can have various sizes (25-200 µm in diameter). Apart from growing adipocytes, adipose tissue mass can also increase by *de novo* formation of mature adipocytes differentiated from committed pre-adipocytes, a process known as hyperplasia (101). In order to expand, adipocytes need to be in close proximity to at least one blood vessel for the supply of oxygen, nutrients and fatty acids from the blood stream and for the elimination of waste products. Therefore, new blood vessels are formed from pre-existing blood vessels (angiogenesis) in obese adipose tissue (102).

Especially hypertrophy is related with cardiometabolic risks, insulin resistance and hepatic fibrosis (103). However, 30% of obese subjects are metabolically healthy.

These “benign obese” people have smaller adipocytes than metabolically unhealthy subjects of comparable weight, and the size of adipocytes correlates with insulin sensitivity. Thus, adipocyte size may be more important than adipose tissue mass for the metabolic health profile of obese people (104).

3.2.2. Inflammatory state of obese adipose tissue

Adipose tissue produces and secretes bioactive proteins, called adipokines, including leptin, adiponectin and tumor necrosis factor-α (TNF-α) into the circulation and thus functions as an endocrine organ regulating metabolism and inflammation. Because of these endocrine mediators, the adipose tissue can interact and communicate with other organs, such as the pancreas, liver and muscle thereby controlling glucose metabolism, insulin sensitivity, immunological processes etc. (105).

In obese individuals, leptin levels are increased in parallel with body fat mass, while adiponectin levels are negatively correlated with adipose tissue mass. In contrast to most other adipokines, adiponectin exerts anti-inflammatory actions (106). The lower levels of adiponectin in obesity are important in the development of insulin resistance since it is an insulin-sensitizing hormone. It stimulates release of anti-inflammatory cytokines e.g. IL-4 and IL-10, and inhibits phagocytotic activity and production of TNF-α in macrophages, the differentiation of monocyte precursors, and the formation of foam cells (related to cardiovascular disease). Leptin is a satiety hormone that can sense the state of energy storage in the body and stimulate satiety or energy expenditure. It is a pro-inflammatory adipokine stimulating monocyte proliferation and differentiation into macrophages and induces the production of pro-inflammatory cytokines such as TNF-α, IL-6 and IL-8 (107).

Due to the presence of immune cells (especially leukocytes), cytokines and chemokines including TNF-α and IL-6 are prominent in adipose tissue. These

cytokines can be pro- or anti-inflammatory. The majority of these cytokines is produced by adipose tissue resident macrophages of which there are two main groups, the M1 or pro-inflammatory classically activated and M2 or anti-inflammatory alternatively activated macrophages. M1, but particularly M2 macrophages are present in lean adipose tissue. However, while becoming obese there is a switch to a greater M1/M2 ratio, as the amount of M1 macrophages increases whereas the number of M2 macrophages remains unchanged (108). Moreover, other white blood cells such as neutrophils, B- and T-cells also produce pro-inflammatory cytokines in obese adipose tissue. Consequently, obesity is characterized by a chronic low-grade pro-inflammatory state of the adipose tissue.

The pro-inflammatory state is maintained by the combination of an excessive uptake of saturated fatty acids (SFA) from the diet, oxidative stress and hypoxia coming together in a vicious circle (Figure 11). Lean adipose tissue has mainly anti-inflammatory capacities due to M2 macrophages and anti-inflammatory adipokines as adiponectin and IL-10. An excess of nutrients, as often seen in obesity, leads to increased release of free fatty acids (FFA) of which especially the SFA are involved in inflammation. SFA bind to Toll-like receptors (TLR) on macrophages leading to secretion of pro-inflammatory cytokines and increase in leptin production (109). Furthermore, the excess of nutrients and subsequent cell expansion (hypertrophy) in obesity causes cellular stress leading to the production of reactive oxygen species (ROS) and stronger activation of pro-inflammatory pathways. Moreover, macrophages are attracted to these stressed adipocytes and recruited into the white adipose tissue, which will lead to enhanced production of pro-inflammatory cytokines. Furthermore, stressed adipocytes are dysfunctional and can go into apoptosis leading to formation of crown-like structures (CLS), which are dead adipocytes surrounded by

macrophages. Altogether, this leads to enhanced stress, adipocyte death and further stress signaling (110, 111). Despite obesity-related angiogenesis, the vascular availability for adipocytes can still be limited due to extreme expansion of the adipose tissue leading to hypoxia. This causes increased leptin, decreased adiponectin, lactate production and ultimately adipocyte apoptosis. Consequently, macrophages are recruited to the hypoxic areas resulting in a higher level of inflammation, stressed and dysfunctional adipocytes (112). Since apoptosis of adipocytes plays a major role in development of insulin resistance and hepatic steatosis, inflammation of white adipose tissue resulting from excess of SFA, oxidative stress and hypoxia, is involved in the development of metabolic disorders, thus comorbidities related to obesity (113).

3.2.3. Anatomical location of white fat is of considerable concern

Fat depots are anatomically localized at different regions in the body and therefore have different characteristics. A major distinction is made between subcutaneous (SC) and visceral adipose tissue. However, visceral adipose tissue can be further subdivided into, among others, gonadal (GN), mesenteric, retroperitoneal, epicardial and omental fat. Interestingly, visceral fat depots are distinct in humans and rodents. Whereas the epididymal fat mass is considerable and the omental fat hardly exists in mice, these depots are nonexistent and well represented, respectively, in human visceral fat (114). However, in both rodents and men, visceral adiposity, in contrast to SC fat, is associated with a metabolically unhealthy profile.

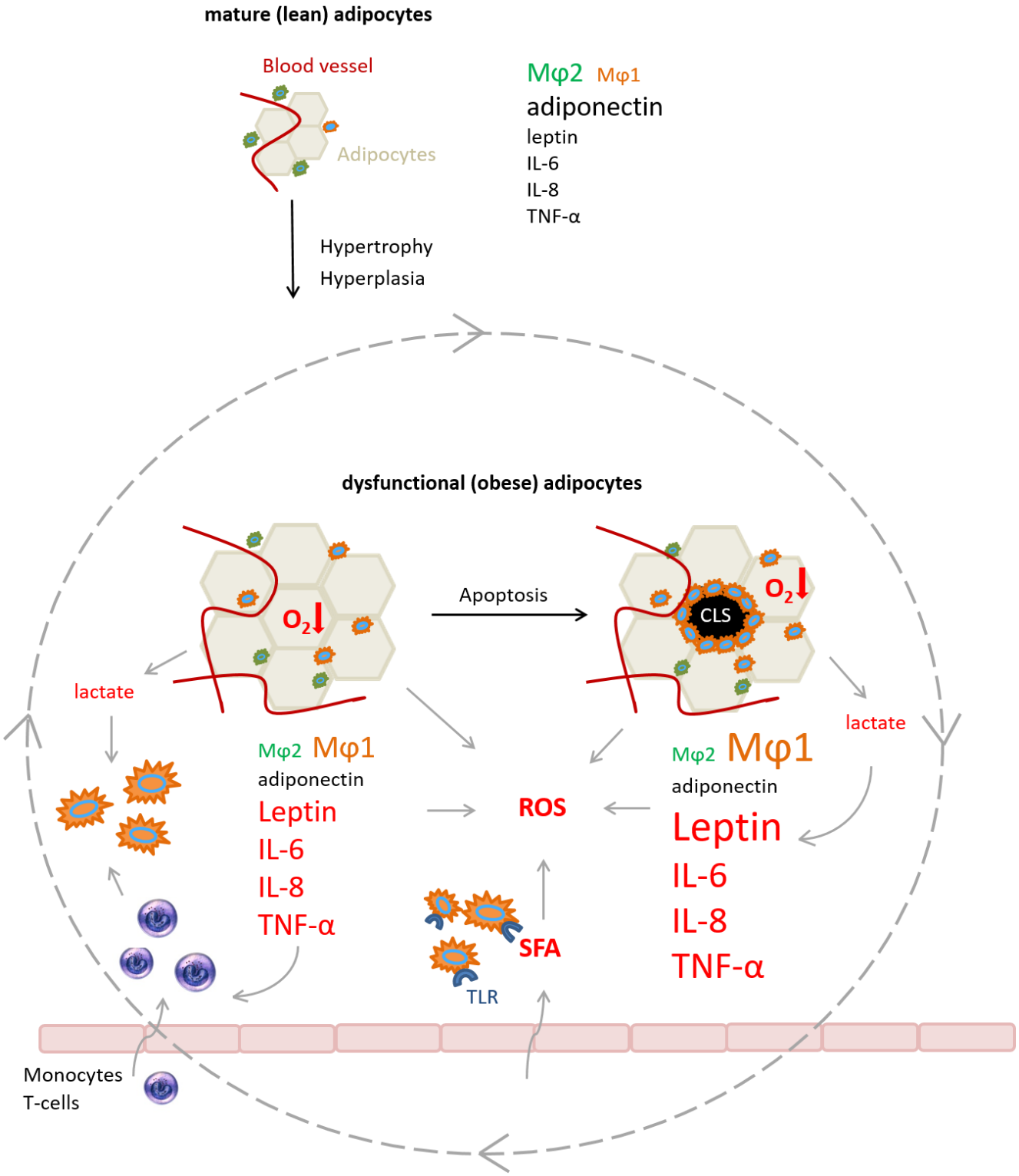

Figure 11: Obesity, a state of low-grade chronic inflammation in the adipose tissue.
Lean adipose tissue contains low levels of pro-inflammatory IL-6, IL-8, TNF-α and leptin, whereas adiponectin levels are relatively high (font size corresponds to amount). Resident macrophages are primarily anti-inflammatory M2 macrophages (green). While becoming obese, adipocytes grow (hypertrophy) and increase in number (hyperplasia). Moreover, new blood vessels will

develop (angiogenesis) to supply the new and larger adipocytes with nutrients and oxygen (O_2). However, local hypoxia ($O_2\downarrow$) can still occur leading to lactate production. Together with an excess of saturated fatty acids (SFA) from the diet and the development of oxidative stress, this leads to the activation of pro-inflammatory pathways. Leptin production increases and pro-inflammatory M1 macrophages (orange) are attracted to the adipose tissue thereby secreting cytokines and chemokines. The obese adipocytes become dysfunctional causing more stress and inflammation resulting in apoptotic adipocytes and formation of crown-like structures (CLS) that will lead to further inflammation and stress. Therefore, obesity is a condition of low-grade chronic inflammation of the adipose tissue in which the adipocytes are trapped in a vicious circle of pro-inflammatory macrophage chemotaxis, cytokine production and stress.
Abbreviations: Mφ1: pro-inflammatory classically activated M1 macrophages; Mφ2: anti-inflammatory alternatively activated M2 macrophages; IL: interleukin; TNF-α: tumor necrosis factor-α; ROS: reactive oxygen species; SFA: saturated fatty acids; TLR: Toll-like receptors; CLS: crown-like structures.

Visceral and SC depots show differences in adipokine production and secretion, inflammatory profile and adipocyte behavior (115). For instance, more infiltration of macrophages and lower secretion of the anti-inflammatory adipokine adiponectin is observed in obese visceral fat, leading to a more pro-inflammatory profile as compared to SC adipose tissue. Furthermore, adiposity is reduced and glucose homeostasis improved when SC adipose tissue is transplanted to the visceral area, indicating that SC fat has potentially favorable metabolic effects (116).

3.3. Comorbidities

Obesity is associated with a variety of life-threatening comorbidities, including cardiovascular diseases, insulin resistance and type 2 diabetes, non-alcoholic fatty liver disease (NAFLD), cancer and respiratory diseases.

Normally, fat storage is limited to the adipose tissue, but in obesity, the overload of fat will also accumulate in other organs throughout the body. This ectopic lipid deposition can give rise to organ dysfunction, as in NAFLD and insulin resistance.

NAFLD is a spectrum of diseases ranging from fat accumulation in the liver (liver steatosis) to non-alcoholic steatohepatitis (NASH). Liver steatosis mostly persists without symptoms and thus remains unnoticed. NASH is characterized by inflammation, hepatocellular injury and fibrosis and is therefore a risk for liver cirrhosis and cancer (117). However, subjects suffering from NASH develop cardiovascular diseases sooner and more frequently than the liver-related side effects. NAFLD is the most frequent liver disease in Western countries and is considered the hepatic manifestation of the metabolic syndrome of which the risk factors are very similar. More specifically, insulin resistance, type 2 diabetes, central obesity and dyslipidemia are the major players in development of NAFLD as well as of the metabolic syndrome (118).

Fat accumulation in the liver, but also in muscle and pancreas, is linked to insulin resistance. Insulin is released from β-cells in the pancreas after nutrient ingestion and is the major regulator of glucose homeostasis. It decreases appetite and stimulates storage and uptake of energy, whereas the breakdown of macromolecules to glucose as well as *de novo* glucose production in the liver is blocked. Insulin resistance is one of the most common comorbidities related to obesity. The β-cells are still capable to produce and secrete sufficient insulin, but the cells are unable to react to the hormone resulting in hyperglycemia. As a response, β-cells increase their insulin secretion, FFA are released from the adipose tissue, production of FFA and hepatic glucose increases, glucose uptake by skeletal muscles is decreased, and β-cells become eventually dysfunctional (119, 120) and type 2 diabetes develops. Furthermore, insulin resistance together with hypercholesterolemia, ectopic fat deposition in the heart and blood vessels, endothelial dysfunction and an inflammatory state as seen in obesity are risk factors for cardiovascular diseases related to atherothrombotic events (121).

Since human platelets express insulin receptors, insulin has an anti-aggregating function in insulin-sensitive subjects, while in insulin-resistant conditions as obesity, the anti-aggregating effects are largely reduced (122). Moreover, in obese subjects, platelet activation, thrombin and fibrinogen levels are increased. Because of coronary artery disease as seen in many obese people, other coagulation factors and anti-fibrinolytic agents, such as TF and PAI-1 are also enhanced, resulting in increased clot formation. Therefore, obesity is a pro-thrombotic state, as a consequence of the obesity-related insulin resistance and inflammation (123).

4. Obesity as risk factor for TTP

The exact etiology of TTP is still unclear. It is generally accepted that mostly ADAMTS13 deficiency plays an important part in the pathophysiology of TTP, but a second triggering event is needed to evoke an acute TTP episode. Recent data suggest that obesity might be such a triggering event and therefore might be a risk factor for TTP.

Multiple independent studies indicated that ADAMTS13 and obesity could possibly interact. Firstly, ADAMTS13 plasma antigen levels and BMI are positively correlated in humans, as observed in a case-control study of patients with myocardial infarction (124). Furthermore, ADAMTS13 expression levels in the liver are higher in obese as compared to lean mice (125). Thus, both in humans and in mice, ADAMTS13 antigen levels and body weight are positively correlated.

As explained above, obesity is a state of chronic inflammation and is, in addition, described as a potential risk factor for TTP development, while ADAMTS13, on the other hand, has anti-inflammatory capacities (75). Since body weight and ADAMTS13 levels are positively correlated, this is rather paradoxical. Furthermore, it would be expected that an increase of ADAMTS13 would protect against TTP and thus that

obesity would be protective against TTP instead of being a risk factor. However, despite these contradictions, there are several indications that obesity is indeed a risk factor for TTP, as observed in the Oklahoma TTP cohort study. This is a population-based inception cohort of 376 patients recruited from 1989 to 2008, with an initial TTP episode that required plasma exchange. This study showed that the prevalence of obesity, especially morbid obesity (BMI of at least 40 kg/m²) was increased in TTP patients (126). Furthermore, half of the patients with severe ADAMTS13 deficiency were obese. Thus, the relative frequency of obesity increased in patients diagnosed with TTP and TTP patients with ADAMTS13 levels lower than 10% were more obese (127). In addition, obesity was associated with TTP development and identified as an independent risk factor for TTP with an odds ratio of 7.6 in a retrospective study with 108 TTP patients (128). In the context of acquired TTP, Lombardi *et al.* found (non-inhibitory) autoantibodies against ADAMTS13 in obese subjects stating that obesity could be a risk factor for acquired TTP (129).

The pathophysiological mechanisms regulating the interaction between obesity and TTP remain, however, unknown.

Chapter 2

Aims of the study

The exact etiology of TTP remains unclear. It is thought that a (genetic) predisposition is underlying TTP development, but that an extra, undefined trigger is required to evoke an acute TTP episode. Despite some controversies, there is evidence that obesity is a possible risk factor for TTP. Moreover, since ADAMTS13 levels and BMI are positively correlated, ADAMTS13 (mainly produced and secreted by the liver) could play a role in adipose tissue expansion. In this project:

1. We investigated whether ADAMTS13 is involved in adipose tissue expansion. Therefore, we kept wild-type (WT) and ADAMTS13 deficient (*Adamts13*$^{-/-}$) mice on a diet high in fat and sugar (HFD) to nutritionally induce obesity, or on a standard diet (SFD) (Chapter 3).
2. We studied whether ADAMTS13 deficiency and obesity are synergistic risk factors for microthrombi formation in the liver, and whether plasmin could compensate for the absence of ADAMTS13 in *Adamts13*$^{-/-}$ mice (Chapter 4).
3. We investigated a potential role for ADAMTS13 in liver steatosis in two different mouse models for NAFLD, i.e. a diet-induced obesity model (Chapter 4) and a steatosis model induced by a diet deficient in methionine and choline (Chapter 5).
4. We evaluated whether obesity is indeed a risk factor for TTP and explored potential underlying mechanisms (Chapter 6).
5. We tried to develop a new murine TTP model by using obese *Adamts13*$^{-/-}$ mice. A new animal model for TTP would be very useful to further unravel the pathophysiology or etiology of TTP, thereby identifying triggering factors, and to develop potential strategies for treatment/prevention of acute TTP episodes (Chapter 6).

Chapter 3

No functional role of ADAMTS13 in adiposity in mice

Published paper

Geys L, Scroyen I, Roose E, Vanhoorelbeke K, Lijnen HR. ADAMTS13 deficiency in mice does not affect adipose tissue development. Biochimica et Biophysica Acta – General Subjects. 2015; 1850(7):1368-1374.

ABSTRACT

Background: BMI and ADAMTS13 levels are positively correlated in man. Development of obesity is associated with angiogenesis and inflammation, and increased ADAMTS13 synthesis in the liver.

Methods: Male wild-type (WT) and ADAMTS13 deficient *(Adamts13$^{-/-}$)* mice were kept on normal chow (SFD) or high fat diet (HFD) for 15 weeks.

Results: HFD feeding of WT mice resulted in significantly enhanced levels of ADAMTS13 antigen and activity as compared to SFD feeding. ADAMTS13 deficiency had no significant effect on body weight gain, subcutaneous (SC) or gonadal (GN) adipose tissue mass, or on adipocyte size. In GN fat of obese (HFD) *Adamts13$^{-/-}$* mice, adipocyte density was higher and blood vessel density lower as compared to obese WT mice. No marked effects of genotype were observed on mRNA expression of adipogenic, endothelial, inflammatory or oxidative stress markers in adipose tissue. Analysis of metabolic parameters and of glucose and insulin tolerance did not reveal significant differences between both obese genotypes, except for higher adiponectin and cholesterol levels in obese *Adamts13$^{-/-}$* as compared to WT mice.

Conclusion: Our data do not support a functional role of ADAMTS13 in adiposity, nor in associated angiogenesis or inflammation in mice.

General significance: ADAMTS13 deficiency may cause thrombotic thrombocytopenic purpura (TTP). Obesity, which is associated with enhanced ADAMTS13 levels, is nevertheless considered an independent risk factor for TTP. To resolve this apparent contradiction, we show that ADAMTS13 does not directly promote development of adipose tissue in a mouse model.

INTRODUCTION

Metabolic disturbances such as obesity and diabetes and their associated complications are a main cause of mortality and morbidity. Development of adipose tissue is a complex process in which extensive modifications occur in adipogenesis, angiogenesis and proteolytic remodeling of extracellular matrix (1). Matrix metalloproteinases are known to play a role in these processes, but little is known on a potential contribution of related classes of proteinases (2, 3).

ADAMTS13 (a disintegrin and metalloproteinase with thrombospondin-1 repeat, member 13) is the proteinase that degrades large multimers of von Willebrand Factor in plasma, thereby preventing development of thrombotic thrombocytopenic purpura (TTP), a life-threatening multisystem disease characterized by the formation of microthrombi in capillaries and arterioles (4). It was suggested that obesity may be a risk factor or trigger for acquired TTP (5); obesity is indeed more frequent in the population of TTP patients than in the general population and represents an independent risk factor for TTP (6). In addition, it has been suggested that ADAMTS13 itself may play a role in adiposity. Indeed, ADAMTS13 plasma levels correlate positively with body mass index (7), and its synthesis is significantly increased in the liver of obese mice (8), likely due to low-grade chronic inflammation (9). However, an inhibitory effect of ADAMTS13 on inflammation has been reported in mouse models of atherosclerosis and cerebral ischemia (10, 11). Furthermore, the thrombospondin-1 (TSP-1) domain of ADAMTS proteinases, such as ADAMTS5, has anti-angiogenic properties (12). Indeed, ADAMTS13 inhibits VEGF-induced angiogenesis by binding to VEGF via its TSP-1 domain (13). However, recently Lee *et al.* found ADAMTS13 to have pro-angiogenic features *in vitro* by upregulating VEGF and VEGFR2 (14).

Because of these apparently contradictory data and the known association of angiogenesis and inflammation with obesity, we have investigated a potential role of ADAMTS13 in development of adipose tissue and associated angiogenesis and inflammation, using an established model of diet-induced obesity in WT and ADAMTS13 deficient mice.

MATERIALS & METHODS

Nutritionally induced obesity model

Male *Adamts13*$^{-/-}$ (n = 20) and WT littermates (n = 18) (genetic background, C57Bl6/J x 129X1/Sv x CASA/RK) (15), from the age of 5 weeks on, were kept in individual micro-isolation cages on a 12h day/night cycle and fed for 15 weeks with a HFD (42% kcal as fat, caloric value 22 kJ/g; E15721-34; Ssniff, Soest, Germany) (n = 17) or a standard fat diet (SFD) (13% kcal as fat, caloric value 10.9 kJ/g; KM-04-k12, Muracon, Carfil, Oud-Turnhout, Belgium) (n = 21). Water was always available *ad libitum*. Body weight and food intake were measured at weekly intervals.

The mice were sedated and blood was taken from the retro-orbital sinus on trisodium citrate (0.01 M), before they were killed by cervical dislocation. Inguinal subcutaneous (SC) and intra-abdominal gonadal (GN) adipose tissues were removed and weighed. Portions were used for RNA or protein extraction or were fixed in 1% formaldehyde for histological analysis. Other organs were also removed and weighed.

All animal experiments were approved by the KU Leuven ethical committee (P082-2011) and performed in accordance with the NIH Guide for the Care and Use of Laboratory Animals (1996) and carried out in accordance with the EU Directive 2010/63/EU for animal experiments.

ADAMTS13 determinations

Murine ADAMTS13 antigen levels in plasma were measured using a home-made ELISA. A 96-well microtiter plate was coated overnight with the in-house developed murine anti-mADAMTS13 monoclonal antibody 20A10 at 5 µg/ml in PBS. After blocking, plasma was diluted in PBS, 0.3% (m/v) skimmed milk and the plate was incubated at 37°C for 1h. An in-house developed polyclonal rabbit anti-mADAMTS13

(5 µg/ml) was incubated for 1h. Bound antibody was detected with HRP-labeled goat anti-rabbit antibody (Jackson Immunoresearch Laboratories Inc., West Grove, PA) (1/25,000 in dilution buffer). A pool of normal murine plasma was used as a reference and set as 100% mADAMTS13 antigen.

The activity of murine ADAMTS13 was measured using the FRETS-VWF73 method (16). Briefly, murine ADAMTS13 in plasma (20 µl) was incubated with 2 µM FRETS-VWF73 in a HEPES buffered saline solution (50 mM HEPES, 5 mM $CaCl_2$, 1 µM $ZnCl_2$, 150 mM NaCl, pH 7.4; HBS), containing 1 mg/ml bovine serum albumin (Sigma, St Louis, MO). Digestion of FRETS-VWF by murine ADAMTS13 generates a fluorescent signal that is measured using the FLUOstar OPTIMA reader (BMG Labtech GmbH, Offenburg, Germany). ADAMTS13 mRNA levels in liver extracts were determined by quantitative real-time PCR using the primers and 6-carboxy-fluorescein (FAM) labeled probes, shown in Table 3.

Metabolic and inflammatory parameters

At the end of the diet, blood was obtained from the tail of unanesthetized mice after fasting for 6h. Blood glucose concentrations were measured using the Accu-chek performa meter and blood glucose test strips (Roche Diagnostics, Basel, Switserland). Total and HDL cholesterol levels were evaluated using routine clinical assays. Leptin and adiponectin levels in plasma were determined with specific ELISA's (R&D Systems, Minneapolis, USA).

Extracts of SC and GN adipose tissues were prepared as described (17), and the protein concentration was determined using the BCA protein assay. IL-6 and TNF-α levels in plasma or extracts were measured using commercially available ELISA's (ELISA Ready-SET-Go!, Affymetrix eBioscience, San Diego, CA).

Table 3: Markers detected by qPCR using TaqMan gene expression assays.

Gene	Assay†	Gene	Assay†
GLUT4	Mm00436615_m1	**IL-6**	Mm00446190_m1
PPAR-γ	Mm01184322_m1	**MCP-1**	Mm00441242_m1
Adiponectin	Mm00456425_m1	**Arginase**	Mm00475988_m1
CD36	Mm00432403_m1	**Mannose receptor**	Mm00485148_m1
VEGF-A	Mm00437304_m1	**Catalase**	Mm00437992_m1
VE-cadherin	Mm00486938_m1	**SOD1**	Mm01700393_g1
endoglin	Mm00468256_m1	**GPX1**	Mm00656767_g1
F4/80	Mm00802529_m1	**XDH1**	Mm00442110_m1
TNF-α	Mm00443258_m1	**β-actin**	Mm01205647_g1

	FW primer	RV primer	probe
ADAMTS13	GGAGCCCAAGGATG TGTGTCTT	TCTCTGGAGGTGAG AGGGAGGAT	6FAM CTTGGCCACCATGC

†Assays purchased from Life Technologies (Carlsbad, CA).

Gene expression studies

mRNA expression levels in adipose tissue extracts were determined by quantitative real-time PCR, as described elsewhere (18). qPCR was done in the ABI 7500 Fast Sequence detector (Life Technologies) to detect the markers listed in Table 3. Transcript levels were determined in duplicate by qPCR reaction using a gene expression assay with specific primers, probes and the Fast mastermix (Life Technologies, Carlsbad, CA). Analyses were performed with the ΔΔCT method using the 7500 System SDS software (Life Technologies). Normalization was carried out to correct for fluctuations caused by sample differences. Fold changes were calculated as $2^{-\Delta\Delta CT}$ relative to the mice fed a SFD for the obese mice (effect of diet), and relative to WT mice for the *Adamts13*$^{-/-}$ mice (effect of genotype). β-actin was used as housekeeping gene.

Histological analysis

Paraffin sections (8 µm) for histology were prepared from isolated SC and GN fat pads. The size and density of adipocytes in the SCAT and GNAT were determined by staining with haematoxylin/eosin (H&E) under standard conditions. The blood vessels in the adipose tissues were analyzed by staining with *Bandeiraea simplicifolia* lectin (19). Analyses were performed by using a Zeiss Axioplan 2 microscope with the AxioVision release 4.8 software (Carl Zeiss, Oberkochen, Germany).

Insulin and glucose tolerance tests

In separate experiments, after 10 weeks of HFD, WT and *Adamts13*$^{-/-}$ mice (n = 10 each) were fasted for 6h and a bolus of 0.1 U/kg human insulin (Eli Lilly Benelux S.A., Brussels, Belgium) or 2 mg/g glucose was administered i.p. Blood glucose levels were determined, as described above, before and 30, 60, 90 and 120 minutes after insulin or glucose injection.

Statistics

Data are presented as means ± standard error of the means (SEM). Statistical significance between groups was analyzed with the non-parametric Mann-Whitney U test, one-way or two-way ANOVA. Correlation analysis was performed using the Spearman rank test. Analysis of the data was performed using Prism 6 (GraphPad Software Inc., San Diego, CA). Values of $p < 0.05$ are considered statistically significant.

RESULTS

Effect of ADAMTS13 deficiency on adiposity

Five weeks old *Adamts13*$^{-/-}$ and WT mice had comparable body weight and showed a very similar weight gain when kept on either SFD (lean) or HFD (obese) for 15 weeks (Figure 12A) (Table 4). Food intake over this period was also comparable for both genotypes (Figure 12B).

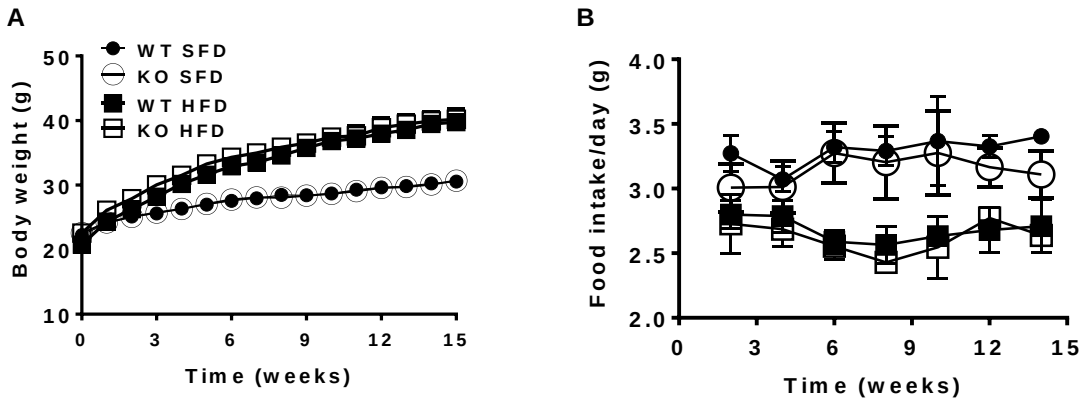

Figure 12: Body weight and food intake of WT and *Adamts13*$^{-/-}$ mice.
Evolution of body weight (A) or food intake (B) of WT (closed symbols) and *Adamts13*$^{-/-}$ (open symbols) mice kept on SFD (circles) or HFD (squares) for 15 weeks. Data are means ± SEM of 8 to 11 experiments in each group. No significant differences were observed between both genotypes (One-way ANOVA).

In plasma of WT mice, significantly elevated levels of both ADAMTS13 antigen and activity were observed after 15 weeks of HFD feeding (Figure 13). ADAMTS13 mRNA expression in the liver was not different between lean or obese WT mice ($p = 0.52$, data not shown). Isolated SC or GN fat mass were not significantly different for WT or *Adamts13*$^{-/-}$ mice on either diet. Adipocytes were markedly enlarged on HFD as compared to SFD, but adipocyte size was similar for both genotypes (Table 4). Adipocyte density in SC adipose tissue was similar for WT and *Adamts13*$^{-/-}$ mice on either SFD or HFD, whereas it was higher in GN fat of obese *Adamts13*$^{-/-}$ versus obese

WT mice (Table 4). The weight of other organs, including liver, heart, spleen, lungs, pancreas, kidneys and hypothalamus was also not different between both genotypes either on SFD or HFD (data not shown).

Table 4: Body weight, adipose tissue mass, adipocyte size and density, blood vessel size and density in GN and SC adipose tissue of WT and *Adamts13*$^{-/-}$ mice fed a SFD or HFD for 15 weeks.

	SFD		HFD	
	WT	***Adamts13*$^{-/-}$**	**WT**	***Adamts13*$^{-/-}$**
n	10	11	8	9
Body weight start (g)	22.3 ± 0.49	22.6 ± 0.65	20.8 ± 0.45	22.4 ± 0.65†
Body weight end [(a)] (g)	31.3 ± 0.48	31.3 ± 0.86	40.9 ± 1.2	40.3 ± 1.7
Body weight gain (g)	8.3 ± 0.28	8.8 ± 0.44	19.8 ± 0.90	17.9 ± 1.3
SC				
weight (mg)	338 ± 15	384 ± 45	1279 ± 80	1096 ± 92
adipocyte size (µm²)	1055 ± 100	1279 ± 156	3092 ± 312	2591 ± 261
adipocyte density (x10^{-6}/µm^2)	1042 ± 70	900 ± 86	362 ± 42	446± 53
vessel size (µm²)	24.6 ± 1.9	24.5 ± 1.1	29.5 ± 1.9	24.2 ± 1.2†
vessel density (x10^{-6}/µm²)	657 ± 58	510 ± 62	386 ± 43	417 ± 27
vessel n°/adipocyte n°	0.62 ± 0.04	0.60 ± 0.06	1.2 ± 0.17	1.0 ± 0.09
GN				
weight (mg)	791 ± 43	855 ± 87	2672 ± 147	2454 ± 241
adipocyte size (µm²)	2229 ± 63	2391 ± 155	5626 ± 266	4519 ± 335
adipocyte density (x10^{-6}/ µm^2)	456 ± 13	441 ± 30	182 ± 9.6	234 ± 19†
vessel size (µm²)	29.5 ± 1.8	27.6 ± 1.5	34.7 ± 1.3	30.9 ± 3.1
vessel density (x10^{-6}/µm²)	337 ± 13	301 ± 20	266 ± 12	203 ± 15††
vessel n°/adipocyte n°	0.78 ± 0.04	0.70 ± 0.04	1.4 ± 0.14	0.95 ± 0.12†

Data are means ± SEM of n experiments in each group. $^{\dagger}p < 0.05$, $^{\dagger\dagger}p < 0.01$ as compared to WT mice on HFD (Mann-Whitney U test). [(a)] Body weight after 6h of fasting.
Abbreviations: SFD: standard fat diet; HFD: high fat diet; WT: wild-type; *Adamts13*$^{-/-}$: ADAMTS13 deficient; SC: subcutaneous adipose tissue; GN: gonadal adipose tissue.

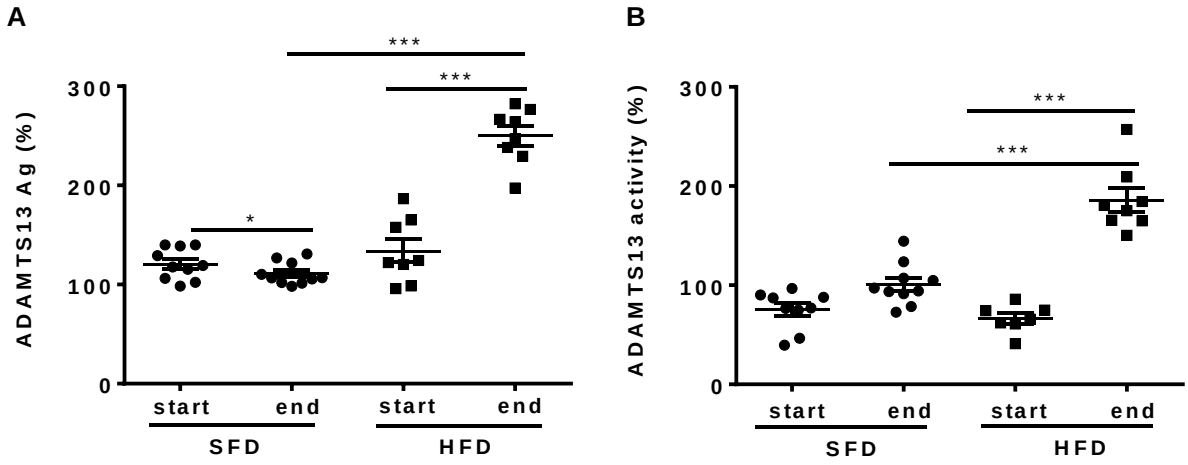

Figure 13: ADAMTS13 antigen and activity levels in plasma of WT mice.
ADAMTS13 antigen (A) and activity (B) levels in plasma (to normal mouse plasma) of WT mice at the start and the end of SFD or HFD feeding for 15 weeks. *, *** p < 0.05, p < 0.001.

Table 5: Adiponectin, leptin, total and HDL cholesterol levels in plasma and glucose levels measured in whole blood of WT and *Adamts13*$^{-/-}$ mice fed a SFD or HFD for 15 weeks.

	SFD		HFD	
	WT	***Adamts13*$^{-/-}$**	**WT**	***Adamts13*$^{-/-}$**
n	10	11	8	9
Adiponectin (µg/ml)	4.1 ± 0.15	4.3 ± 0.33	3.5 ± 0.13**	4.6 ± 0.35††
Leptin (ng/ml)	1.8 ± 0.40	3.4 ± 0.7	18.7 ± 1.2***	16.3 ± 3.7$^{\#}$
Total cholesterol (mg/dl)	56.3 ± 1.1	59.7 ± 3.5	100 ± 7.5***	126 ± 7.9$^{\#\#\#\dagger}$
HDL cholesterol (mg/dl)	45.6 ± 2.4	47.2 ± 2.8	93.4 ± 6.4***	108 ± 7.3$^{\#\#\#}$
Glucose (mg/dl)	124 ± 7.8	129 ± 7.0	152 ± 8.8	169 ± 4.1

Data are means ± SEM of n experiments in each group. †p < 0.05, †† p < 0.01 as compared to WT mice on HFD. ** p < 0.01, *** p < 0.001 as compared to WT mice fed a SFD. # p < 0.05, ### p < 0.001 as compared to *Adamts13*$^{-/-}$ mice fed a SFD (Mann-Whitney U test).
Abbreviations: SFD: standard fat diet; HFD: high fat diet; WT: wild-type; *Adamts13*$^{-/-}$: ADAMTS13 deficient.

Gene expression analysis of the adipogenic markers GLUT4, PPAR-γ, adiponectin and CD36 in adipose tissues did not reveal effects of ADAMTS13 deficiency in lean or obese mice, with the exception of lower GLUT4 expression in SC fat of lean *Adamts13*$^{-/-}$ mice (0.80 ± 0.05 versus 1.03 ± 0.09 for lean WT mice, $p < 0.05$ by Mann-Whitney U test) (data not shown). Determination of plasma adiponectin levels by ELISA (Table 5) revealed lower levels in obese versus lean WT mice, but not in obese versus lean *Adamts13*$^{-/-}$ mice. Higher levels were observed in obese *Adamts13*$^{-/-}$ versus obese WT mice.

Effect of ADAMTS13 deficiency on adipose tissue related angiogenesis

Quantitative analysis of blood vessel size and density in SC and GN adipose tissues of WT and *Adamts13*$^{-/-}$ mice on HFD revealed a few significant differences for obese *Adamts13*$^{-/-}$ as compared to obese WT mice (Table 4):

1) blood vessels in SC adipose tissue were smaller
2) blood vessel density in GN adipose tissue was lower
3) blood vessel density normalized to adipocyte density was lower in GN fat

On SFD, no differences were observed between WT and *Adamts13*$^{-/-}$ adipose tissues. For WT mice, no correlations were observed between plasma ADAMTS13 antigen or activity levels and blood vessel size or density in SC or GN adipose tissues.

We also monitored expression of some endothelial markers by qPCR. This revealed no effects of either diet or genotype on relative expression in GN adipose tissue of endoglin (1.01 ± 0.09 for lean *Adamts13*$^{-/-}$ versus 1.02 ± 0.04 for lean WT mice, with corresponding values of 1.0 ± 0.06 versus 0.89 ± 0.08 for obese *Adamts13*$^{-/-}$ versus obese WT mice). Expression of VEGF-A was lower for obese as compared to lean GN fat for both WT (0.60 ± 0.07 versus 1.05 ± 0.11; $p < 0.01$) and *Adamts13*$^{-/-}$ (0.58 ± 0.06 versus 0.99 ± 0.10; $p < 0.01$ by Mann-Whitney U test) mice, but was not different

between genotypes. Expression of VE-cadherin was higher for obese as compared to lean GN fat for both WT (1.60 ± 0.17 versus 1.02 ± 0.05; $p < 0.01$) and *Adamts13*$^{-/-}$ (1.64 ± 0.17 versus 1.13 ± 0.06; $p<0.01$ by Mann-Whitney U) mice, but was also not different between genotypes.

Effect of ADAMTS13 deficiency on adipose tissue related inflammation or oxidative stress

Analysis of the effect of diet on expression of inflammatory gene markers in SC adipose tissues of WT mice revealed significantly reduced expression of IL-6 on HFD as compared to SFD, whereas expression of F4/80, TNF-α, MCP-1, arginase or mannose R was not different (Figure 14A, I). In GN adipose tissue of WT mice, expression of IL-6 was also significantly reduced on HFD as compared to SFD, whereas F4/80, TNF-α and mannose R expression was enhanced (Figure 14A, II). In SC adipose tissue of *Adamts13*$^{-/-}$ mice on HFD versus SFD, enhanced expression of F4/80, arginase and mannose R, and reduced expression of IL-6 was observed (Figure 14A, I). Similarly, in GN adipose tissue of obese versus lean *Adamts13*$^{-/-}$ mice, expression of IL-6 was significantly reduced and expression of F4/80 and arginase was enhanced (Figure 14A, II).

Analysis of the effect of genotype on expression of inflammatory gene markers revealed significantly lower expression of F4/80, TNF-α, IL-6 and mannose R in SC fat, and of F4/80 in GN fat of lean *Adamts13*$^{-/-}$ versus WT mice. For obese *Adamts13* $^{-/-}$ mice as compared to obese WT mice, only higher expression of arginase in SC fat was observed (albeit not statistically different) (Figure 14B, I). Expression of MCP-1 in SC or GN adipose tissues was not affected by diet or genotype.

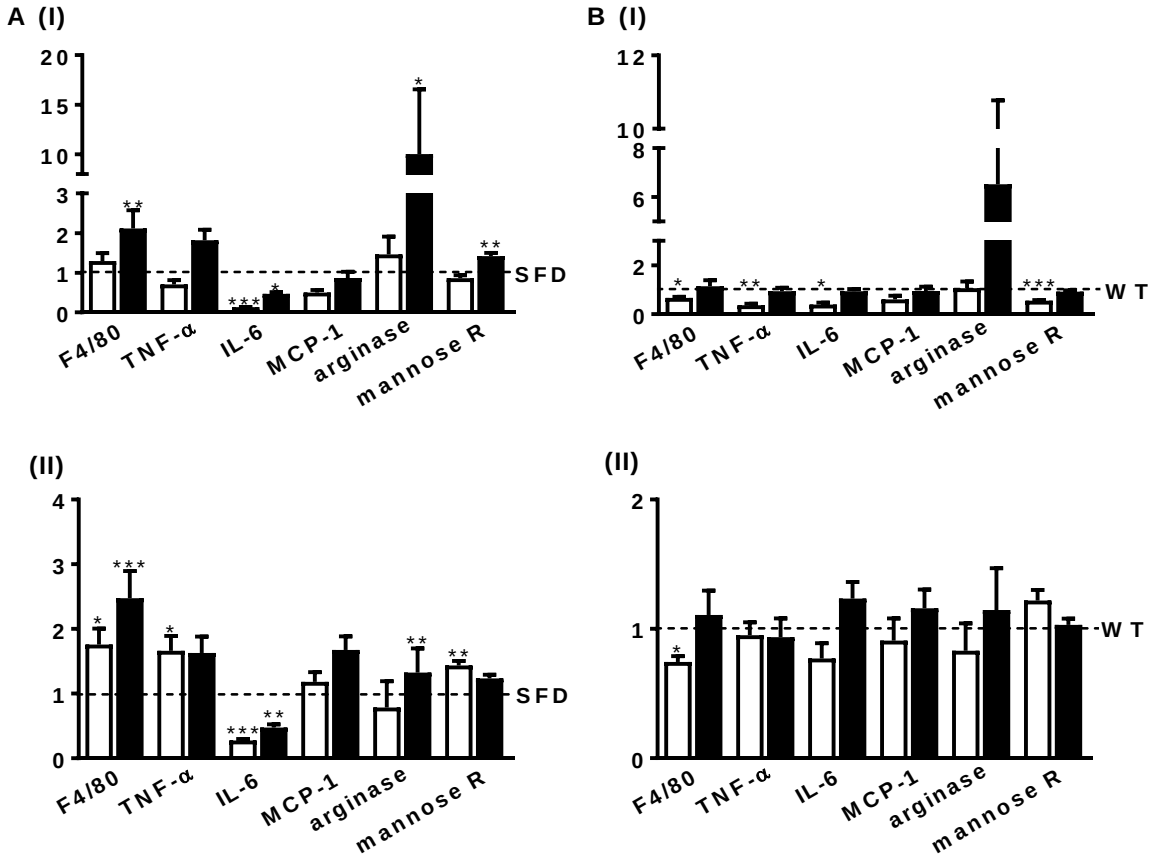

Figure 14: Gene expression of inflammatory markers in SC and GN adipose tissue.
(A) Effect of diet on expression of inflammatory markers in SC (I) or GN (II) adipose tissues. Gene expression is shown for obese relative to lean WT (white bars) or obese relative to lean *Adamts13*$^{-/-}$ (black bars) mice. *, **, *** p < 0.05, p < 0.01 and p < 0.001 for obese versus lean mice. (B) Effect of genotype on expression of inflammatory markers in SC (I) or GN (II) adipose tissues. Gene expression is shown for lean (white bars) or obese (black bars) *ADAMTS13*$^{-/-}$ relative to WT mice. *, **, *** p < 0.05, p < 0.01 and p < 0.001 for *Adamts13*$^{-/-}$ versus WT mice (Mann-Whitney U test).

In protein extracts of SC and GN adipose tissues as well as plasma of lean and obese WT and *Adamts13*$^{-/-}$ mice TNF-α and IL-6 could not be detected (detection limit of 78 pg/ml and 145 pg/ml, respectively) by ELISA.

Analysis of the effect of diet on expression of oxidative stress markers in SC adipose tissues revealed enhanced expression of NOX4 for obese *Adamts13*$^{-/-}$ and reduced expression of XDH1 for obese WT mice (Figure 15A, I). In GN adipose tissues, NOX4

expression was enhanced for obese WT as well as *Adamts13*$^{-/-}$ mice, whereas SOD1 and GPX1 expression were reduced in obese as compared to lean WT mice (Figure 15A, II).

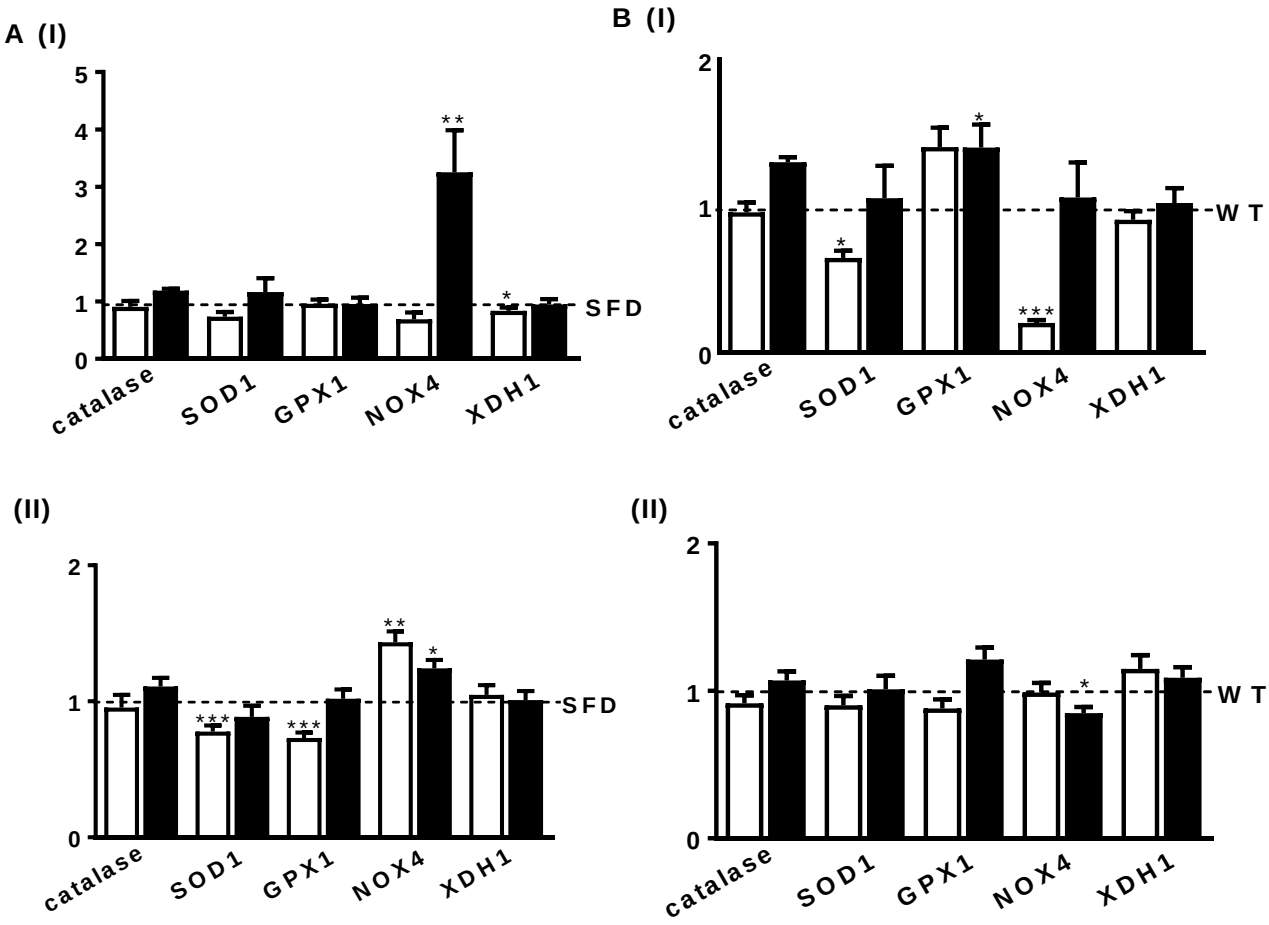

Figure 15: Gene expression of oxidative stress markers in SC and GN adipose tissue.
(A) Effect of diet on expression of oxidative stress markers in SC (I) or GN (II) adipose tissues. Gene expression is shown for obese relative to lean WT (white bars) or obese relative to lean *Adamts13*$^{-/-}$ (black bars) mice. *, **, *** p < 0.05, p < 0.01 and p < 0.001 for obese versus lean mice. (B) Effect of genotype on expression of oxidative stress markers in SC (I) or GN (II) adipose tissues. Gene expression is shown for lean (white bars) or obese (black bars) *Adamts13*$^{-/-}$ relative to WT mice. *, **, *** p < 0.05, p < 0.01 and p < 0.001 for *Adamts13*$^{-/-}$ versus WT mice (Mann-Whitney U test).

Analysis of the effect of genotype on expression of oxidative stress markers in SC adipose tissues revealed reduced expression of NOX4 and SOD1 for lean *Adamts13*$^{-/-}$ versus lean WT mice, and enhanced expression of GPX1 for obese *Adamts13*$^{-/-}$ versus obese WT mice (Figure 15B, I). In GN adipose tissues, only reduced expression of NOX4 for obese *Adamts13*$^{-/-}$ versus obese WT mice was observed (Figure 15B, II). Expression of catalase in SC or GN adipose tissues was not affected by diet or genotype.

Effect of ADAMTS13 deficiency on metabolic parameters

Analysis of plasma metabolic parameters evidenced the effects of HFD versus SFD, as shown by enhanced leptin, total cholesterol and HDL cholesterol levels in WT as well as *Adamts13*$^{-/-}$ mice (Table 5). No significant effects of genotype were observed on these metabolic parameters, except for higher total cholesterol levels for obese *Adamts13*$^{-/-}$ versus WT mice. Total plasma cholesterol levels for WT mice were strongly positively correlated with both ADAMTS13 antigen ($r = 0.81$, $p < 0.0001$) and activity ($r = 0.67$, $p = 0.002$). Glucose levels for obese *Adamts13*$^{-/-}$ mice were not significantly different as compared to obese WT mice. In separate experiments glucose tolerance and insulin sensitivity tests were performed with obese WT and *Adamts13*$^{-/-}$ mice. No significant differences were observed between WT ($n = 10$) and *Adamts13*$^{-/-}$ ($n = 10$) mice (Figure 16).

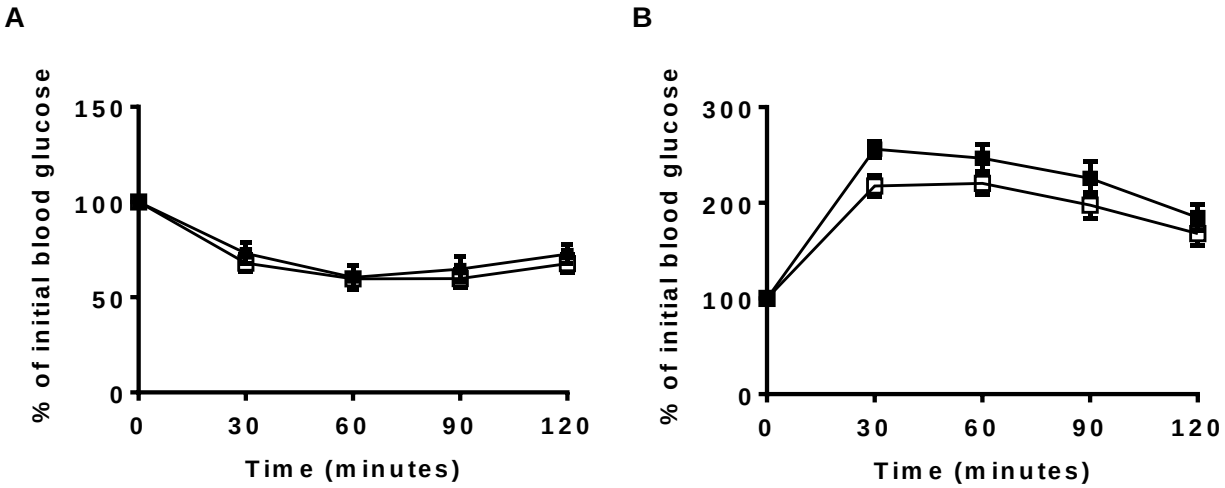

Figure 16: Insulin and glucose tolerance in WT and *Adamts13*$^{-/-}$ mice after a HFD.
Insulin sensitivity (A) and glucose tolerance (B) test of WT (closed symbols) or *Adamts13*$^{-/-}$ (open symbols) mice kept on HFD. Data are means ± SEM of 10 experiments in each group. No significant differences were observed between both genotypes (Two-way ANOVA).

DISCUSSION

The rationale for this study was based on several published observations relating to a potential functional role of ADAMTS13 in adiposity (7), angiogenesis (13), and oxidative stress/inflammation (20). Therefore, we have investigated a potential role of ADAMTS13 in adipose tissue development and associated angiogenesis and inflammation using an established mouse model of nutritionally induced obesity (21). The difference in body weight, weight of SC and GN fat depots, adipocyte size and density between mice fed a SFD or HFD and the enhanced levels of leptin and cholesterol, confirm that the HFD was effective in inducing obesity in both genotypes. However, no differences were found in body weight, food intake, adipocyte size or expression of adipogenic markers between the two genotypes. These data indicate that there is no relevant functional role of ADAMTS13 in adiposity in mice. The enhanced plasma ADAMTS13 levels in obese as compared to lean WT mice could not be explained by increased expression in the liver, the main organ of its synthesis (22), but may be due to enhanced release.

For adipose tissue to expand, each adipocyte needs to be in close proximity to blood vessels for the supply of nutrients and oxygen, for the transport of lipids and signaling molecules and for the elimination of waste products (23). It was previously established that adipogenesis is related to angiogenesis (24). Thus, ADAMTS13 inhibits VEGF-induced angiogenesis by binding to VEGF via its TSP-1 domain (14). In our study, obese *Adamts13*$^{-/-}$ mice showed smaller blood vessels in their SC fat depots as compared to WT mice and had fewer blood vessels in their GN adipose tissue. There were, however, no differences in gene expression of endoglin, VEGF-A or VE-cadherin in GN adipose tissues of WT or *Adamts13*$^{-/-}$ mice. It is generally accepted that adipose tissue associated angiogenesis is mainly regulated by VEGF (23). Thus, the

anti-angiogenic effect of ADAMTS13 in adipose tissue related angiogenesis is at best marginal and does not affect *in vivo* adipose tissue development. Obesity is associated with a state of low-grade chronic inflammation, which triggers some related comorbidities. Pro-inflammatory cytokines are secreted and leptin production by dysfunctional adipocytes is increased leading to insulin resistance. Adiponectin is an anti-inflammatory insulin-sensitizing hormone that inhibits several obesity-related processes such as formation of foam cells and production of TNF-α in macrophages (25). It is known that adiponectin concentrations decrease with increasing body weight in mice as well as in humans (26). Interestingly, in our study adiponectin levels were comparable in lean and obese *Adamts13*$^{-/-}$ mice, but were higher in obese *Adamts13*$^{-/-}$ mice as compared to their WT counterparts. The fact that adiponectin levels in *Adamts13*$^{-/-}$ mice do not decrease upon HFD feeding may suggest a somewhat improved metabolic profile.

In agreement with a previous study of Crawley *et al.* (7) in man, we observed a strong positive correlation between cholesterol levels and ADAMTS13 levels in WT mice. However, total plasma cholesterol levels were higher in obese *Adamts13*$^{-/-}$ versus obese WT mice. This apparent contradiction questions the functional association between ADAMTS13 and cholesterol levels. Furthermore, insulin and glucose tolerance tests on obese mice did not reveal differences between the two genotypes and blood glucose levels at the start of the tests were comparable for obese WT and *Adamts13*$^{-/-}$ mice. These findings indicate that there is no direct effect of ADAMTS13 on glycemia in nutritionally induced obese mice.

Reactive oxygen species and oxidative stress are involved in adipocyte dysfunction. Stressed adipocytes send out signals that recruit macrophages in white adipose tissue leading to production of pro-inflammatory cytokines resulting in further enhanced

stress and adipocyte death (27). Based on the literature it was anticipated that obesity (28) as well as ADAMTS13 deficiency (20) would be associated with enhanced inflammation. Therefore, we monitored expression of pro- and anti-inflammatory gene markers in SC and GN adipose tissues of lean and obese WT and *Adamts13*$^{-/-}$ mice. More specifically, as general macrophage markers F4/80 and MCP-1 were used. TNF-α and mannose receptor or arginase were used as markers for M1 (classically activated, pro-inflammatory) or M2 (alternatively activated, anti-inflammatory) macrophages, respectively. IL-6 can act as a pro-inflammatory as well as an anti-inflammatory cytokine (29). It is secreted by adipocytes in obese subjects (30). The major changes that were observed (≥ 2-fold difference; $p < 0.05$) for the effect of diet (HFD versus SFD) were: 1) reduced expression of IL-6 in SC and GN fat of both WT and *Adamts13*$^{-/-}$ mice; 2) enhanced expression of the macrophage marker F4/80 in GN fat of *Adamts13*$^{-/-}$ mice (as expected); and 3) enhanced expression of anti-inflammatory arginase and mannose receptor in SC fat of *Adamts13*$^{-/-}$ mice (reduction was expected). For the effect of genotype (*Adamts13*$^{-/-}$ versus WT), we observed: 1) in SC fat of lean mice reduced expression of TNF-α (increase expected), of IL-6 and of mannose receptor; 2) enhanced arginase expression in SC fat of obese *Adamts13*$^{-/-}$ mice and 3) reduced expression of F4/80 in both SC and GN adipose tissue of lean *Adamts13*$^{-/-}$ versus WT mice. In obese adipose tissues, no relevant effects of genotype were observed on expression of inflammatory gene markers. In lean SC adipose tissues, however, expression of pro-inflammatory TNF-α and F4/80 and of anti-inflammatory mannose receptor was significantly reduced in *Adamts13*$^{-/-}$ as compared to WT mice. These differences were not consistently detected in lean GN adipose tissues, except for lower expression of F4/80 in *Adamts13*$^{-/-}$ tissues. Because of the confounding effects of the combination of obesity and ADAMTS13 deficiency, and the

differences between SC and GN adipose tissues, these data do not allow to predict whether ADAMTS13 is pro- or anti-inflammatory in adipose tissue. In any case, the observed changes in expression of inflammatory markers are not reflected in differences in adipose tissue development between WT and *Adamts13*$^{-/-}$ mice. Similar analysis for expression of oxidative stress gene markers revealed only an effect of HFD on enhanced expression of NOX4 in *Adamts13*$^{-/-}$ mice (as expected), and no effects of genotype. As chronic inflammation and enhanced oxidative stress are considered consequences of obesity, and ADAMTS13 deficiency did not affect adiposity, significant differences in associated inflammation or oxidative stress between both obese genotypes would not be expected.

Thus, despite several indications from previous studies, our study does not support a functional role of ADAMTS13 in obesity nor in associated angiogenesis or inflammation, at least in mice. However, it cannot be excluded that ADAMTS13 plays a more prominent role in adipose tissue development in humans.

REFERENCES

1. Crandall DL, Hausman GJ, Kral JG. A review of the microcirculation of adipose tissue: anatomic, metabolic, and angiogenic perspectives. Microcirculation. 1997;4(2):211-32.
2. Christiaens V, Scroyen I, Lijnen HR. Role of proteolysis in development of murine adipose tissue. Thromb Haemost. 2008;99(2):290-4.
3. Sun K, Kusminski CM, Scherer PE. Adipose tissue remodeling and obesity. J Clin Invest. 2011;121(6):2094-101.
4. Le Goff C, Cormier-Daire V. The ADAMTS(L) family and human genetic disorders. Hum Mol Genet. 2011;20(R2):R163-7.
5. Lombardi AM, Fabris R, Scarda A, Zanato V, Dal Pra C, Scarparo P, et al. Presence of anti-ADAMTS13 antibodies in obesity. Eur J Clin Invest. 2012;42(11):1197-204.
6. Nicol KK, Shelton BJ, Knovich MA, Owen J. Overweight individuals are at increased risk for thrombotic thrombocytopenic purpura. Am J Hematol. 2003;74(3):170-4.
7. Crawley JT, Lane DA, Woodward M, Rumley A, Lowe GD. Evidence that high von Willebrand factor and low ADAMTS-13 levels independently increase the risk of a non-fatal heart attack. J Thromb Haemost. 2008;6(4):583-8.
8. Liu MY, Zhou Z, Ma R, Tao Z, Choi H, Bergeron AL, et al. Gender-dependent up-regulation of ADAMTS-13 in mice with obesity and hypercholesterolemia. Thromb Res. 2012;129(4):536-9.
9. Hijona E, Hijona L, Arenas JI, Bujanda L. Inflammatory mediators of hepatic steatosis. Mediators Inflamm. 2010;2010:837419.
10. Gandhi C, Khan MM, Lentz SR, Chauhan AK. ADAMTS13 reduces vascular inflammation and the development of early atherosclerosis in mice. Blood. 2012;119(10):2385-91.
11. Jin SY, Tohyama J, Bauer RC, Cao NN, Rader DJ, Zheng XL. Genetic ablation of Adamts13 gene dramatically accelerates the formation of early atherosclerosis in a murine model. Arterioscler Thromb Vasc Biol. 2012;32(8):1817-23.
12. Kumar S, Sharghi-Namini S, Rao N, Ge R. ADAMTS5 functions as an anti-angiogenic and anti-tumorigenic protein independent of its proteoglycanase activity. Am J Pathol. 2012;181(3):1056-68.
13. Lee M, Rodansky ES, Smith JK, Rodgers GM. ADAMTS13 promotes angiogenesis and modulates VEGF-induced angiogenesis. Microvasc Res. 2012;84(2):109-15.
14. Lee M, Keener J, Xiao J, Long Zheng X, Rodgers GM. ADAMTS13 and its variants promote angiogenesis via upregulation of VEGF and VEGFR2. Cell Mol Life Sci. 2014.
15. Motto DG, Chauhan AK, Zhu G, Homeister J, Lamb CB, Desch KC, et al. Shigatoxin triggers thrombotic thrombocytopenic purpura in genetically susceptible ADAMTS13-deficient mice. J Clin Invest. 2005;115(10):2752-61.
16. Kokame K, Nobe Y, Kokubo Y, Okayama A, Miyata T. FRETS-VWF73, a first fluorogenic substrate for ADAMTS13 assay. Br J Haematol. 2005;129(1):93-100.
17. Lijnen HR, Maquoi E, Demeulemeester D, Van Hoef B, Collen D. Modulation of fibrinolytic and gelatinolytic activity during adipose tissue development in a mouse model of nutritionally induced obesity. Thromb Haemost. 2002;88(2):345-53.
18. Scroyen I, Cosemans L, Lijnen HR. Effect of tissue inhibitor of matrix metalloproteinases-1 on in vitro and in vivo adipocyte differentiation. Thromb Res. 2009;124(5):578-83.
19. Laitinen L. Griffonia simplicifolia lectins bind specifically to endothelial cells and some epithelial cells in mouse tissues. Histochem J. 1987;19(4):225-34.
20. Chauhan AK, Kisucka J, Brill A, Walsh MT, Scheiflinger F, Wagner DD. ADAMTS13: a new link between thrombosis and inflammation. J Exp Med. 2008;205(9):2065-74.
21. Christiaens V, Van Hul M, Lijnen HR, Scroyen I. CD36 promotes adipocyte differentiation and adipogenesis. Biochim Biophys Acta. 2012;1820(7):949-56.
22. Zhou W, Inada M, Lee TP, Benten D, Lyubsky S, Bouhassira EE, et al. ADAMTS13 is expressed in hepatic stellate cells. Lab Invest. 2005;85(6):780-8.
23. Hausman GJ, Richardson RL. Adipose tissue angiogenesis. J Anim Sci. 2004;82(3):925-34.
24. Christiaens V, Lijnen HR. Angiogenesis and development of adipose tissue. Mol Cell Endocrinol. 2010;318(1-2):2-9.
25. Koerner A, Kratzsch J, Kiess W. Adipocytokines: leptin--the classical, resistin--the controversical, adiponectin--the promising, and more to come. Best Pract Res Clin Endocrinol Metab. 2005;19(4):525-46.
26. Yadav A, Kataria MA, Saini V. Role of leptin and adiponectin in insulin resistance. Clin Chim Acta. 2013;417:80-4.

27. Gregor MF, Hotamisligil GS. Thematic review series: Adipocyte Biology. Adipocyte stress: the endoplasmic reticulum and metabolic disease. J Lipid Res. 2007;48(9):1905-14.
28. Weisberg SP, McCann D, Desai M, Rosenbaum M, Leibel RL, Ferrante AW, Jr. Obesity is associated with macrophage accumulation in adipose tissue. J Clin Invest. 2003;112(12):1796-808.
29. Scheller J, Chalaris A, Schmidt-Arras D, Rose-John S. The pro- and anti-inflammatory properties of the cytokine interleukin-6. Biochim Biophys Acta. 2011;1813(5):878-88.
30. Skurk T, Alberti-Huber C, Herder C, Hauner H. Relationship between adipocyte size and adipokine expression and secretion. J Clin Endocrinol Metab. 2007;92(3):1023-33.

Chapter 4

ADAMTS13 deficiency promotes microthrombosis in a murine model of diet-induced liver steatosis

Published paper

Geys L, Bauters D, Roose E, Tersteeg C, Vanhoorelbeke K, Hoylaerts MF, Lijnen HR, Scroyen I. ADAMTS13 deficiency promotes microthrombosis in a murine model of diet-induced liver steatosis. Thrombosis and Haemostasis. 2017; 117(1):19-26.

ABSTRACT

ADAMTS13 cleaves ultra-large multimeric von Willebrand Factor (VWF), thereby preventing formation of platelet-rich microthrombi. ADAMTS13 is mainly produced by hepatic stellate cells, and numerous studies have suggested a functional role of ADAMTS13 in the pathogenesis of liver diseases. We used a model of high fat diet-induced steatosis in ADAMTS13 deficient (*Adamts13*$^{-/-}$) and wild-type (WT) control mice to investigate a potential role of ADAMTS13 in formation of hepatic microthrombi and development of non-alcoholic steatohepatitis (NASH).

Microthrombi were more abundant in the liver of obese *Adamts13*$^{-/-}$ as compared to obese WT or to lean *Adamts13*$^{-/-}$ mice. Obese *Adamts13*$^{-/-}$ mice displayed lower platelet counts and higher prevalence of ultra-large VWF multimers. Hepatic plasmin-α_2-antiplasmin complex levels were comparable for obese WT and *Adamts13*$^{-/-}$ mice and were lower for lean *Adamts13*$^{-/-}$ than WT mice, not supporting marked activation of the fibrinolytic system. High fat diet feeding, as compared to normal chow, resulted in enhanced liver triglyceride levels for both genotypes ($p < 0.0001$) and steatosis ($p < 0.0001$ for WT mice, $p = 0.002$ for *Adamts13*$^{-/-}$ mice) without differences between the genotypes. Expression of markers of inflammation, oxidative stress, steatosis and fibrosis was affected by diet, but not by genotype.

Thus, our data confirm that obesity promotes NASH, but do not support a detrimental role of ADAMTS13 in its development. However, ADAMTS13 deficiency in obese mice promotes hepatic microthrombosis, whereas a compensatory role of plasmin in removal of microthrombi in the absence of ADAMTS13 could not be demonstrated.

INTRODUCTION

ADAMTS13 (a disintegrin and metalloproteinase with thrombospondin type-1 repeat, member 13) specifically cleaves multimeric von Willebrand Factor (VWF), hereby preventing accumulation of ultra-large VWF (UL-VWF) multimers and the subsequent platelet clumping and formation of microthrombi that disturbs the microcirculation and impairs oxygen supply to organs (1). Hence, ADAMTS13 deficiency, caused by mutations in the ADAMTS13 gene (2-6) or by inhibitory autoantibodies (7, 8) may result in development of thrombotic thrombocytopenic purpura (TTP), a rare but life-threatening disease (1). Recently, it was reported that plasmin might function as a backup for ADAMTS13 in the degradation of complexes between platelets and UL-VWF multimers in patients with TTP (9). On the basis of these findings, it was suggested that plasmin may also be involved in the removal of microthrombi in patients with liver disease (10). ADAMTS13 is mainly produced by stellate cells in the liver (11), and numerous studies have suggested a functional role of ADAMTS13 in the pathogenesis of liver diseases (reviewed in (12)). A beneficial effect of ADAMTS13 activity was observed on liver disease severity, and increased ADAMTS13 activity is related with a better prognosis of liver cirrhosis (13), alcoholic hepatitis (14) and hepatic veno-occlusive disease (15). However, a detrimental effect of ADAMTS13 was also reported on hepatocellular carcinoma risk in patients suffering from chronic liver disease (16). In rats, steatohepatitis and liver fibrosis are associated with enhanced systemic ADAMTS13 antigen and activity levels (17). In addition, we previously found enhanced ADAMTS13 levels in obese mice (18). Therefore, in this study, we have used a model of diet-induced non-alcoholic steatohepatitis (NASH) in ADAMTS13 deficient mice to elucidate a potential role of ADAMTS13 and obesity in hepatic microthrombosis and steatosis.

MATERIALS & METHODS

Animal models

Male *Adamts13*$^{-/-}$ and wild-type (WT) littermate mice (genetic background, C57Bl6/J x 129X1/Sv x CASA/RK) were used and genotyped as described (19). The mice were kept from the age of 5 weeks on in individual micro-isolation cages on a 12h day/night cycle and fed for 15 weeks with a high fat diet (HFD) (42% kcal as fat, caloric value 22 kJ/g; E15721-34; Ssniff, Soest, Germany) (n = 9 or 8 for *Adamts13*$^{-/-}$ or WT) or a standard fat diet (SFD) (13% kcal as fat, caloric value 10.9 kJ/g; KM-04-k12; Muracon, Carfil, Oud-Turnhout, Belgium) (n = 11 or 10 for *Adamts13*$^{-/-}$ or WT). Water was always available *ad libitum*. Body weight and food intake were measured at weekly intervals (18). At the end of the diet, after fasting for 6h, blood was taken from the tail of unanesthetized mice. Blood glucose concentrations were measured using the Accu-chek performa meter (Roche diagnostics, Roche, Basel, Switserland) and blood glucose test strips (Roche diagnostics). At the end of the experiment, the mice were sedated and blood was taken from the retro-orbital sinus on trisodium citrate (0.01 M), before they were perfused by saline and killed by cervical dislocation. Livers were removed and weighed. Portions were used for RNA or protein extraction or were fixed in 4% formaldehyde for histological analysis.

All animal experiments were approved by the KU Leuven ethical committee (P158-2011) and performed in accordance with the NIH Guide for the Care and Use of Laboratory Animals (1996) and the EU Directive 2010/63/EU for animal experiments.

Metabolic and inflammatory parameters

Total triglyceride, alkaline phosphatases, alanine aminotransferase (ALT) and aspartate aminotransferase (AST) levels in plasma were evaluated using routine clinical assays. Mouse plasminogen activator inhibitor 1 (PAI-1) antigen levels in

plasma were measured by a combined monoclonal-polyclonal antibody assay calibrated with recombinant mouse PAI-1, as described previously (18, 20). C-reactive protein (CRP) levels in plasma were determined by ELISA (Quantikine ELISA kit, R&D Systems, Minneapolis, USA). Liver tissue extracts were prepared by adding alcoholic KOH (30%) to a sample of 30 mg. Samples were incubated overnight at 55°C to digest the tissue, and 1M $MgCl_2$ was added to the digested sample (1:1 vol/vol), mixed well, incubated on ice for 10 minutes and centrifuged for 30 minutes. The supernatant was analyzed using the triglycerides FS* kit (Diasys, Holzheim, Germany). Plasmin-α_2-antiplasmin (PAP) and thrombin-antithrombin III (TAT) complex levels were determined in plasma and liver extracts by home-made ELISA (21) or by a commercial ELISA (ab137994, Abcam, Cambridge, Great-Britain), respectively. Protein extraction of liver tissue was performed in 10 μL/μg tissue of a 10 mM sodium phosphate buffer, pH 7.2, containing 150 mM NaCl, 1% Triton X-100, 0.1% SDS, 0.5% sodium deoxycholate and 0.2% NaN_3. After centrifugation, the protein concentration of the supernatant was determined (BCA assay, Thermofisher Scientific Waltham, MA).

RNA extraction and expression analysis

RNA extraction from livers was performed using the RNeasy mini kit (Qiagen, Basel, Switzerland) according to the manufacturer's protocol. Therefore, the livers were transferred in RLT buffer (lysis buffer) before homogenizing (*FastPrep-24; MP* Biomedicals, Illkirch, France). To prevent the lipids from obstructing the membrane of the RNeasy column, the lysates were centrifuged for 3 minutes at 13,000 rpm. The resulting supernatant was transferred to a new tube. An equal volume of 50% ethanol was added to all samples to allow binding of the RNA on the membrane of the RNeasy spin column. DNAse treatment was performed to prevent contamination with genomic DNA. RNA was eluted in 60 μL RNAse-free water. RNA concentrations were measured

using a nanodrop spectrometer (ThermoFisher Scientific) and samples were stored at -80°C. Next, 10 ng/µL RNA was reverse transcribed into cDNA using the Multiscribe™ Reverse Transcriptase kit, according to the manufacturer's protocol (Life Technologies, Carlsbad, CA). Quantitative real-time PCR (qPCR) was performed to amplify the isolated RNA. qPCR was done in the ABI 7500 Fast Sequence detector (Life Technologies) to detect the markers listed in Table 6.

Table 6: Markers detected by qPCR using TaqMan gene expression assays

Gene	Assay†	Gene	Assay†
F4/80	Mm00802529_m1	**FATP**	Mm00449511_m1
TNF-α	Mm00443258_m1	**MCAD**	Mm01323360_g1
MCP-1	Mm00441242_m1	**CD36**	Mm00432403_m1
IL-6	Mm 00446190_m1	**PPAR-γ**	Mm00440939_m1
IL-1	Mm 01336189_m1	**TIMP-1**	Mm 00441818_m1
Arginase	Mm00475988_m1	**PAI-1**	Mm 00435860_m1
Mannose receptor	Mm00485148_m1	**α-SMA**	Mm00725412_s1
SREBP-1	Mm00550338_m1	**Col1a1**	Mm00801666_g1
FAS	Mm01253300_g1	**TGF-β**	Mm01178820_m1
β-actin	Mm01205647_g1		

†Assays purchased from Life Technologies (Carlsbad, CA).

Transcript levels were determined in duplicate by qPCR reaction using a gene expression assay with specific primers, probes and the Fast mastermix (Life Technologies). Analyses were performed with the ΔΔCT method using the 7500 System SDS software (Life Technologies). Normalization was carried out to correct for fluctuations caused by sample differences. Fold changes were calculated as $2^{-\Delta\Delta CT}$ relative to the mice fed a SFD for obese mice (effect of diet) and relative to WT mice for the *Adamts13*$^{-/-}$ mice (effect of genotype). β-actin was used as housekeeping gene (18).

Histological analysis

Paraffin sections (4 μm) for histology were prepared from isolated livers. The degree of steatosis was visualized by staining with haematoxylin/eosin (H&E) under standard conditions, and sections were inspected for the presence of microthrombi. These were further evaluated by staining for VWF, TSP-1 and fibrin. Antigens were unmasked using trypsin treatment for 7 minutes or antigen retrieval solution (Dako) for VWF or TSP-1 and fibrin stainings, respectively. To remove endogenous peroxidase activity, sections were incubated in 0.3% hydrogen peroxide in PBS. The sections were incubated overnight with a polyclonal rabbit anti-human VWF antibody (DAKO, code A0082, Heverlee, Belgium) at a dilution of 1/500 in blocking buffer, a TSP-1 (0.87 μg/mL in-house rabbit anti-human TSP-1, preadsorbed with liver extract from *Tsp1*$^{-/-}$ mice, to eliminate interfering TSP-2 signals) or a goat anti-human fibrinogen 1/200 antibody (Nordic Immunology cat no: GAHu/Fbg/7S stock 10 mg/ml) in blocking buffer. Afterwards, a biotin labeled goat-anti-rabbit antibody (DAKO, E0432) or rabbit anti-goat-HRP (P0449) was used as secondary antibody (1/300 dilution). VWF and TSP-1 were visualized by the ABC-kit (Vector Laboratories, CA, USA) and DAB, whereas fibrin was visualized using DAB. Microthrombi in the liver were quantitated as blood vessels of 15-100 μm obstructed with VWF positive thrombi relative to total blood vessels of 15-100 μm. In addition, the size was scored (+, ++, or +++, corresponding to respectively less than 2/3, 2/3 or totally obstructing blood vessels) in 2 to 3 sections taken throughout the liver of 3-6 mice in each group. Analyses were performed with a Zeiss Axioplan 2 microscope and the AxioVision release 4.8 software (Carl Zeiss, Oberkochen, Germany) and Image J.

VWF antigen and multimers

Murine VWF antigen levels were measured in plasma using a home-made ELISA. A 96-well microtiter plate was coated overnight with a polyclonal rabbit anti-human VWF antibody (Dako). After blocking, plasma was diluted in PBS, 0.3% non-fat milk and the plate was incubated at 37°C for 1.5h. Bound antigen was detected with 2 biotinylated in-house developed murine anti-mVWF monoclonal antibodies (2C12-bio, 15H7-bio). HRP-labeled streptavidin (Sigma Aldrich) was added (1/10 000 in PBS 0.3% non-fat milk).

The multimeric pattern of plasma VWF was analyzed by gel electrophoresis as described by Lotta *et al.* (22). Low (L), medium (M) and high (H) molecular weight (MW) multimers were visualized using an in-house developed anti-VWF antibody.

Statistical analysis

Data are presented as means ± standard error of the means (SEM). Statistical significance between groups was analyzed with the non-parametric Mann-Whitney U test. Scores of microthrombi in liver sections were analyzed by one-way ANOVA. Analysis of the data was performed using Prism 6 (GraphPad Software Inc., San Diego, CA). Values of $p < 0.05$ are considered statistically significant.

RESULTS

Effect of diet and genotype on microthrombosis and fibrinolysis

When mice were kept on a SFD or HFD for 15 weeks, total body weight (Figure 17A) as well as liver weight (Figure 17B) were markedly enhanced for both obese *Adamts13*$^{-/-}$ and WT mice as compared to lean (SFD) mice, but there were no significant differences between genotypes.

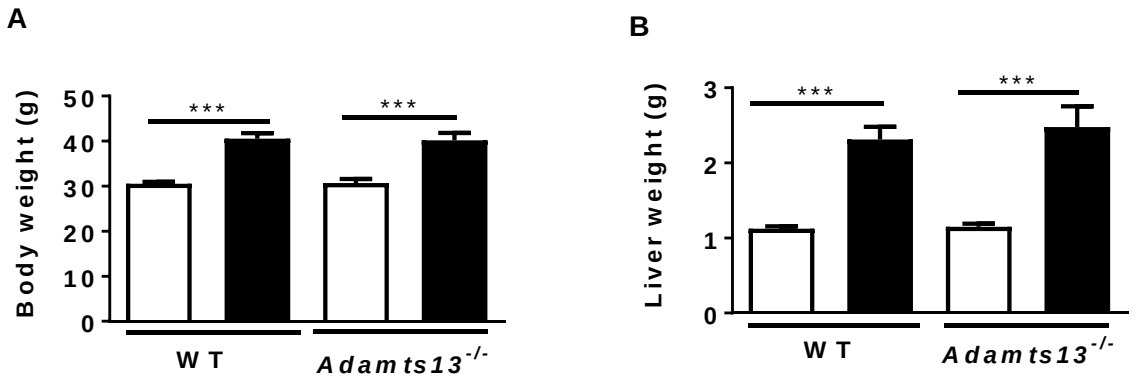

Figure 17: Body weight (A) and liver weight (B) are shown for wild-type (WT) and *Adamts13*$^{-/-}$ mice kept on standard fat diet (white bars) or high fat diet (black bars). Data represent means ± SEM of 8 to 10 experiments. *** p < 0.001.

Staining of liver sections indicated the presence of fibrin, whereas TSP-1 staining showed abundance of platelets for obese *Adamts13*$^{-/-}$ as compared to WT mice (Figure 18). Furthermore, VWF-staining (Figure 19A) and quantitative analyses revealed significantly higher prevalence of microthrombi for *Adamts13*$^{-/-}$ mice on HFD as compared to WT mice on HFD ($p = 0.001$) or SFD ($p = 0.05$) (Figure 19B). Scoring of microthrombi size confirmed a significant abundance for obese *Adamts13*$^{-/-}$ versus obese WT mice ($p = 0.02$) or versus lean *Adamts13*$^{-/-}$ mice ($p = 0.001$) (Figure 19C). No significant difference was observed between SFD and HFD feeding of WT mice, or between WT and *Adamts13*$^{-/-}$ mice on SFD.

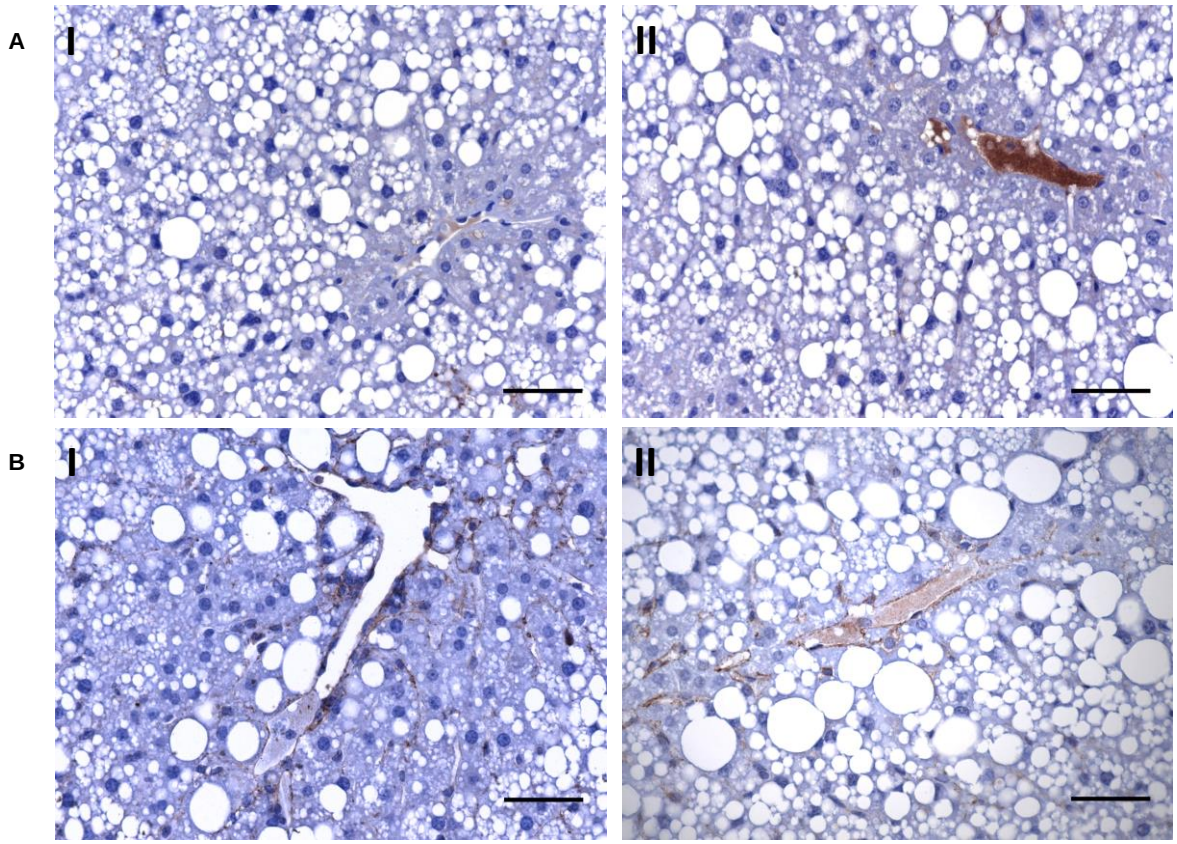

Figure 18: Characterization of hepatic microthrombi.

Fibrin (A) and TSP-1 (B) staining of liver sections of obese (HFD) WT (panels I) and *Adamts13*$^{-/-}$ mice (panels II). Scale bars represent 50 µm.

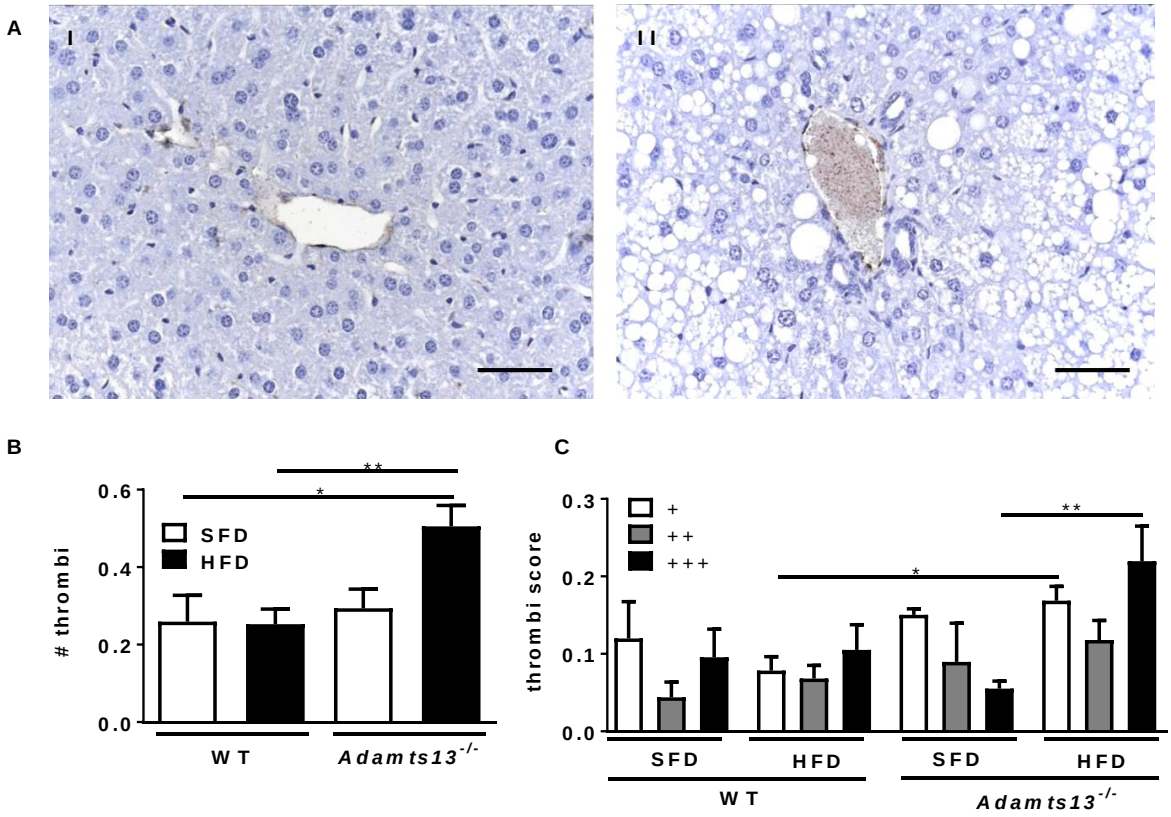

Figure 19: Quantitation of microthrombi in the liver of WT and *Adamts13*$^{-/-}$ mice.
(A) VWF staining of liver sections of a lean WT mouse (I) (score +) and an obese *Adamts13*$^{-/-}$ mouse (II) (score +++). Scale bars represent 50 µm. (B) Total number of thrombi normalized to total number of blood vessels in WT and *Adamts13*$^{-/-}$ mice fed a SFD (white bars) or HFD (black bars). (C) Number of thrombi normalized to total number of blood vessels between 15 and 100 µm that are totally obstructing (+++), 2/3 obstructing (++) or less than 2/3 obstructing (+) blood vessels. Data represent means ± SEM of 4 experiments. * p < 0.05, ** p < 0.01.

TAT levels in plasma (Table 7) or in liver extracts (Figure 20A) were somewhat higher upon HFD as compared to SFD feeding. For liver extracts, TAT levels were significantly different between lean WT and *Adamts13*$^{-/-}$ mice, whereas, in plasma no significant differences were found between the genotypes.

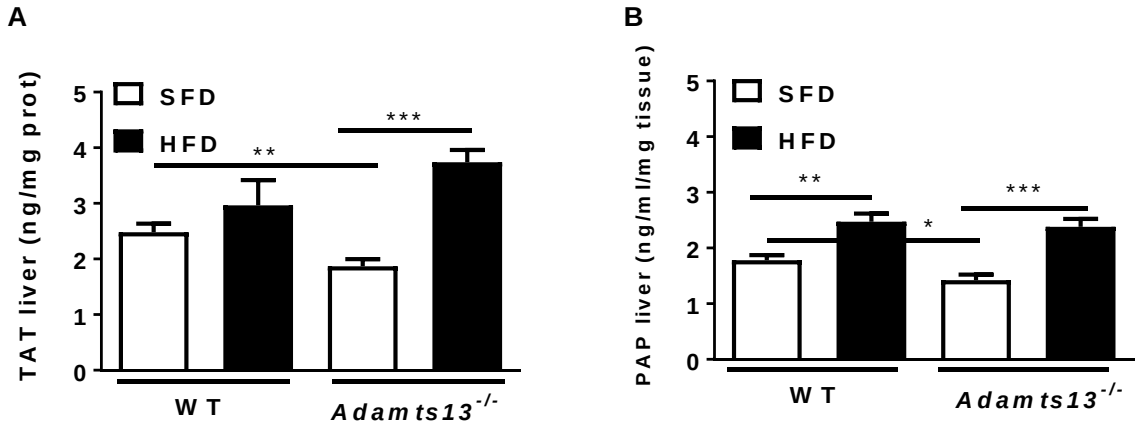

Figure 20: Thrombin-antithrombin III (TAT) complex levels (A) and plasmin-α2-antiplasmin (PAP) complex levels (B) in liver extracts. Data represent means ± SEM of 8 to 10 experiments. * p < 0.05, ** p < 0.01, *** p < 0.001.

Platelet counts at the end of the diet were lower for obese *Adamts13*$^{-/-}$ mice versus obese WT or lean *Adamts13*$^{-/-}$ mice (Figure 21A). VWF antigen levels were higher for lean, but not for obese *Adamts13*$^{-/-}$ versus WT mice (Figure 21B). Analysis of VWF multimer composition in plasma (Figure 21C) revealed more abundant HMW multimers for both lean and obese *Adamts13*$^{-/-}$ versus WT mice.

To examine whether plasmin compensates for the absence of ADAMTS13 as previously suggested (9), plasmin-α_2-antiplasmin (PAP) complex levels were measured. This is a sensitive parameter to monitor activation of the fibrinolytic system. PAP complex levels in plasma were below 5 nM in all samples and were not different between genotypes. As compared to WT mice, PAP complex levels in liver extracts were lower for *Adamts13*$^{-/-}$ mice on SFD and were not enhanced on HFD (Figure 20B), not supporting marked activation of the fibrinolytic system in the absence of ADAMTS13.

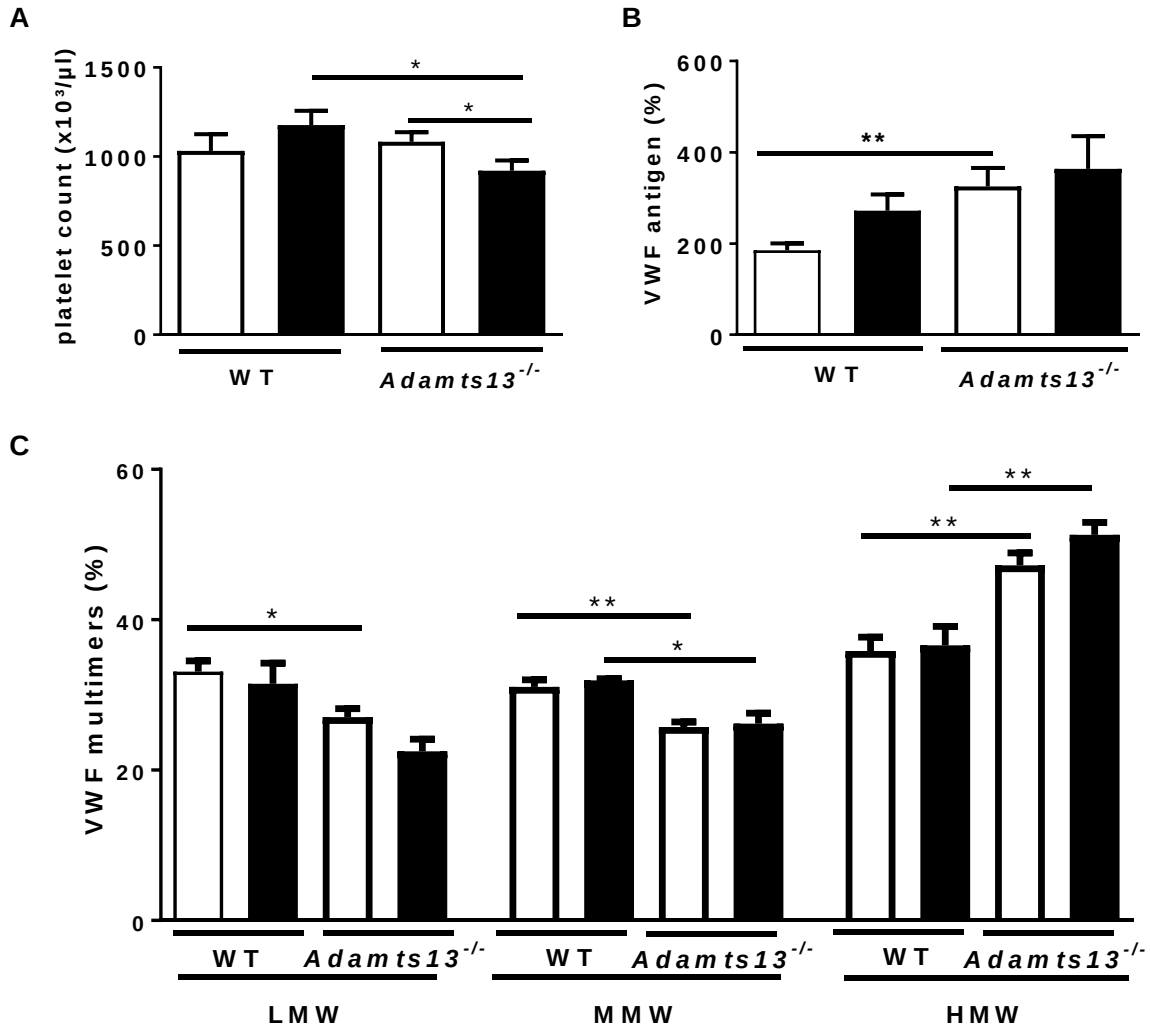

Figure 21: Effect of diet and genotype on platelet counts and VWF composition.
(A) platelet count, (B) plasma levels of VWF antigen and (C) VWF multimers are shown for wild-type (WT) and ADAMTS13 deficient (*Adamts13*$^{-/-}$) mice kept on standard fat diet (white bars) or high fat diet (black bars). Data represent means ± SEM of 8 to 10 experiments. * $p < 0.05$, ** $p < 0.01$.

Effect of diet and genotype on liver steatosis

Plasma levels of the liver enzymes alkaline phosphatases and ALT were elevated for obese versus lean *Adamts13*$^{-/-}$ mice, but not for WT mice. AST levels were not affected by either diet or genotype. Plasma PAI-1 and CRP levels were significantly elevated after HFD feeding in both genotypes (Table 7). Histological analysis of liver steatosis by H&E staining (Figure 22A) revealed a higher degree of steatosis in obese as

compared to lean mice, without however, significant difference between genotypes. Quantitative analysis revealed that HFD feeding significantly enhanced liver steatosis in both genotypes, but showed no difference between genotypes (Figure 22B). Determination of triglycerides in liver extracts confirmed significantly higher levels after HFD as compared to SFD feeding, but did not show a difference between genotypes (Figure 22C). Determination of plasma triglyceride levels did not reveal significant effects of diet or genotype (Table 7). Glucose levels correlated positively with liver weight for WT mice ($r = 0.81$; $p < 0.0001$) and for *Adamts13*$^{-/-}$ mice ($r = 0.54$; $p < 0.01$). Obese *Adamts13*$^{-/-}$ mice had lower glucose levels than obese WT mice.

Table 7: Plasma levels of liver enzymes and inflammatory markers of WT and *Adamts13*$^{-/-}$ mice.

	WT		***Adamts13*$^{-/-}$**	
	SFD	**HFD**	**SFD**	**HFD**
Glucose (mg/dl)	124 ± 7.99	211 ± 16.2***	129 ± 7.95	156 ± 7.68*$^{\#\#}$
Triglycerides (mg/dl)	42 ± 1.8	40 ± 7.0	38 ± 1.4	33 ± 2.1
Alkaline phosphates (U/l)	41 ± 1.9	47 ± 5.2	39 ± 2.1	55 ± 5.8 **
AST (U/l)	191 ± 29	151 ± 21.1	167 ± 21.3	237 ± 39.4
ALT (U/l)	72 ± 9.1	95 ± 12	59 ± 3.9	122 ± 27.3**
PAI-1 (ng/ml)	7.4 ± 2.2	30 ± 11*	13 ± 5.2	42 ± 18
CRP (µg/ml)	5.8 ± 0.33	9.4 ± 1.3*	5.6 ± 0.52	6.4 ± 0.89**
PAP (ng/ml)	437 ± 50.4	559 ± 48.2	331 ± 38.8	483 ± 65.3
TAT (ng/ml)	93 ± 34	115 ± 39	60 ± 15	118 ± 30

Data are means ± SEM of 8 to 10 experiments. * $p < 0.05$, ** $p < 0.01$, *** $p < 0.001$ for HFD versus SFD fed mice; $^{\#\#}$ $p < 0.01$ for *Adamts13*$^{-/-}$ versus WT mice.

Abbreviations: WT: wild-type; SFD: standard fat diet; HFD: high fat diet; AST: aspartate aminotransaminase; ALT: alanine aminotransferase; PAI: plasminogen activator inhibitor; CRP: C-reactive protein; PAP: plasmin-α2-antiplasmin complex; TAT: thrombin-antithrombin III complex.

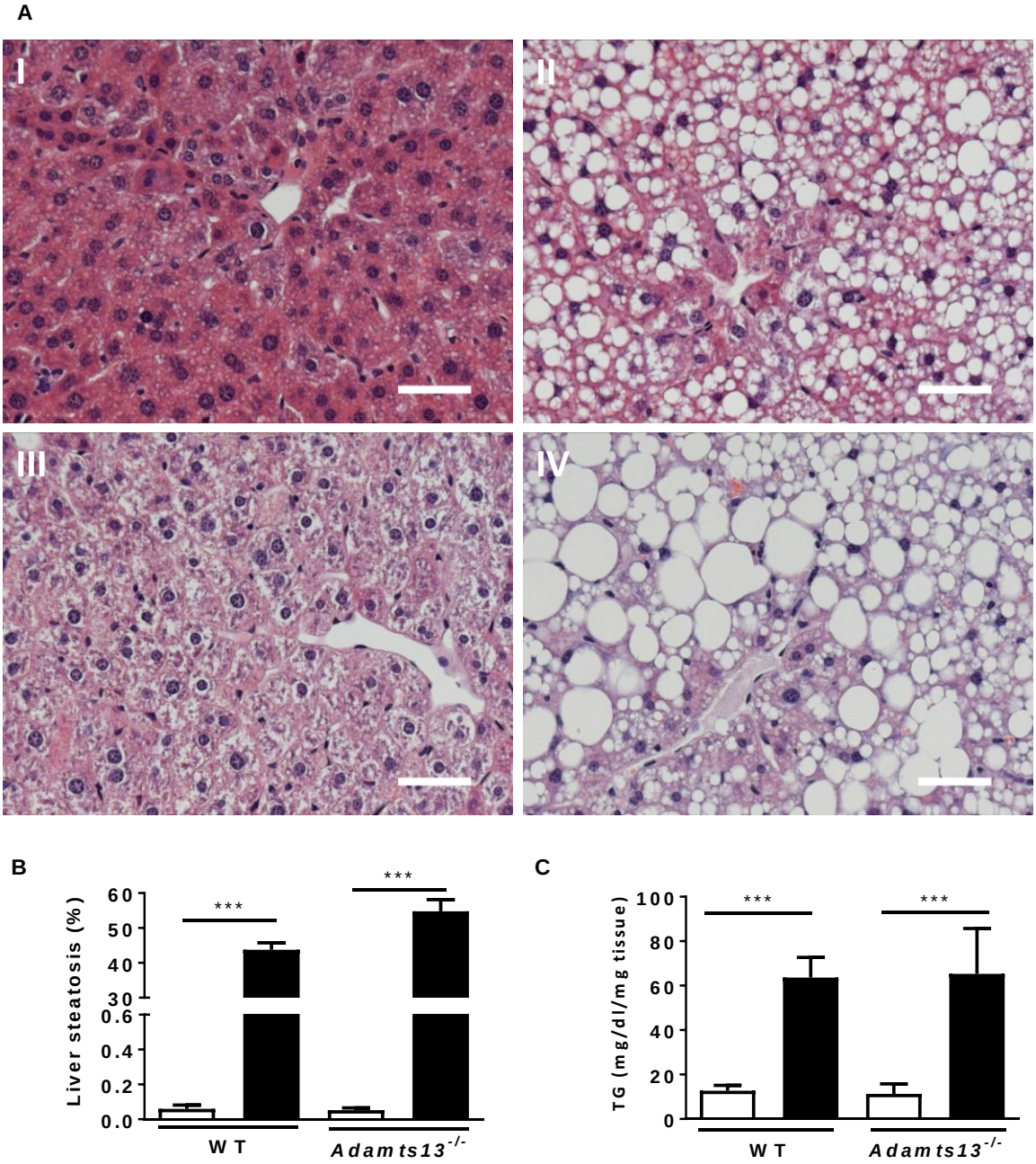

Figure 22: Effect of diet-induced obesity and ADAMTS13 deficiency on liver steatosis.
(A) Haematoxylin/eosin staining (40x) of liver sections of WT mice on SFD (I) or HFD (II) and of *Adamts13*$^{-/-}$ mice on SFD (III) or HFD (IV). The scale bars correspond to 50 µm. (B) Quantitative analysis of steatosis of liver sections and (C) triglycerides (TG). Data represent means ± SEM of 8 to 10 experiments. *** p < 0.001.

Effect of diet and genotype on expression of macrophage/inflammatory, steatosis, fibrosis and oxidative stress markers

Gene expression analysis in liver tissues was performed to evaluate the effects of diet or genotype on markers of macrophages/inflammation, oxidative stress, steatosis/triglyceride metabolism and fibrosis (Figure 23). Analysis of the effect of diet on expression of inflammatory gene markers in the liver of *Adamts13*$^{-/-}$ mice revealed significantly enhanced expression of F4/80, TNF-α and MCP-1 (as expected) and reduced expression of IL-6, IL-1 and arginase in mice on HFD compared to SFD. Essentially similar observations were made for obese as compared to lean WT mice (Figure 23A). Analysis of the effect of genotype showed reduced expression of F4/80, MCP-1 and IL-6 and enhanced expression of TNF-α for lean *Adamts13*$^{-/-}$ versus lean WT mice, whereas on HFD only TNF-α expression was elevated for *Adamts13*$^{-/-}$ versus WT mice. Expression of Mannose R was not affected by either diet or genotype. Analysis of the effect of diet on expression of oxidative stress markers in the liver revealed markedly reduced expression of catalase, SOD1, NOX4 and XDH1 for obese versus lean mice, but no marked differences between genotypes (data not shown). Analysis of the effect of diet on expression of markers of triglyceride metabolism in the liver revealed markedly enhanced expression of CD36 on HFD versus SFD for *Adamts13*$^{-/-}$ as well as WT mice. Expression of SREBP-1, FAS, FATP, MCAD and PPAR-α were not drastically different between both genotypes (Figure 23B). Analysis of the effect of diet on expression of fibrosis markers showed higher levels of TIMP-1, col1a1 and TGF-β after a HFD in both *Adamts13*$^{-/-}$ and WT mice, but no differences between genotypes (Figure 23C).

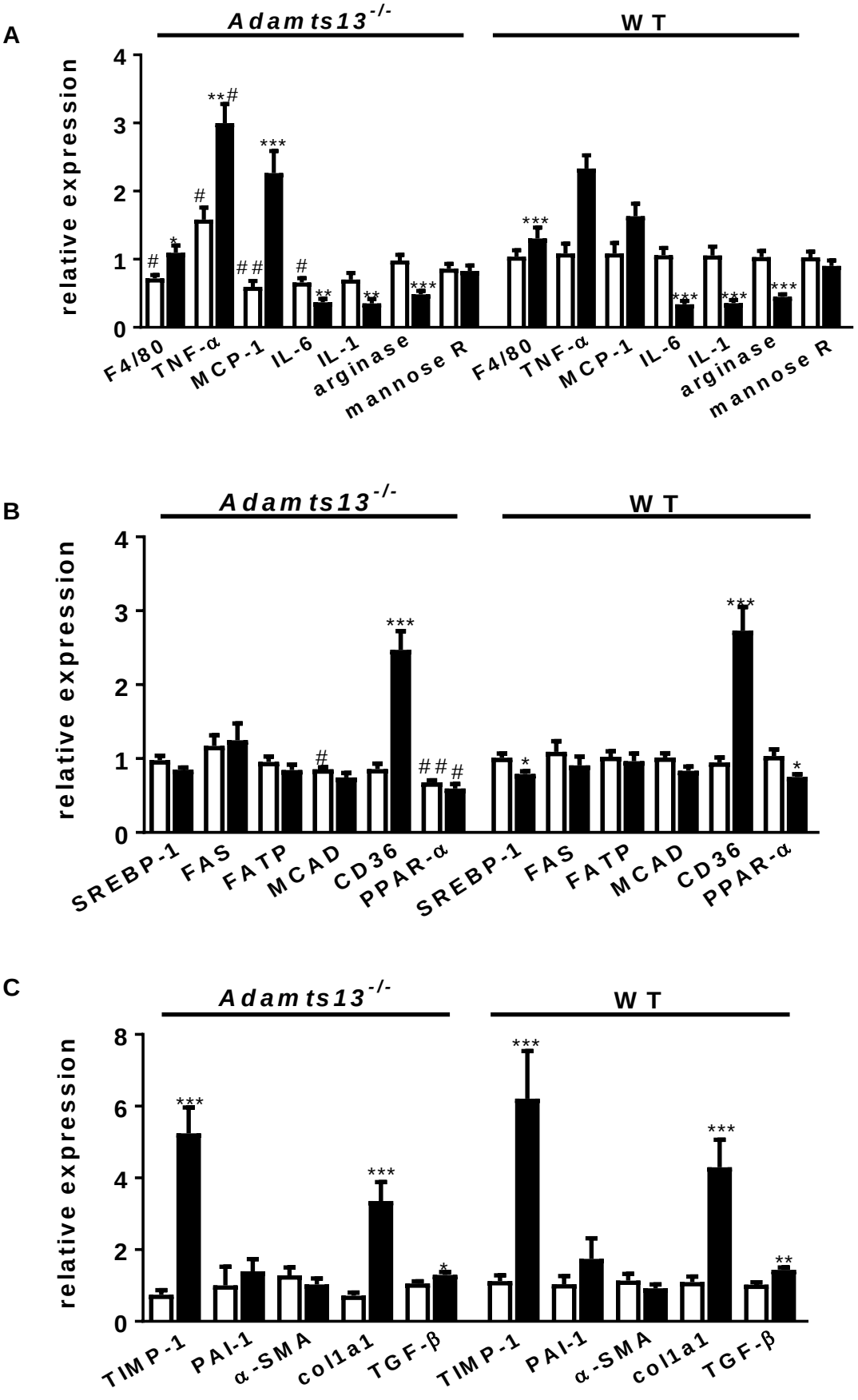
A
Adamts13-/-
WT
relative expression
F4/80
TNF-α
MCP-1
IL-6
IL-1
arginase
mannose R
B
Adamts13-/-
WT
relative expression
SREBP-1
FAS
FATP
MCAD
CD36
PPAR-α
C
Adamts13-/-
WT
relative expression
TIMP-1
PAI-1
α-SMA
col1a1
TGF-β

Figure 23: Effect of diet and genotype on expression of markers of macrophages/inflammation, steatosis/ triglyceride metabolism and fibrosis in the liver.
Relative gene expression is shown for WT and *Adamts13*$^{-/-}$ mice fed a SFD (lean, white bars) or a HFD (obese, black bars). * p < 0.05, ** p < 0.01, *** p < 0.001 for obese versus lean mice. # p < 0.05, ## p < 0.01, for *Adamts13*$^{-/-}$ versus WT mice on the same diet. Markers of macrophages/inflammation in panel A, markers of steatosis/triglyceride metabolism in panel B and markers of fibrosis in panel C.

Thus, the combination of obesity and ADAMTS13 deficiency (*Adamts13*$^{-/-}$ mice on HFD versus WT mice on SFD) resulted for the inflammatory makers in significantly higher expression of TNF-α and MCP-1 and lower expression of IL-6, IL-1 and arginase, for the oxidative stress markers in reduced expression of NOX4 and XDH1, for fibrosis markers in higher expression levels of TIMP-1, col1a1 and TGF-β and for the markers of triglyceride metabolism in reduced expression of SREBP-1, MCAD and PPAR-α and enhanced expression of CD36. Most of these differences are, however, due to the HFD feeding and not to the genotype.

DISCUSSION

An apparent paradox with respect to the potential role of ADAMTS13 in development of acute liver failure has recently been recognized. On the one hand, ADAMTS13 activity was found to be inversely related to disease severity and outcome, possibly due to formation of platelet-rich thrombi in the diseased liver. On the other hand, however, no UL-VWF multimers were found in the systemic circulation, and high molecular weight (HMW) VWF levels and VWF function were even reduced as compared to healthy controls (23). We have in the present study directly investigated a potential role of ADAMTS13 in liver steatosis and monitored activation of the fibrinolytic system. Therefore, we used ADAMTS13 deficient mice with diet-induced steatosis, achieved by feeding mice with a HFD for 15 weeks.

In a previous study, we have shown that obesity in WT mice is associated with enhanced ADAMTS13 antigen and activity levels, but that ADAMTS13 deficiency does not markedly affect adipose tissue development (18). In the present study, histopathological examination of liver sections revealed a more abundant presence of microthrombi for obese versus lean ADAMTS13 deficient mice, but not for obese WT mice. This finding is compatible with higher prevalence of HMW VWF multimers (lack of cleavage by ADAMTS13), promoting microthrombi and with lower platelet count (incorporated in microthrombi) for obese *Adamts13*$^{-/-}$ mice. These thrombi indeed were predominantly platelet-rich as shown by TSP-1 staining. Enhanced microthrombosis is observed only with the combination of obesity and ADAMTS13 deficiency, indicating that both conditions are required. Circulating PAP levels were comparable for both genotypes, but lower levels were found in the liver of ADAMTS13 deficient mice on SFD (no differences between obese WT and obese *Adamts13*$^{-/-}$ mice). These findings do not support more extensive activation of the fibrinolytic system in the obese

ADAMTS13 deficient mice, and are not compatible with a compensatory action of plasmin to remove hepatic microthrombi in absence of ADAMTS13. This, therefore, could suggest that more extensive endothelial damage is required for activation of the fibrinolytic system, and subsequent degradation of UL-VWF multimers.

Common liver diseases include syndromes ranging from isolated steatosis to non-alcoholic steatohepatitis (NASH), characterized by fat accumulation in the liver in combination with hepatocyte ballooning, inflammation and liver damage, with or without fibrosis (14). Increasing age, obesity and diabetes are known risk factors for development of NASH (15). It is also recognized that the increased prevalence of obesity and metabolic syndrome is paralleled by an increase in non-alcoholic fatty liver disease (NAFLD) (16, 17). NASH is an independent risk factor for cardiovascular diseases (18), and is associated with an increased risk for development of cirrhosis and liver-related deaths (15); it is becoming a major indication for liver transplantation (24). Our present data indicate that obesity triggers NAFLD, but that ADAMTS13 deficiency does not distinctly affects its development. Liver steatosis was indeed found to be significantly more pronounced upon HFD as compared to SFD feeding, but was overall not different between *Adamts13*$^{-/-}$ and WT mice. Indeed, similar levels of triglycerides in the liver and comparable hepatic expression of steatosis and fibrosis markers were observed for both genotypes on either diet. Analysis of the liver enzymes alkaline phosphatases, AST and ALT did reveal effects of the diet, but no marked differences between genotypes. Park *et al*. (25) reported that enhanced production of the cytokines TNF-α and IL-6 plays a central role in liver inflammation in dietary and genetic obesity. We also observed enhanced liver expression of TNF-α upon HFD feeding of WT and ADAMTS13 deficient mice, but lower expression of IL-6. It was previously recognized that the role of IL-6 in obesity may be more complex than

anticipated (26). Thus, whereas obesity promotes liver steatosis in both genotypes, ADAMTS13 deficiency does not appear to aggravate it for lean or obese mice. Furthermore, our finding of more pronounced microthrombosis in obese *Adamts13*$^{-/-}$ mice without aggravating steatohepatitis does not suggest a causative relation between both processes.

In summary, our study shows that ADAMTS13 deficiency in obese mice promotes formation of hepatic microthrombi, and does not support a compensatory role of plasmin in removal of microthrombi in the absence of ADAMTS13. Our data furthermore confirm that obesity promotes NASH, but do not support a detrimental role of ADAMTS13 in development of liver steatosis in obese mice.

REFERENCES

1. Le Goff C, Cormier-Daire V. The ADAMTS(L) family and human genetic disorders. Hum Mol Genet. 2011;20(R2):R163-7.
2. Fujimura Y, Matsumoto M, Yagi H, Yoshioka A, Matsui T, Titani K. Von Willebrand factor-cleaving protease and Upshaw-Schulman syndrome. Int J Hematol. 2002;75(1):25-34.
3. Levy GG, Nichols WC, Lian EC, Foroud T, McClintick JN, McGee BM, et al. Mutations in a member of the ADAMTS gene family cause thrombotic thrombocytopenic purpura. Nature. 2001;413(6855):488-94.
4. Kokame K, Matsumoto M, Soejima K, Yagi H, Ishizashi H, Funato M, et al. Mutations and common polymorphisms in ADAMTS13 gene responsible for von Willebrand factor-cleaving protease activity. Proc Natl Acad Sci U S A. 2002;99(18):11902-7.
5. Levy GG, Motto DG, Ginsburg D. ADAMTS13 turns 3. Blood. 2005;106(1):11-7.
6. Savasan S, Lee SK, Ginsburg D, Tsai HM. ADAMTS13 gene mutation in congenital thrombotic thrombocytopenic purpura with previously reported normal VWF cleaving protease activity. Blood. 2003;101(11):4449-51.
7. Furlan M, Robles R, Galbusera M, Remuzzi G, Kyrle PA, Brenner B, et al. von Willebrand factor-cleaving protease in thrombotic thrombocytopenic purpura and the hemolytic-uremic syndrome. N Engl J Med. 1998;339(22):1578-84.
8. Tsai HM, Lian EC. Antibodies to von Willebrand protease in acute thrombotic thrombocytopenic purpura. N Engl J Med. 1998;339(22):1585-94.
9. Tersteeg C, de Maat S, De Meyer SF, Smeets MW, Barendrecht AD, Roest M, et al. Plasmin cleavage of von Willebrand factor as an emergency bypass for ADAMTS13 deficiency in thrombotic microangiopathy. Circulation. 2014;129(12):1320-31.
10. Hugenholtz GC, Lisman T. Letter by Hugenholtz and Lisman regarding article, "plasmin cleavage of von Willebrand factor as an emergency bypass for ADAMTS13 deficiency in thrombotic microangiopathy". Circulation. 2015;131(2):e18.
11. Uemura M, Tatsumi K, Matsumoto M, Fujimoto M, Matsuyama T, Ishikawa M, et al. Localization of ADAMTS13 to the stellate cells of human liver. Blood. 2005;106(3):922-4.
12. Uemura M, Fujimura Y, Ko S, Matsumoto M, Nakajima Y, Fukui H. Pivotal role of ADAMTS13 function in liver diseases. Int J Hematol. 2010;91(1):20-9.
13. Takaya H, Uemura M, Fujimura Y, Matsumoto M, Matsuyama T, Kato S, et al. ADAMTS13 activity may predict the cumulative survival of patients with liver cirrhosis in comparison with the Child-Turcotte-Pugh score and the Model for End-Stage Liver Disease score. Hepatol Res. 2012;42(5):459-72.
14. Uemura M, Matsuyama T, Ishikawa M, Fujimoto M, Kojima H, Sakurai S, et al. Decreased activity of plasma ADAMTS13 may contribute to the development of liver disturbance and multiorgan failure in patients with alcoholic hepatitis. Alcohol Clin Exp Res. 2005;29(12 Suppl):264S-71S.
15. Matsumoto M, Kawa K, Uemura M, Kato S, Ishizashi H, Isonishi A, et al. Prophylactic fresh frozen plasma may prevent development of hepatic VOD after stem cell transplantation via ADAMTS13-mediated restoration of von Willebrand factor plasma levels. Bone Marrow Transplant. 2007;40(3):251-9.
16. Ikeda H, Tateishi R, Enooku K, Yoshida H, Nakagawa H, Masuzaki R, et al. Prediction of hepatocellular carcinoma development by plasma ADAMTS13 in chronic hepatitis B and C. Cancer Epidemiol Biomarkers Prev. 2011;20(10):2204-11.
17. Watanabe N, Ikeda H, Kume Y, Satoh Y, Kaneko M, Takai D, et al. Increased production of ADAMTS13 in hepatic stellate cells contributes to enhanced plasma ADAMTS13 activity in rat models of cholestasis and steatohepatitis. Thromb Haemost. 2009;102(2):389-96.
18. Geys L, Scroyen I, Roose E, Vanhoorelbeke K, Lijnen HR. ADAMTS13 deficiency in mice does not affect adipose tissue development. Biochim Biophys Acta. 2015;1850(7):1368-74.
19. Motto DG, Chauhan AK, Zhu G, Homeister J, Lamb CB, Desch KC, et al. Shigatoxin triggers thrombotic thrombocytopenic purpura in genetically susceptible ADAMTS13-deficient mice. J Clin Invest. 2005;115(10):2752-61.
20. Van De Craen B, Scroyen I, Vranckx C, Compernolle G, Lijnen HR, Declerck PJ, et al. Maximal PAI-1 inhibition in vivo requires neutralizing antibodies that recognize and inhibit glycosylated PAI-1. Thromb Res. 2012;129(4):e126-33.
21. Lijnen HR, Van Hoef B, Dewerchin M, Collen D. Alpha(2)-antiplasmin gene deficiency in mice does not affect neointima formation after vascular injury. Arterioscler Thromb Vasc Biol. 2000;20(6):1488-92.

22. Lotta LA, Wu HM, Mackie IJ, Noris M, Veyradier A, Scully MA, et al. Residual plasmatic activity of ADAMTS13 is correlated with phenotype severity in congenital thrombotic thrombocytopenic purpura. Blood. 2012;120(2):440-8.
23. Hugenholtz GC, Adelmeijer J, Meijers JC, Porte RJ, Stravitz RT, Lisman T. An unbalance between von Willebrand factor and ADAMTS13 in acute liver failure: implications for hemostasis and clinical outcome. Hepatology. 2013;58(2):752-61.
24. Charlton MR. Fibrosing NASH: on being a blind man in a dark room looking for a black cat (that isn't there). Gastroenterology. 2011;140(1):25-8.
25. Park EJ, Lee JH, Yu GY, He G, Ali SR, Holzer RG, et al. Dietary and genetic obesity promote liver inflammation and tumorigenesis by enhancing IL-6 and TNF expression. Cell. 2010;140(2):197-208.
26. Tilg H, Moschen AR. Evolution of inflammation in nonalcoholic fatty liver disease: the multiple parallel hits hypothesis. Hepatology. 2010;52(5):1836-46.

Chapter 5

Role of ADAMTS13 in murine diet-induced liver steatosis

Paper in press

Geys L, Roose E, Vanhoorelbeke K, Bedossa P, Scroyen I, Lijnen HR. Role of ADAMTS13 in diet-induced liver steatosis. Molecular Medicine Reports. 2017.

ABSTRACT

Previous studies, mainly based on increased or decreased plasma levels, have reported conflicting data on a potential functional role of ADAMTS13 in the pathogenesis of liver diseases, including non-alcoholic steatohepatitis (NASH). The aim of this study was to evaluate whether ADAMTS13 deficiency affects development of NASH.

Therefore, male wild-type (WT) and ADAMTS13 deficient (*Adamts13*$^{-/-}$) mice were kept on a steatosis-inducing diet devoid of methionine and choline (MCD) or a control diet (MCC) for 4 weeks. Induction of NASH did not affect plasma ADAMTS13 antigen levels of WT mice. MCD as compared to MCC feeding resulted in lower body and liver weight without, however, differences between genotypes. Plasma levels of the liver enzymes AST and ALT were significantly higher for MCD versus MCC fed *Adamts13*$^{-/-}$ and WT mice, but were not different between genotypes. Liver triglyceride levels were also higher after MCD feeding, but were not different between WT and *Adamts13*$^{-/-}$ mice. *Adamts13*$^{-/-}$ mice on both diets displayed higher insulin sensitivity as compared to WT mice. On the MCC diet, neither genotype showed clear histological abnormalities in the liver, whereas severe steatosis and fibrosis were observed on MCD diet, but comparable for both genotypes. This was supported by comparably enhanced hepatic expression in both genotypes on MCD diet of the steatosis marker CD36 and of the fibrosis marker TIMP-1.

Thus, our data do not support a functional role of ADAMTS13 in this murine model of NASH.

INTRODUCTION

Non-alcoholic fatty liver disease (NAFLD) is characterized by excessive fat accumulation in the liver of patients without a history of alcohol abuse. NAFLD is classified into simple steatosis and non-alcoholic steatohepatitis (NASH). In patients with NASH, in addition to steatosis, also intralobular inflammation and hepatocellular ballooning are observed, frequently with progressive fibrosis (1). Over time, NASH may progress to liver cirrhosis and hepatocellular carcinoma (2-4). It is recognized that the increased prevalence of obesity and metabolic syndrome is paralleled by an increase in NAFLD (5, 6), as up to 80% of obese subjects suffer from NAFLD (7). Worldwide about 20% of all adults have NAFLD and 2 to 3% suffer from NASH (8).

ADAMTS13 (a disintegrin and metalloproteinase with thrombospondin-1 repeat, member 13) is a proteinase that specifically cleaves multimeric von Willebrand factor (VWF), thereby preventing accumulation of ultra-large VWF (UL-VWF) multimers and subsequent platelet clumping and formation of microthrombi that disturb the microcirculation and impair oxygen supply to organs (9). ADAMTS13 is mainly produced by stellate cells in the liver (10), of which proliferation contributes to steatohepatitis and fibrosis. This is compatible with enhanced ADAMTS13 antigen and activity levels observed in rats suffering from diet-induced steatosis and fibrosis (11). Several previous studies have, however, reported conflicting data on a potential functional role of ADAMTS13 in the pathogenesis of liver diseases (reviewed in (12)). A beneficial effect of ADAMTS13 activity was observed on liver disease severity, and increased ADAMTS13 activity was related with a better prognosis of liver cirrhosis (13), alcoholic hepatitis (14) and hepatic veno-occlusive disease (15). In contrast, a detrimental effect of ADAMTS13 was reported on hepatocellular carcinoma risk in patients suffering from chronic liver disease (16). Thus, it is not clear whether NASH is

related with increased or decreased levels of ADAMTS13, nor whether ADAMTS13 plays a functional role in its development. In order to resolve these apparent contradictions, we have subjected wild-type and ADAMTS13 deficient mice to a steatosis-inducing diet.

MATERIALS & METHODS

Animal model

Male ADAMTS13 deficient (*Adamts13*$^{-/-}$) and wild-type (WT) mice (genetic background, C57Bl6/J x 129X1/Sv x CASA/RK) were used and genotyped as described (17, 18). The mice were kept from the age of 5 weeks on in individual micro-isolation cages on a 12h day/night cycle and fed for 4 weeks with a lipogenic diet devoid of methionine and choline (MCD; #02960034, MPbiomedicals, Illkirch Cedex, France) or the MCD diet supplemented with 3 g/kg DL-methionine and 2 g/kg choline chloride (control diet, MCC; #02960414, MPbiomedicals) (n = 10 or 5 for *Adamts13*$^{-/-}$ or WT mice on each diet). Water was always available *ad libitum*. Body weight and food intake were measured at weekly intervals. At the end of the diet, after fasting for 6h, blood was taken from the tail of unanesthetized mice for determination of blood glucose concentrations using the Accu-chek performa meter and blood glucose test strips (Roche diagnostics, Roche, Basel, Switserland). At the end of the experiment, the mice were sedated and blood was taken from the retro-orbital sinus on trisodium citrate (0.01 M), before they were killed by cervical dislocation. Platelets were counted (Cell Dyn 3200R, Abbott Diagnostics, Illinois, USA). Livers, SC and GN adipose tissues were removed and weighed. Portions were used for RNA or protein extraction or were fixed in 4% formaldehyde for histological analysis.

All animal experiments were approved by the KU Leuven ethical committee (P158-2011) and performed in accordance with the NIH Guide for the Care and Use of Laboratory Animals (1996) and the EU Directive 2010/63/EU for animal experiments.

Metabolic and inflammatory parameters

Total, HDL and LDL cholesterol, triglycerides, alkaline phosphatases, alanine aminotransferase (ALT) and aspartate aminotransaminase (AST) levels in plasma

were evaluated using routine clinical assays. Insulin levels in plasma were determined by ELISA (Ultrasensitive mouse insulin ELISA 10-1249-01; Mercodia AB, Uppsala, Sweden). The homeostasis model assessment of insulin resistance (HOMA-IR) was determined using the formula: [fasting plasma insulin (ng/ml) × fasting blood glucose (mg/dl)]/405. Liver tissue extracts were prepared by adding alcoholic KOH (30%) to a sample of 30 mg. Samples were incubated overnight at 55°C to digest the tissue, and 1 M $MgCl_2$ was added to the digested sample (1:1 vol/vol), mixed well, incubated on ice for 10 minutes and centrifuged for 30 minutes. The supernatant was analyzed using the triglycerides FS* kit (Diasys, Holzheim, Germany).

Histological and microscopic analysis

Liver samples were fixed in 4% buffered formaldehyde and embedded in paraffin. Sections (4 µm) were stained with haematoxylin/eosin (H&E) or picrosirius red to assess steatosis or fibrosis, respectively. All liver biopsies were analyzed by an expert liver pathologist, blinded to the genotype and diet. Steatosis and fibrosis were diagnosed and semiquantitatively scored according to the NASH-Clinical Research Network criteria (19, 20). Hepatocyte ballooning was classified as 0 (none), 1 (few) or 2 (many cells/prominent ballooning). Foci of lobular inflammation were scored as 0 (no foci), 1 (< 2 foci per 200× field), 2 (2–4 foci per 200× field) and 3 (> 4 foci per 200× field). Fibrosis was scored as stage F0 (no fibrosis), stage F1a (mild, zone 3, perisinusoidal fibrosis), stage F1b (moderate, zone 3, perisinusoidal fibrosis), stage F1c (portal/periportal fibrosis), stage F2 (perisinusoidal and portal/periportal fibrosis), stage F3 (bridging fibrosis) and stage F4 (cirrhosis). Severity of the disease was assessed using the NAS (NAFLD activity score) as the unweighted sum of scores of steatosis, hepatocyte ballooning and lobular inflammation (21). Percentage of fibrosis was quantitated by morphometry from digitalized sirius red stained sections (22).

RNA extraction and expression analysis

RNA extraction from livers was performed using the RNeasy mini kit (Qiagen, Basel, Switzerland) according to the manufacturer's protocol. Ten ng/µl RNA was reverse transcribed into cDNA using the Multiscribe^{TM} Reverse Transcriptase kit (Life Technologies, Carlsbad, CA). RT-qPCR was done in the ABI 7500 Fast Sequence detector (Life Technologies) to detect the markers listed in Table 8. Analyses were performed with the ΔΔCT method (23) using the 7500 System SDS software (Life Technologies). Normalization was carried out to correct for fluctuations caused by sample differences. Fold changes for MCD diet fed mice were calculated as $2^{-\Delta\Delta CT}$ relative to MCC diet. β-actin was used as housekeeping gene.

VWF and ADAMTS13 antigen

Murine VWF and ADAMTS13 antigen levels were measured in plasma using home-made ELISA's (24, 25).

Statistical analysis

Data are presented as means ± standard error of the means (SEM). Statistical significance between groups was analyzed with the non-parametric Mann-Whitney U test. Analysis of the data was performed using Prism 6 (GraphPad Software Inc., San Diego, CA). Values of $p < 0.05$ are considered statistically significant.

Table 8: Markers detected by qPCR using TaqMan gene expression assays.

Gene	Assay†	Gene	Assay†
F4/80	Mm00802529_m1	**PPAR-α**	Mm00440939_m1
TNF-α	Mm00443258_m1	**TIMP-1**	Mm0441818_m1
MCP-1	Mm00441242_m1	**PAI-1**	Mm0435860_m1
IL-6	Mm0446190_m1	**α-SMA**	Mm00725412_s1
Arginase	Mm00475988_m1	**Col1a1**	Mm00801666_g1
Mannose receptor	Mm00485148_m1	**TGF-β**	Mm01178820_m1
FAS	Mm01253300_g1	**β-actin**	Mm01205647_g1
CD36	Mm00432403_m1		

	FW primer	RV primer	probe
ADAMTS13	GGAGCCCAAGGATG TGTGTCTT	TCTCTGGAGGTGAG AGGGAGGAT	6FAM CTTGGCCACCATGC

†Assays purchased from Life Technologies (Carlsbad, CA).

RESULTS

Feeding WT and *Adamts13*$^{-/-}$ mice with the MCD diet for 4 weeks as compared to the control MCC diet, resulted in rapid and progressive weight loss for both genotypes (Figure 24A). Food intake was comparable for WT and *Adamts13*$^{-/-}$ mice kept on MCC (3.3 versus 3.0 g/mouse/day) or on MCD diet (2.4 versus 2.2 g/mouse/day). At the end of the diets, total body weight was comparable for WT and *Adamts13*$^{-/-}$ mice on MCC diet (30.0 ± 1.4 versus 27.4 ± 0.6 g) as well as on MCD diet (17.2 ± 0.4 versus 17 ± 0.4 g). As expected, subcutaneous (SC) and gonadal (GN) fat mass were markedly lower for both genotypes when kept on MCD versus MCC diet (Figure 24B, C).

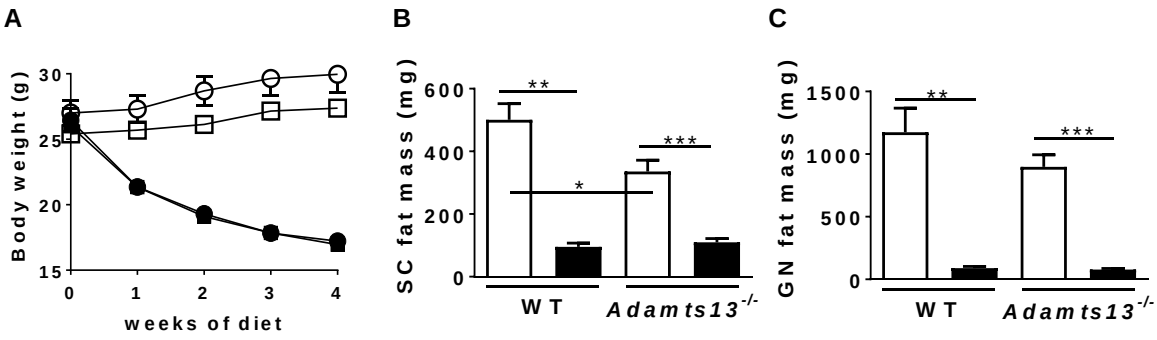

Figure 24: Effect of MCD and MCC diets on body and fat mass of wild-type (WT) and ADAMTS13 deficient (*Adamts13*$^{-/-}$) mice.

Body weight evolution (A) and weight of subcutaneous (SC) fat (B) and gonadal (GN) fat (C) of mice kept on MCD (black symbols and bars) or MCC (white symbols and bars) diet for 4 weeks. Data are means ± SEM of 10 (*Adamts13*$^{-/-}$) (squares) or 5 (WT) (circles) experiments for each diet. *, **, *** p < 0.05, p < 0.01, p < 0.001.

For WT mice, plasma ADAMTS13 antigen levels were not significantly different on MCC or MCD diet (183 ± 12 *versus* 205 ± 17 % of pooled plasma), and relative expression of ADAMTS13 mRNA in the liver was comparable on both diets (0.91 ± 0.07 *versus* 1.0 ± 0.05). VWF antigen levels were comparable for both genotypes on either diet (Table 9). However, platelet counts were significantly lower for *Adamts13*$^{-/-}$ mice fed the MCD versus MCC, but this was not seen in WT mice (Table 9). Analysis

of plasma metabolic parameters (Table 9) revealed for MCD *versus* MCC diets for both genotypes: 1) lower glucose levels; 2) lower total and HDL cholesterol levels; 3) higher LDL cholesterol levels ($p < 0.05$ for *Adamts13*$^{-/-}$ mice; trend for WT mice, as for the MCC diet n = 2, because of undetectable levels of LDL cholesterol in other samples); and 4) comparable triglyceride levels. Insulin levels were markedly lower on MCD versus MCC diet (only significant for the *Adamts13*$^{-/-}$ mice due to small sample sizes for WT mice), and were reduced for *Adamts13*$^{-/-}$ versus WT mice on MCC. Thus, HOMA-IR revealed higher insulin sensitivity for *Adamts13*$^{-/-}$ mice on MCC diet (Table 9).

Total liver weight was reduced upon MCD feeding, but was not affected by genotype (Figure 25A). Liver enzymes AST and ALT were markedly higher in MCD fed as compared to MCC fed mice, but were not different between genotypes (Table 9). Liver triglyceride levels were also enhanced upon MCD feeding, but not affected by genotype (Figure 25B).

H&E staining of liver sections revealed more pronounced steatosis in MCD as compared to MCC fed mice of both genotypes (Figure 26A), as confirmed by quantitative analysis (Figure 25C).

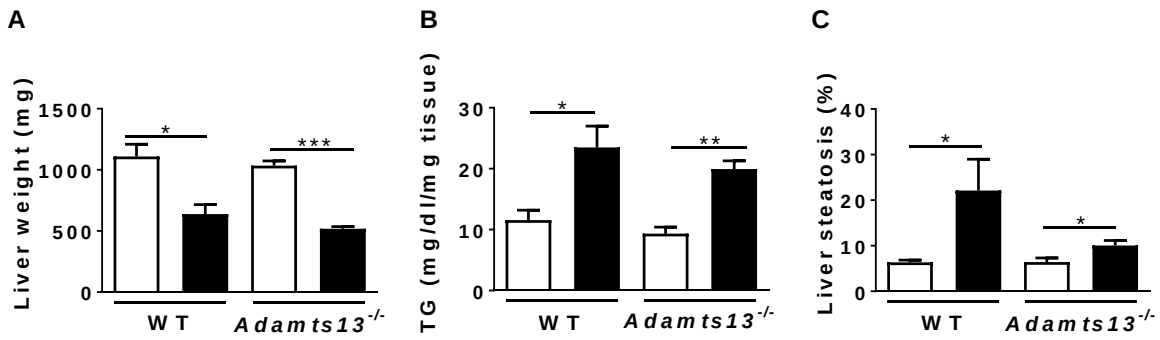

Figure 25: Effect of MCD and MCC diets on liver of wild-type (WT) and ADAMTS13 deficient (*Adamts13*$^{-/-}$) mice.

Weight of liver (A) of mice kept on MCD (black bars) or MCC (white bars) diet for 4 weeks. Liver triglyceride (TG) levels (B) and quantitation of liver steatosis (C). Data are means ± *SEM* of 10 (*Adamts13*$^{-/-}$) or 5 (WT) experiments for each diet. *, **, *** $p < 0.05$, $p < 0.01$, $p < 0.001$ for MCD versus MCC.

Further histological analysis of liver sections revealed that after 4 weeks of MCC diet feeding, both WT (3/5 with score 1) and *Adamts13*$^{-/-}$ (3/10 with score 1) mice showed only mild steatosis, whereas they all scored 0 for hepatocyte ballooning, lobular inflammation, and fibrosis (Figure 26A and Table 10). However, after MCD feeding, both WT and *Adamts13*$^{-/-}$ mice presented with histological abnormalities with markedly enhanced scores for steatosis, ballooning, lobular inflammation and NAS without, however, significant differences between genotypes (Figure 26C). Also fibrosis stage and score were deteriorated in MCD versus MCC fed mice, but did not show a clear genotype effect (Figure 26B and Table 10).

Table 9: Plasma levels of metabolic parameters, liver enzymes, endogenous VWF and platelet count of WT and *Adamts13*$^{-/-}$ mice kept on MCC or MCD diet for 4 weeks.

	WT		***Adamts13*$^{-/-}$**	
	MCC	**MCD**	**MCC**	**MCD**
Glucose (mg/dl)	194 ± 20.4	94 ± 8.98**	177 ± 6.09	93 ± 3.86****
Insulin (ng/ml)	0.58 ± 0.12	0.17 ± 0.07	0.26 ± 0.06#	0.05 ± 0.01*
HOMA-IR	0.30 ± 0.06	0.05 ± 0.02*	0.12 ± 0.03#	0.01 ± 0.002**
Triglycerides (mg/dl)	45 ± 4.6	36 ± 0.95	35 ± 1.7	31 ± 1.0#
Cholesterol (mg/dl)	89 ± 14	31 ± 5*	84 ± 5	30 ± 1***
HDL cholesterol (mg/dl)	82 ± 13	22 ± 2*	75 ± 4#	17 ± 1***
LDL cholesterol (mg/dl)	1.5 ± 1.5	7.5 ± 0.9	3.8 ± 0.9	7.0 ± 0.9*
Alkaline phosphatases (U/l)	63 ± 7.6	76 ± 12	56 ± 3.2	77 ± 3.0*
AST (U/l)	58 ± 13	185 ± 62.0*	78 ± 12	173 ± 14.4***
ALT (U/l)	22 ± 2.0	193 ± 53.4**	39 ± 9.0	227 ± 24.0****
Platelet count (x10³/µl)	917 ± 84.3	752 ± 117	829 ± 25	565 ± 65**
mVWF (% to NMP)	302 ± 2.53	250 ± 38.9	247 ± 40.3	168 ± 37.5

Data are means ± *SEM* of 10 (*Adamts13*$^{-/-}$) or 5 (WT) experiments for each diet. * $p < 0.05$, ** $p < 0.01$, *** $p < 0.001$, **** $p < 0.0001$ for MCD versus MCC fed mice; # $p < 0.05$ for *Adamts13*$^{-/-}$ versus WT mice.

Abbreviations: WT: wild-type; *Adamts13*$^{-/-}$: ADAMTS13 deficient; MCD: methionine and choline deficient diet; MCC: control diet; HOMA-IR: Homeostasis Model Assessment of Insulin Resistance; HDL: high density lipoprotein; LDL: low density lipoprotein; AST: aspartate aminotransaminase; ALT: alanine aminotransferase; mVWF: murine von Willebrand factor; NMP: normal mouse plasma.

Relative expression of markers of triglyceride metabolism, fibrosis and inflammation were not markedly affected by genotype on either diet (data not shown). Histological observations on steatosis and fibrosis were compatible with markedly enhanced gene expression of the steatosis maker CD36 and the fibrosis marker TIMP-1 for MCD versus MCC fed mice of both genotypes (Figure 27A, B). Analysis of hepatic inflammatory markers revealed enhanced expression of TNF-α for WT mice on MCD versus MCC feeding (Figure 27C).

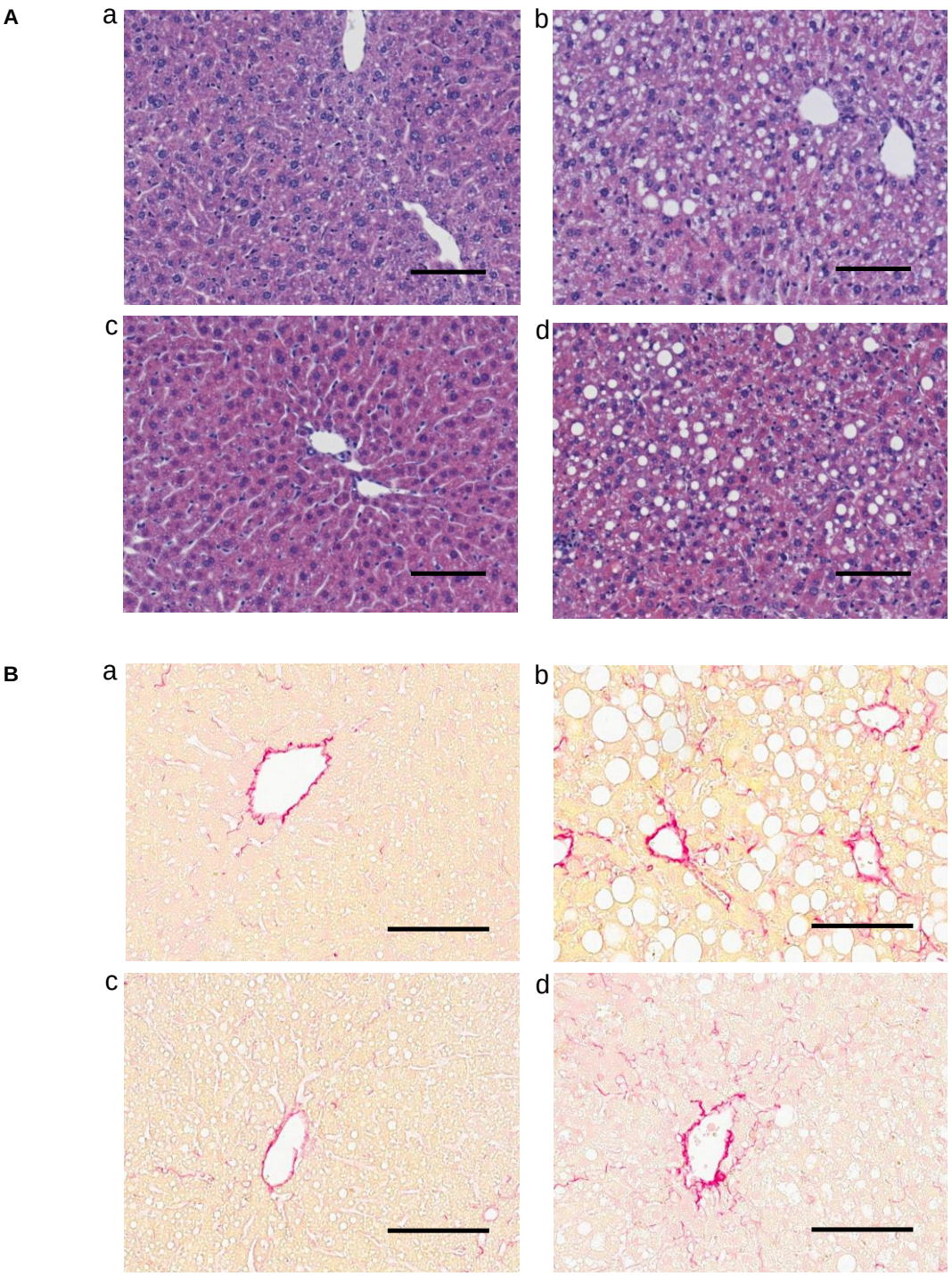
A
a
b
c
d
B
a
b
c
d

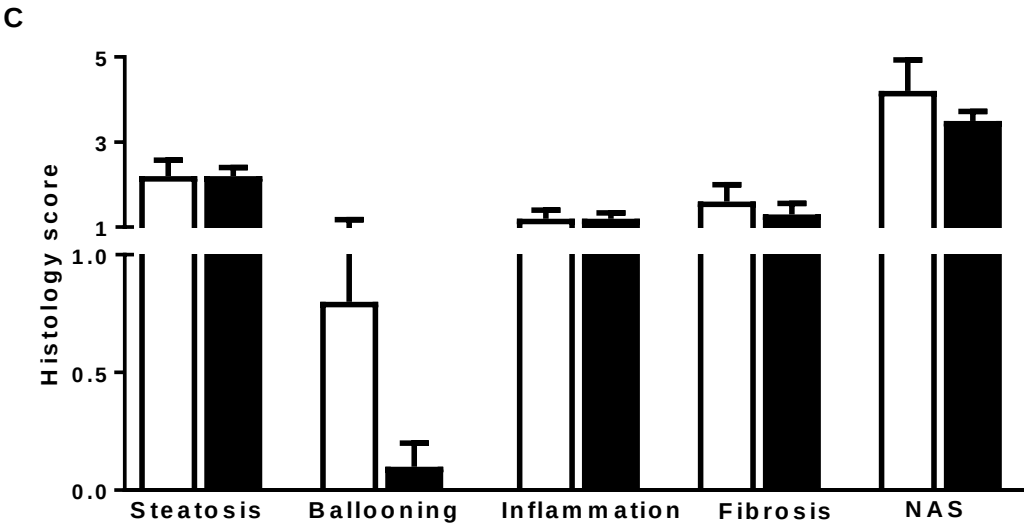

Figure 26: MCD diet-induced steatohepatitis in WT and *Adamts13*$^{-/-}$ mice.
H&E (A) and sirius red (B) stainings of liver sections of WT (a, b) and *Adamts13*$^{-/-}$ (c, d) mice kept on MCC (a, c) or MCD (b, d) diet for 4 weeks. Scale bars represent 100 µm. (C) Histological scoring of steatosis, hepatocyte ballooning, inflammation, fibrosis and NAS for mice kept on MCD diet. Data are means ± SEM of 10 (*Adamts13*$^{-/-}$, black bars) or 5 (WT, white bars) determinations.

DISCUSSION

Deficiency of ADAMTS13, the VWF cleaving proteinase, causes thrombotic thrombocytopenic purpura (TTP), a rare but severe thrombotic disease (26). A functional role of ADAMTS13 has also been suggested in liver diseases, but available data are controversial (12). We have previously shown that ADAMTS13 antigen and activity levels are enhanced in obese mice, whereas ADAMTS13 deficiency did not affect development of NASH in obese mice (27, 28). In the present study, we show that a steatosis-inducing diet, independent of obesity, induces NASH to a comparable extent in ADAMTS13 deficient and WT mice.

In patients, visceral obesity is frequently associated with NAFLD and NASH. These conditions may be associated with reduced ADAMTS13 activity, as reported in an

obese patient with recurrent TTP; defective ADAMTS13 synthesis was suggested as a possible consequence of NASH (29).

Table 10: Histological scoring* of liver sections of mice kept on MCC or MCD diet for 4 weeks.

	MCC		MCD	
	WT	***Adamts13*$^{-/-}$**	**WT**	***Adamts13*$^{-/-}$**
Microvesicular steatosis				
Score 0 (<5%)	2/5	7/10	0/5	0/10
Score 1 (5-33%)	3/5	3/10	1/5	1/10
Score 2 (33–66%)	0/5	0/10	2/5	6/10
Score 3 (>66%)	0/5	0/10	2/5	3/10
Hepatocyte ballooning				
Score 0	5/5	10/10	2/5	9/10
Score 1	0/5	0/10	2/5	1/10
Score 2	0/5	0/10	1/5	0/10
Lobular inflammation				
Score 0	5/5	10/10	0/5	0/10
Score 1	0/5	0/10	4/5	8/10
Score 2	0/5	0/10	1/5	2/10
Score 3	0/5	0/10	0/5	0/10
Fibrosis				
F0	5/5	10/10	1/5	1/10
Stage F1a	0/5	0/10	0/5	6/10
Stage F1b	0/5	0/10	4/5	2/10
Stage F1c	0/5	0/10	0/5	0/10
Stage F2	0/5	0/10	0/5	1/10

***See Materials & Methods**

Abbreviations: MCD: methionine and choline deficient diet; MCC: control diet; WT: wild-type; *Adamts13*$^{-/-}$: ADAMTS13 deficient.

Furthermore, an apparent paradox with respect to the potential role of ADAMTS13 in development of acute liver failure has recently been recognized. On the one hand, ADAMTS13 activity was found to be inversely related to disease severity and outcome, whereas on the other hand, no UL-VWF multimers were found in the systemic

circulation, and high molecular weight VWF levels and VWF function were even reduced in patients with acute liver failure as compared to healthy controls (30).

Since NASH is difficult to study in humans because of the slow progression of the disease and of ethical considerations, animal models of NASH are crucial to better understand the pathogenesis of the disease. The model of feeding rodents with a diet deficient in both methionine and choline (MCD) used in this study, is one of the most common in NASH research (31-34). It is characterized by macrovesicular steatosis, hepatocellular death, inflammation, oxidative stress and fibrosis. Due to this diet, the mice lose weight and the metabolic profile is opposite to that of typical human NASH, e.g. the mice do not develop hyperlipidemia or hypertriglyceridemia and do not present with insulin resistance. However, liver injury and steatohepatitis are histologically similar to humans (35-37). The severity of NASH induced in rodents by the MCD diet depends on the administration scheme, but also on species, gender and strain of the animal (38, 39). With the administration scheme used in this study, 4 weeks of MCD/MCC, we have previously observed a protective effect of ADAMTS5 deficiency (C57Bl/6J background) on development of NASH (40). A similar administration scheme was used by Rinella *et al.* (34). Although we have not performed a time course, different effects of ADAMTS13 deficiency at earlier time points (e.g. 2 weeks) cannot be totally excluded.

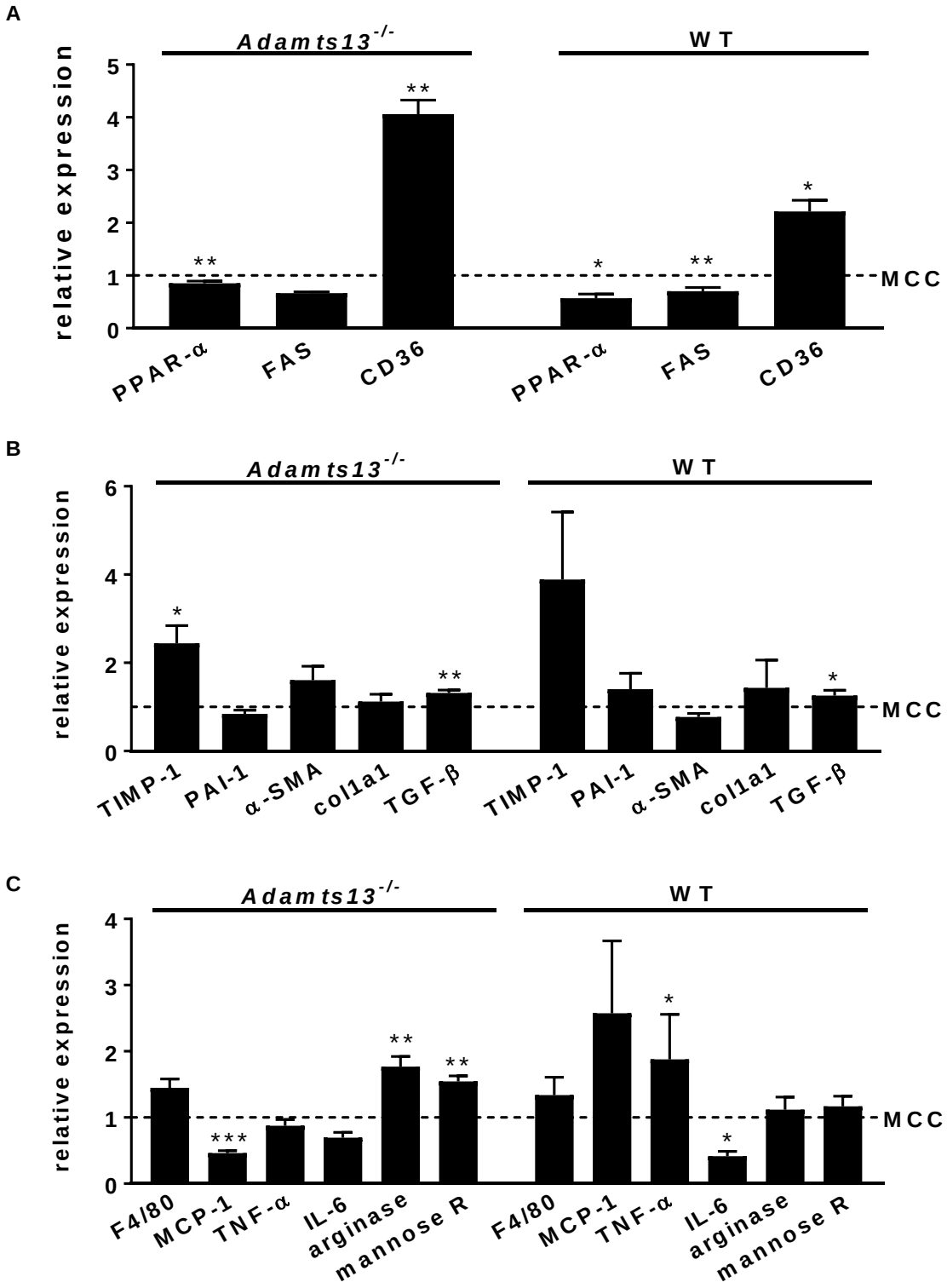

Figure 27: Effect of MCD diet on expression of hepatic markers of steatosis/triglyceride metabolism (A), fibrosis (B) and inflammation (C).

Gene expression relative to the MCC diet is shown for MCD fed mice. Data represent means ± SEM of 10 (*Adamts13*$^{-/-}$) or 5 (WT) experiments for each diet. *, **, *** $p < 0.05$, $p < 0.01$, $p < 0.001$ for MCD versus MCC.

It was reported that steatosis in mice kept on the MCD diet develops within 2 to 4 weeks and progression to fibrosis by 8 to 10 weeks (41-43). Our mice indeed developed steatosis on the 4-weeks diet, which was not restricted to centrolobular or periportal liver portions, but was diffusely spread throughout the liver tissue. More pronounced steatosis and higher liver triglyceride levels were found upon MCD feeding of both genotypes, but without differences between genotypes. None of the mice developed severe fibrosis, although mRNA expression of the fibrosis markers TIMP-1 and TGF-β in liver tissue was enhanced after the short-term MCD diet. These findings were supported by similar hepatic expression profiles of steatosis and fibrosis markers for both genotypes. The liver enzymes alkaline phosphatases, AST and ALT were enhanced on the MCD diet, indicating liver damage, but without marked differences between genotypes. Platelet counts tended to be lower after MCD diet feeding, most pronounced in *Adamts13*$^{-/-}$ mice. To our knowledge, this has not been reported previously and remains unexplained.

In the present study, we observed that both the WT and the ADAMTS13 deficient mice fed with the MCD diet lose weight and present with low fasting blood glucose, but do not develop insulin resistance, in agreement with previous studies (31, 32, 37). Actually, we observed improved insulin sensitivity upon MCD feeding of both genotypes, whereas the HOMA-IR on either diet was lower for *Adamts13*$^{-/-}$ versus WT mice. In contrast, in mice with high fat induced obesity, glucose and insulin sensitivity were not different between WT and *Adamts13*$^{-/-}$ mice (27).

Taken together, our present and previous (27) data do not support a functional role for ADAMTS13 in the development of steatohepatitis in mouse models of diet-induced steatosis. This is in agreement with a recent study in patients with NASH, showing that plasma ADAMTS13 levels were not different from controls (44).

REFERENCES

1. Cassiman D, Jaeken J. NASH may be trash. Gut. 2008;57(2):141-4.
2. Powell EE, Cooksley WG, Hanson R, Searle J, Halliday JW, Powell LW. The natural history of nonalcoholic steatohepatitis: a follow-up study of forty-two patients for up to 21 years. Hepatology. 1990;11(1):74-80.
3. Harrison SA, Torgerson S, Hayashi PH. The natural history of nonalcoholic fatty liver disease: a clinical histopathological study. Am J Gastroenterol. 2003;98(9):2042-7.
4. Cohen JC, Horton JD, Hobbs HH. Human fatty liver disease: old questions and new insights. Science. 2011;332(6037):1519-23.
5. Bedogni G, Miglioli L, Masutti F, Tiribelli C, Marchesini G, Bellentani S. Prevalence of and risk factors for nonalcoholic fatty liver disease: the Dionysos nutrition and liver study. Hepatology. 2005;42(1):44-52.
6. Blachier M, Leleu H, Peck-Radosavljevic M, Valla DC, Roudot-Thoraval F. The burden of liver disease in Europe: a review of available epidemiological data. J Hepatol. 2013;58(3):593-608.
7. Sanyal AJ, American Gastroenterological A. AGA technical review on nonalcoholic fatty liver disease. Gastroenterology. 2002;123(5):1705-25.
8. Neuschwander-Tetri BA. Nonalcoholic steatohepatitis and the metabolic syndrome. Am J Med Sci. 2005;330(6):326-35.
9. Le Goff C, Cormier-Daire V. The ADAMTS(L) family and human genetic disorders. Hum Mol Genet. 2011;20(R2):R163-7.
10. Uemura M, Tatsumi K, Matsumoto M, Fujimoto M, Matsuyama T, Ishikawa M, et al. Localization of ADAMTS13 to the stellate cells of human liver. Blood. 2005;106(3):922-4.
11. Watanabe N, Ikeda H, Kume Y, Satoh Y, Kaneko M, Takai D, et al. Increased production of ADAMTS13 in hepatic stellate cells contributes to enhanced plasma ADAMTS13 activity in rat models of cholestasis and steatohepatitis. Thromb Haemost. 2009;102(2):389-96.
12. Uemura M, Fujimura Y, Ko S, Matsumoto M, Nakajima Y, Fukui H. Pivotal role of ADAMTS13 function in liver diseases. Int J Hematol. 2010;91(1):20-9.
13. Takaya H, Uemura M, Fujimura Y, Matsumoto M, Matsuyama T, Kato S, et al. ADAMTS13 activity may predict the cumulative survival of patients with liver cirrhosis in comparison with the Child-Turcotte-Pugh score and the Model for End-Stage Liver Disease score. Hepatol Res. 2012;42(5):459-72.
14. Uemura M, Matsuyama T, Ishikawa M, Fujimoto M, Kojima H, Sakurai S, et al. Decreased activity of plasma ADAMTS13 may contribute to the development of liver disturbance and multiorgan failure in patients with alcoholic hepatitis. Alcohol Clin Exp Res. 2005;29(12 Suppl):264S-71S.
15. Matsumoto M, Kawa K, Uemura M, Kato S, Ishizashi H, Isonishi A, et al. Prophylactic fresh frozen plasma may prevent development of hepatic VOD after stem cell transplantation via ADAMTS13-mediated restoration of von Willebrand factor plasma levels. Bone Marrow Transplant. 2007;40(3):251-9.
16. Ikeda H, Tateishi R, Enooku K, Yoshida H, Nakagawa H, Masuzaki R, et al. Prediction of hepatocellular carcinoma development by plasma ADAMTS13 in chronic hepatitis B and C. Cancer Epidemiol Biomarkers Prev. 2011;20(10):2204-11.
17. Motto DG, Chauhan AK, Zhu G, Homeister J, Lamb CB, Desch KC, et al. Shigatoxin triggers thrombotic thrombocytopenic purpura in genetically susceptible ADAMTS13-deficient mice. J Clin Invest. 2005;115(10):2752-61.
18. De Maeyer B, De Meyer SF, Feys HB, Pareyn I, Vandeputte N, Deckmyn H, et al. The distal carboxyterminal domains of murine ADAMTS13 influence proteolysis of platelet-decorated VWF strings in vivo. J Thromb Haemost. 2010;8(10):2305-12.
19. Kleiner DE, Brunt EM, Van Natta M, Behling C, Contos MJ, Cummings OW, et al. Design and validation of a histological scoring system for nonalcoholic fatty liver disease. Hepatology. 2005;41(6):1313-21.
20. Verbeek J, Lannoo M, Pirinen E, Ryu D, Spincemaille P, Vander Elst I, et al. Roux-en-y gastric bypass attenuates hepatic mitochondrial dysfunction in mice with non-alcoholic steatohepatitis. Gut. 2015;64(4):673-83.
21. Bedossa P, Poitou C, Veyrie N, Bouillot JL, Basdevant A, Paradis V, et al. Histopathological algorithm and scoring system for evaluation of liver lesions in morbidly obese patients. Hepatology. 2012;56(5):1751-9.
22. Bedossa P, Dargere D, Paradis V. Sampling variability of liver fibrosis in chronic hepatitis C. Hepatology. 2003;38(6):1449-57.

23. Livak KJ, Schmittgen TD. Analysis of relative gene expression data using real-time quantitative PCR and the 2(-Delta Delta C(T)) Method. Methods. 2001;25(4):402-8.
24. Verhenne S, Denorme F, Libbrecht S, Vandenbulcke A, Pareyn I, Deckmyn H, et al. Platelet-derived VWF is not essential for normal thrombosis and hemostasis but fosters ischemic stroke injury in mice. Blood. 2015;126(14):1715-22.
25. Deforche L, Tersteeg C, Roose E, Vandenbulcke A, Vandeputte N, Pareyn I, et al. Generation of Anti-Murine ADAMTS13 Antibodies and Their Application in a Mouse Model for Acquired Thrombotic Thrombocytopenic Purpura. PLoS One. 2016;11(8):e0160388.
26. Murrin RJ, Murray JA. Thrombotic thrombocytopenic purpura: aetiology, pathophysiology and treatment. Blood Rev. 2006;20(1):51-60.
27. Geys L, Scroyen I, Roose E, Vanhoorelbeke K, Lijnen HR. ADAMTS13 deficiency in mice does not affect adipose tissue development. Biochim Biophys Acta. 2015;1850(7):1368-74.
28. Geys L, Bauters D, Roose E, Tersteeg C, Vanhoorelbeke K, Hoylaerts MF, et al. ADAMTS13 deficiency promotes microthrombosis in a murine model of diet-induced liver steatosis. Thromb Haemost. 2016;116(6).
29. Lombardi AM, Fabris R, Berti de Marinis G, Marson P, Navaglia F, Plebani M, et al. Defective ADAMTS13 synthesis as a possible consequence of NASH in an obese patient with recurrent thrombotic thrombocytopenic purpura. Eur J Haematol. 2014;92(6):497-501.
30. Hugenholtz GC, Adelmeijer J, Meijers JC, Porte RJ, Stravitz RT, Lisman T. An unbalance between von Willebrand factor and ADAMTS13 in acute liver failure: implications for hemostasis and clinical outcome. Hepatology. 2013;58(2):752-61.
31. Takahashi Y, Soejima Y, Fukusato T. Animal models of nonalcoholic fatty liver disease/nonalcoholic steatohepatitis. World J Gastroenterol. 2012;18(19):2300-8.
32. Machado MV, Michelotti GA, Xie G, Almeida Pereira T, Boursier J, Bohnic B, et al. Mouse models of diet-induced nonalcoholic steatohepatitis reproduce the heterogeneity of the human disease. PLoS One. 2015;10(5):e0127991.
33. Caballero F, Fernandez A, Matias N, Martinez L, Fucho R, Elena M, et al. Specific contribution of methionine and choline in nutritional nonalcoholic steatohepatitis: impact on mitochondrial S-adenosyl-L-methionine and glutathione. J Biol Chem. 2010;285(24):18528-36.
34. Rinella ME, Elias MS, Smolak RR, Fu T, Borensztajn J, Green RM. Mechanisms of hepatic steatosis in mice fed a lipogenic methionine choline-deficient diet. J Lipid Res. 2008;49(5):1068-76.
35. Weltman MD, Farrell GC, Liddle C. Increased hepatocyte CYP2E1 expression in a rat nutritional model of hepatic steatosis with inflammation. Gastroenterology. 1996;111(6):1645-53.
36. Weltman MD, Farrell GC, Hall P, Ingelman-Sundberg M, Liddle C. Hepatic cytochrome P450 2E1 is increased in patients with nonalcoholic steatohepatitis. Hepatology. 1998;27(1):128-33.
37. Rinella ME, Green RM. The methionine-choline deficient dietary model of steatohepatitis does not exhibit insulin resistance. J Hepatol. 2004;40(1):47-51.
38. Fan JG, Qiao L. Commonly used animal models of non-alcoholic steatohepatitis. Hepatobiliary Pancreat Dis Int. 2009;8(3):233-40.
39. Kirsch R, Clarkson V, Shephard EG, Marais DA, Jaffer MA, Woodburne VE, et al. Rodent nutritional model of non-alcoholic steatohepatitis: species, strain and sex difference studies. J Gastroenterol Hepatol. 2003;18(11):1272-82.
40. Bauters D, Spincemaille P, Geys L, Cassiman D, Vermeersch P, Bedossa P, et al. ADAMTS5 deficiency protects against non-alcoholic steatohepatitis (NASH) in obesity. Liver Int. 2016.
41. Dela Pena A, Leclercq I, Field J, George J, Jones B, Farrell G. NF-kappaB activation, rather than TNF, mediates hepatic inflammation in a murine dietary model of steatohepatitis. Gastroenterology. 2005;129(5):1663-74.
42. Leclercq IA, Farrell GC, Field J, Bell DR, Gonzalez FJ, Robertson GR. CYP2E1 and CYP4A as microsomal catalysts of lipid peroxides in murine nonalcoholic steatohepatitis. J Clin Invest. 2000;105(8):1067-75.
43. Ip E, Farrell G, Hall P, Robertson G, Leclercq I. Administration of the potent PPARalpha agonist, Wy-14,643, reverses nutritional fibrosis and steatohepatitis in mice. Hepatology. 2004;39(5):1286-96.
44. Potze W, Siddiqui MS, Boyett SL, Adelmeijer J, Daita K, Sanyal AJ, et al. Preserved hemostatic status in patients with non-alcoholic fatty liver disease. J Hepatol. 2016.

Chapter 6

ADAMTS13 deficiency and obesity as risk factors for Thrombotic Thrombocytopenic Purpura in mice

Article in preparation

Geys L, Roose E, Scroyen I, Rottensteiner H, Tersteeg C, Hoylaerts MF, Vanhoorelbeke K, Lijnen HR. ADAMTS13 deficiency and obesity as risk factors for Thrombotic Thrombocytopenic Purpura.

ABSTRACT

Background: Thrombotic thrombocytopenic purpura (TTP) is caused by absence of ADAMTS13 activity. Thrombocytopenia is presumably related to formation of microthrombi rich in von Willebrand Factor (VWF) and platelets. Obesity may be a risk factor for TTP; it is associated with abundance of macrophages that may phagocytose platelets.

Aims: To evaluate the role of obesity and ADAMTS13 deficiency in TTP, and to establish whether macrophages contribute to thrombocytopenia.

Methods: Lean or obese ADAMTS13 deficient (*Adamts13*$^{-/-}$) and wild-type (WT) mice (n = 10 in each group) were triggered with 250 U/kg of recombinant human VWF (rVWF), and TTP characteristics were evaluated 24h later. In separate experiments, macrophages were depleted in the liver and spleen of lean and obese WT or *Adamts13*$^{-/-}$ mice (n = 5 in each group) by injection of clodronate liposomes, 48h before injection of rVWF.

Results: Obese *Adamts13*$^{-/-}$ mice had a lower platelet count than their lean counterparts (894 ± 35 x 10^3 versus 1010 ± 35 x 10^3 platelets/µL; $p < 0.05$) suggesting that they might be more susceptible to TTP development. Lean *Adamts13*$^{-/-}$ mice triggered with rVWF did not develop TTP, while typical TTP symptoms developed in obese *Adamts13*$^{-/-}$ mice, including severe thrombocytopenia (35 ± 13 x 10^3 versus 803 ± 113 x 10^3 platelets/µL; $p = 0.0001$) and higher LDH levels (630 ± 123 versus 329 ± 57 mU/mL; $p < 0.05$). Removal of hepatic and splenic macrophages by clodronate injection in obese *Adamts13*$^{-/-}$ mice before treatment with rVWF resulted in preservation of platelet counts measured 24h after the trigger (1327 ± 80 x 10^3/µL versus 187 ± 47 x 10^3/µL for control PBS liposomes; $p = 0.008$). *In vitro* experiments

with cultured macrophages confirmed VWF dose-dependent increase of platelet phagocytosis ($p = 0.001$).

Conclusions: Obese *Adamts13*$^{-/-}$ mice are more susceptible to induction of acute episodes of TTP than lean mice. Phagocytosis of platelets by macrophages contributes to thrombocytopenia after rVWF injection in this model.

INTRODUCTION

Thrombotic thrombocytopenic purpura (TTP) is a life-threatening disease caused by absence of ADAMTS13 (a disintegrin and metalloproteinase with thrombospondin-type 1 repeat, member 13) activity, which cleaves pro-thrombotic ultra-large von Willebrand Factor (UL-VWF) multimers. Consequently, TTP is characterized by formation of platelet-rich microthrombi in capillaries and arterioles that can lead to organ failure and death. Other symptoms are severe thrombocytopenia, microangiopathic hemolytic anemia, fever and neurological dysfunctions (1). Pregnancy, alcohol abuse, infections and surgery are common risk factors for TTP development (2). However, investigation of potential triggers for TTP development is hampered by the lack of suitable animal models. Indeed, *Adamts13*$^{-/-}$ mice do not spontaneously develop TTP, but this can be triggered by injection of high dose recombinant VWF (rVWF) (3) or of Shiga toxin (Stx) (4). We previously observed higher levels of ADAMTS13 antigen and activity in obese as compared to lean mice (5). This is in agreement with higher expression levels of ADAMTS13 in livers of obese mice (6). Therefore, obesity would not be expected to be a risk factor for TTP, as it is associated with higher levels of the VWF cleaving proteinase ADAMTS13. Moreover, ADAMTS13 has anti-inflammatory potential (7), whereas obesity is a state of low-grade chronic inflammation (8). Recent emerging data, however, suggest that obesity may be a trigger for acute TTP in humans. Thus, in patients with BMI > 30 kg/m^2 obesity was identified as a potential inducer of TTP with an odds ratio of 7.6 (9), and in the Oklahoma Registry of TTP patients more than 25% were morbidly obese (BMI > 40 kg/m^2) (10). Furthermore, a positive correlation was established between ADAMTS13 levels and BMI in humans (11). In the present study, we have evaluated the combined effect of obesity and ADAMTS13 deficiency in mice on development of a TTP phenotype.

It was also reported that macrophages play a role in thrombocytopenia associated with von Willebrand Disease (12). In TTP patients, it is assumed that severe thrombocytopenia is a consequence of the formation of microthrombi that are VWF and platelet-rich (13). Since macrophages are able to phagocytose and clear platelets from the circulation (14), we have also investigated whether platelet clearance in the liver and spleen by macrophages could contribute to TTP-related thrombocytopenia.

MATERIALS & METHODS

Animal model

Male ADAMTS13 deficient (*Adamts13*$^{-/-}$) and wild-type (WT) littermate mice (genetic background: C57Bl6/J x 129X1/Sv x CASA/RK) (4) were kept on a standard fat diet (SFD) (KM-04-k12, Muracon, Carfil, Oud-Turnhout, Belgium; 13% kcal as fat, caloric value 10.9 kJ/g) or a high fat diet (HFD) (E15721–34, Ssniff, Soest, Germany; 42 % kcal as fat, caloric value 22 kJ/g) (n = 20 WT and *Adamts13*$^{-/-}$ mice each for both diets) for 15 weeks from the age of 5 weeks on. Body weight was measured weekly. At the start and end of the diet, blood was taken from the retro-orbital plexus on trisodium citrate (0.01 M) or EDTA (0.5 M) under anesthesia with isoflurane, and whole blood cell analysis was performed (Cell Dyn 3200R, Abbott Diagnostics, Illinois, USA). At the end of the diet, mice (n = 9-11 per group) were injected in the tail vein with a threshold dose of rVWF (250 U/kg) (Baxalta Innovations GmbH, Vienna, Austria) to trigger TTP (see below). Twenty-four hours later, blood was taken and organs were harvested after anesthetizing with pentobarbital. Blood smears were stained with May-Grünwald-Giemsa to visualize schistocytes, and photographed on a Zeiss Axioplan 2 microscope (Carl Zeiss, Oberkochen, Germany). In separate experiments, obese (HFD) and lean (SFD) WT as well as *Adamts13*$^{-/-}$ mice were injected i.v. with 10 µL/g body weight liposome-encapsulated dichloromethylene bisphosphonate (clodronate) or control PBS liposomes (n = 5 with clodronate and PBS each) 48h before injection with rVWF (250 U/kg). *In vivo* platelet clearance was monitored in obese *Adamts13*$^{-/-}$ mice injected with clodronate or PBS 24h before injection with rVWF (250 U/kg).

All animal experiments were approved by the KU Leuven ethical committee (P153–2015) and performed in accordance with the NIH Guide for the Care and Use of Laboratory Animals (1996) and the EU Directive 2010/63/EU for animal experiments.

Determination of threshold dose of rVWF

To determine the threshold dose that does not reduce platelet counts below 600 x 10^3/µL (level of thrombocytopenia), lean *Adamts13*$^{-/-}$ mice were injected with different doses (0, 100, 250, 500, 1000, 1300 and 2000 U/kg) of rVWF (3). Blood was taken via the retro-orbital plexus under anesthesia with isoflurane at several time points (24, 48, 72, 96 and 120h) after injection to measure the platelet count.

Analysis

Murine ADAMTS13 and VWF levels in plasma were determined by ELISA as described previously (5, 15). Pooled plasma of WT mice was used as reference. Macrophages were stained with a F4/80 antibody (Serotec, Raleigh, NC), followed by signal amplification with the tyramide signal amplification biotin system (Perkin Elmer, Waltham, MA) and visualization with a streptavidin-enzyme conjugate, followed by DAB. Data are quantitatively expressed as percentage staining of section area. Analyses were performed with a Zeiss Axioplan 2 microscope and the AxioVision release 4.8 software (Carl Zeiss). Gene expression analysis of F4/80, MRC-1, IL-1β and TNF-α in liver tissue was analyzed by qPCR as described previously (5). Lactate dehydrogenase (LDH) activity levels were measured in plasma by the Lactate Dehydrogenase Activity Assay according to manufacturer's protocol (BioVision Incorporated, Milpitas, CA).

Platelet isolation and labeling

For the *in vitro* study, lean WT mice were anesthetized with pentobarbital and blood was obtained by cardiac puncture, diluted (6/1) in ACD buffer (93 mM sodium citrate, 7 mM citric acid, 14 mM dextrose, pH 6.8 supplemented with apyrase (100 mU/mL) (A6410, Sigma: Darmstadt, Germany); platelet-rich plasma (PRP) was obtained by centrifugation at 1600g for 30s followed immediately by centrifugation at 115g for 5

minutes. The PRP was diluted in ACD (1/3) and centrifuged at 950g for 5 minutes, followed by resuspension of the platelet pellet in Tyrode buffer (137 mM NaCl, 12 mM $NaHCO_3$, 2 mM KCl, 0.34 mM Na_2HPO_4, 1 mM $MgCl_2$, 2 mM $CaCl_2$, 5.5 mM glucose, and 5 mM HEPES [N-2-hydroxyethylpiperazine-N′-2-ethanesulfonic acid], pH 7.4). Washed platelets were labeled with CMFDA-Green (10 µM for 30 min at 37°C) (Molecular Probes, Life Technologies). Afterwards 1 µM prostaglandin E1 (PGE1; Sigma Aldrich, Saint-Quentin, France) was added before centrifugation (to remove non-incorporated dye), to suppress platelet activation.

For the *in vivo* study, obese WT mice were anesthetized with pentobarbital and blood was obtained by cardiac puncture in ACD-C buffer (124 mM tri-sodium citrate, 130 mM citric acid, 110 mM dextrose, pH 6.5), washed in wash buffer (140 mM NaCl, 5 mM KCl, 12 mM tri-sodium citrate, pH 6.5, supplemented with 100 mU/mL apyrase and 1 µM PGE1). PRP, obtained by centrifugation at 1600g for 30s followed immediately by centrifugation at 115g for 5 minutes. was supplemented by ACD (1/10), 100 mU/mL apyrase and 1 µM PGE1, and washed in wash buffer and centrifuged for 5 minutes at 950g; platelets were finally diluted in Tyrode buffer (10 mM HEPES, 140 mM NaCl, 3 mM KCl, 5 mM $NaHCO_3$, 0.5 mM $MgCl_2$, and 10 mM glucose, pH 7.4). Washed platelets were labeled with CMTMR-Orange (10 µM for 30 min at 37°C) (Molecular Probes, Life Technologies) in Tyrode buffer supplemented with 100 mU/mL apyrase and 1 µM PGE1. To remove non-incorporated dye, platelets were centrifuged for 5 minutes at 950g.

In vitro platelet phagocytosis by macrophages

Four days after i.p. injection of 4% thioglycollate, peritoneal macrophages were harvested in RPMI medium (Thermofisher Scientific, Gent, Belgium) and incubated with red blood cell (RBC) lysis buffer (eBioscience, San Diego, USA) for 5 minutes. Cells were counted and seeded at a density of 500 x 10^3 cells per well (3.8 cm^2) in RPMI medium supplemented with 10% fetal bovine serum (FBS) and 1% penicillin/streptomycin (PenStrep; Invitrogen, Paisly, UK). After attaching overnight, macrophages were washed with PBS to remove non-adherent cells and incubated for 45 minutes in an atmosphere of 95% humidified air–5 % CO_2 at 37°C with 5 µM Cell Tracker Orange CMTMR in DMEM/F12 (Thermofisher Scientific) supplemented with 10 mM L-glutamine (Thermofisher Scientific) and 1% PenStrep. Afterwards, remaining dye was removed by washing with PBS. CMFDA-Green labeled washed murine platelets were added at a density of 5 platelets per macrophage, together with increasing doses of rVWF (0-15 U/mL) and botrocetin (3 µg/mL/U rVWF; Sigma-Aldrich, Overijse, Belgium) to promote rVWF binding to platelets. Cells were incubated for 20h in DMEM/F12 medium supplemented with 10 mM L-glutamine, 10% FBS and 1% PenStrep at 37°C after which they were washed and fixed with 4% formaldehyde (Thermofisher Scientific) in PBS. Phagocytosis was analyzed and quantitated by using a fluorescence Zeiss Axioplan 2 microscope (Carl Zeiss). For each condition, total amount of macrophages, total amount of platelets, macrophages with phagocytosed platelets (yellow) and total number of phagocytosed platelets were assessed.

In vivo platelet clearance/aggregation

Obese *Adamts13*$^{-/-}$ mice were injected with 10 µL/g body weight PBS or clodronate liposomes. Twenty-four hours later, 200 µL of washed fluorescently labeled (CMTMR-Orange) platelets obtained from obese WT mice (diluted in Tyrode buffer

supplemented with 1 µM PGE1 to a final concentration of 500 x 10^3 platelets/µL) was injected via the tail vein in obese *Adamts13*$^{-/-}$ mice. Threshold dose of rVWF (250 U/kg) was injected i.v. 1h after injection of fluorescent-labeled platelets. Twenty-four hours later, blood was taken via retro-orbital bleeding (0.5 M EDTA), platelets were counted and blood smears were prepared with 4 µL of blood. Mice were perfused by saline and killed by cervical translocation, before liver and spleen were removed. Microaggregates/single platelets were qualitatively visualized using the fluorescence Zeiss Axioplan 2 microscope (Carl Zeiss).

Statistical analysis

Data are presented as means ± standard error of the means (SEM). Statistical significance between groups was analyzed with the non-parametric Mann-Whitney U or non-parametric Wilcoxon test. Analysis of the data was performed using Prism 7 (GraphPad Software Inc., San Diego, CA). Values of $p < 0.05$ are considered statistically significant.

RESULTS

Obese Adamts13$^{-/-}$ mice do not develop TTP

After 15 weeks of HFD, both WT and *Adamts13$^{-/-}$* mice gained significantly more weight as compared to SFD feeding (Figure 28A). This was associated with significantly enhanced ADAMTS13 antigen levels after HFD feeding of WT mice, but with reduced levels after SFD feeding (Figure 28B).

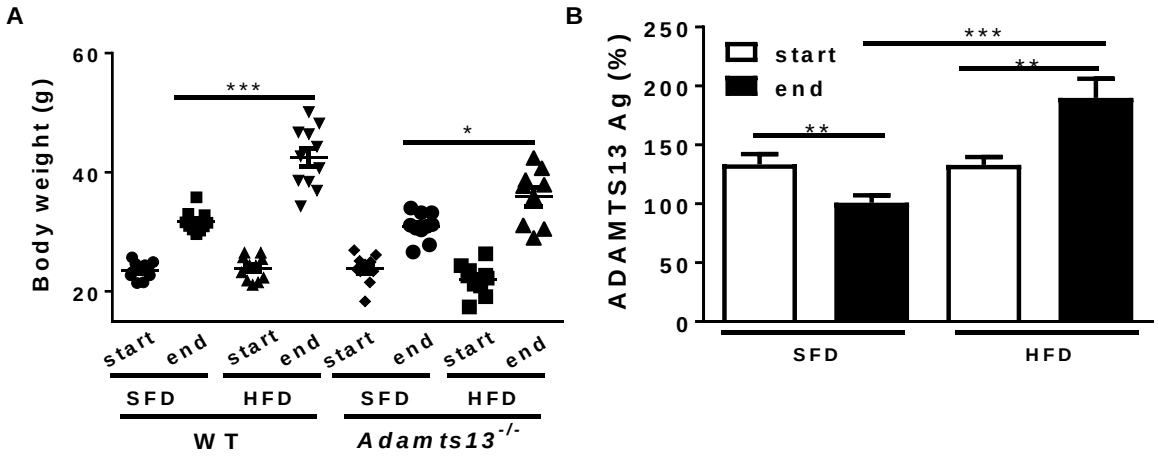

Figure 28: Phenotype of wild-type (WT) and ADAMTS13 deficient (*Adamts13$^{-/-}$*) mice kept on a standard fat (SFD) or high fat diet (HFD).
(A) Body weight at the start and end of the diet. (B) ADAMTS13 antigen (Ag) levels, as compared to a reference plasma pool, in plasma of WT mice at the start and end of the diet. Data are means ± SEM of 9-11 experiments with * p < 0.05, ** p < 0.01 and *** p < 0.001 (Mann-Whitney U test).

At the start of the diet, plasma VWF antigen levels were not different in the four groups (data not shown). After 15 weeks on HFD, VWF levels were significantly increased as compared to SFD feeding of both genotypes. On SFD, there was no significant difference between genotypes, whereas on HFD the VWF levels were lower for the *Adamts13$^{-/-}$* mice (Figure 29A). Plasma levels of lactate dehydrogenase (LDH) activity were higher after HFD in *Adamts13$^{-/-}$* mice reflecting more organ damage, but were not affected by genotype (Figure 29B). Hemoglobin and hematocrit levels were not different between WT and *Adamts13$^{-/-}$* mice on SFD or HFD (Table 11). Obese as

compared to lean mice of both genotypes displayed enhanced hepatic macrophage content, as determined by quantitative analysis of F4/80 staining (Figure 29C). Platelet count was comparable for WT and *Adamts13*$^{-/-}$ mice at the start of the diet. At the end of the diet, platelet counts were reduced for obese as compared to lean WT as well as *Adamts13*$^{-/-}$ mice (Figure 29D), suggesting that obesity may represent a risk for enhanced platelet consumption or clearance.

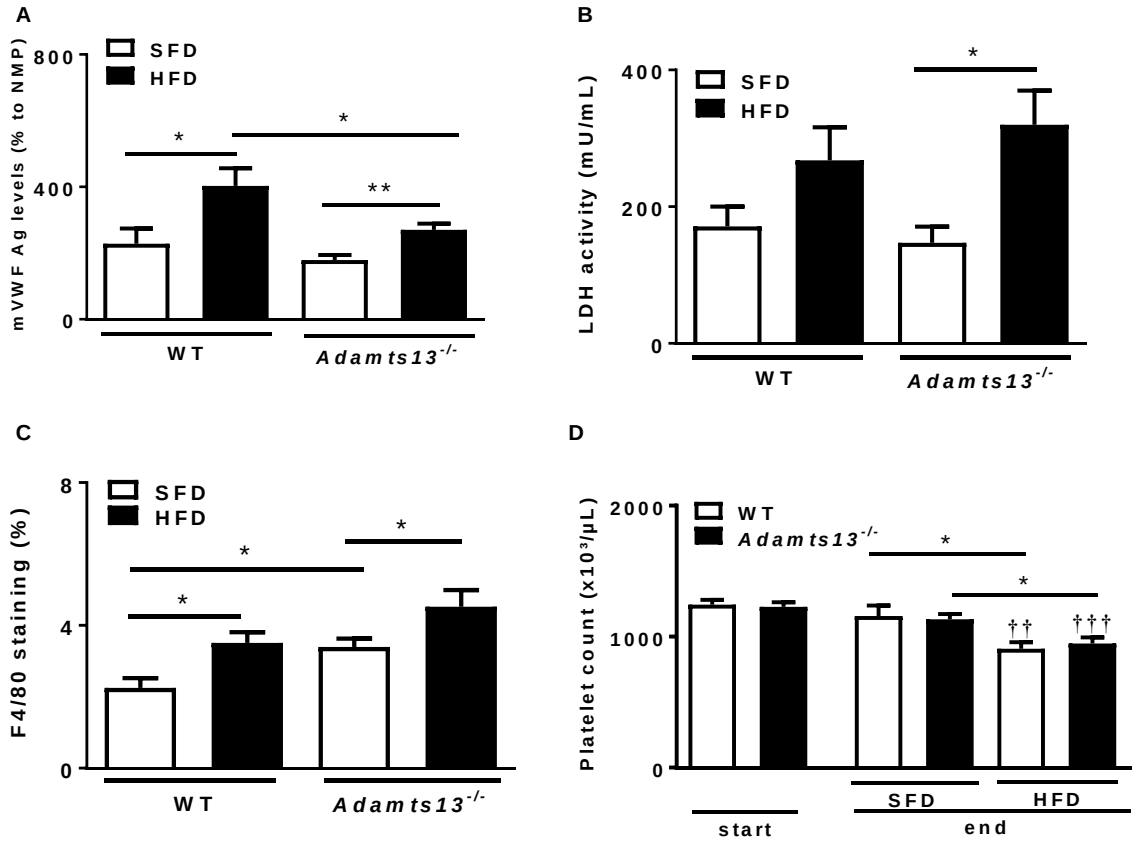

Figure 29: Phenotype of wild-type (WT) and ADAMTS13 deficient (*Adamts13*$^{-/-}$) mice kept on a standard fat (SFD) or high fat diet (HFD).

(A) Endogenous plasma VWF Ag levels, (B) LDH activity and (C) hepatic macrophage content (F4/80 staining) of WT and *Adamts13*$^{-/-}$ mice at the end of the diet. (D) Platelet count at the start and end of the diet of WT and *Adamts13*$^{-/-}$ mice. Data are means ± SEM of 9-11 experiments with * p < 0.05, ** p < 0.01; †† p < 0.01, ††† p < 0.001 as compared to the start of the diet (Mann-Whitney U test).

Table 11: Blood cell analysis of WT and *Adamts13*$^{-/-}$ mice fed a SFD or HFD for 15 weeks.

	SFD		HFD	
	WT	***Adamts13*$^{-/-}$**	**WT**	***Adamts13*$^{-/-}$**
n	5	11	8	9
WBC (x10^3/µL)	8.27 ± 0.66	10.4 ± 0.70*	10.8 ± 1.1	8.99 ± 0.73
Neutrophils (%)	14.7 ± 2.3	10.6 ± 0.96	9.56 ± 1.4	9.83 ± 1.8
Lymphocytes (%)	79.9 ± 2.3	84.6 ± 1.4	85.04 ± 2.0	82.3 ± 2.4
RBC (x10^6/µL)	8.70 ± 0.16	8.66 ± 0.29	9.31 ± 0.38	8.97 ± 0.21
Hemoglobin (g/dL)	12.6 ± 0.13	12.6 ± 0.47	13.5 ± 0.55	12.9 ± 0.32
Hematocrit (%)	13.9 ± 0.17	13.8 ± 0.51	14.8 ± 0.59	14.2 ± 0.34

Data are means ± SEM of n experiments in each group. * p < 0.05 as compared to WT mice on SFD (Mann-Whitney U test). Abbreviations: SFD, standard fat diet; HFD, high fat diet.

rVWF induces TTP symptoms in obese Adamts13$^{-/-}$ *mice*

A previous study reported that injection of 2000 U/kg rVWF in *Adamts13*$^{-/-}$ mice induced TTP (3). However, we observed that this high dose rVWF also caused severe thrombocytopenia in WT mice (data not shown). Therefore, we determined the threshold dose of rVWF that significantly decreased platelet counts, but not below the level of thrombocytopenia (< 600 x 10³/µL). Therefore, decreasing doses of rVWF (2000 to 100 U/kg) were injected in lean *Adamts13*$^{-/-}$ mice and platelet counts were monitored between 24 and 120h after injection (data not shown). Doses of rVWF between 500 and 2000 U/kg caused severe thrombocytopenia (platelet counts between 65 and 343 x 10³/µL) after 24h in all mice, whereas up to 250 U/kg only a moderate decrease of platelet count was observed. Therefore, a dose of 250 U/kg was selected as threshold for further experiments, and platelet counts were measured 24h after injection. Using this approach, injection of rVWF in obese WT or *Adamts13*$^{-/-}$ mice was associated with lower platelet counts as compared to lean mice (Figure 30A). In obese *Adamts13*$^{-/-}$ mice, platelet counts after injection dropped by 96% (948 ± 46 x

10^3/µL at the end of the diet versus 35 ± 13 x 10^3/µL 24h after rVWF injection), as compared to a drop by 29% for lean *Adamts13*$^{-/-}$ mice (1,133 ± 40 x 10^3/µL versus 803 ± 113 x 10^3/µL). In contrast, platelet counts of lean or obese WT mice were not affected by rVWF injection. Thus, obesity in an *Adamts13*$^{-/-}$ background promotes induction of severe thrombocytopenia upon rVWF injection. In addition, plasma levels of LDH activity were significantly higher for obese as compared to lean *Adamts13*$^{-/-}$ mice or to obese WT mice (Figure 30B), indicating more severe organ damage in obese *Adamts13*$^{-/-}$ mice 24h after rVWF injection. Endogenous VWF antigen levels were higher in obese as compared to lean WT as well as *Adamts13*$^{-/-}$ mice, without marked effects of genotype (Figure 30C).

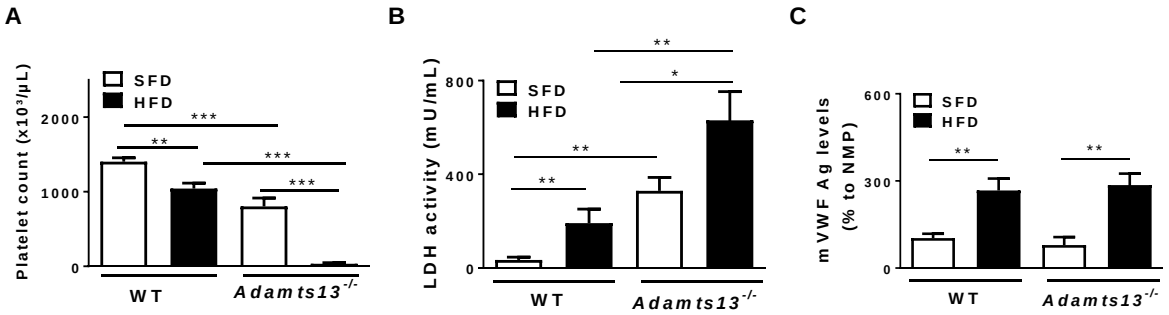

Figure 30: TTP characteristics after injection of rVWF in lean (SFD) and obese (HFD) WT or *Adamts13*$^{-/-}$ mice.

(A) Platelet count, (B) LDH activity and (C) endogenous levels of VWF antigen. Data are means ± SEM of 9-11 experiments with * p < 0.05, ** p < 0.01 and *** p < 0.001 (Mann-Whitney U test).

Hemoglobin (Figure 31A) and hematocrit (Figure 31B) levels were not different between obese and lean *Adamts13*$^{-/-}$ mice, not supporting hemolytic anemia or effects on hematopoiesis. Furthermore, analysis of schistocytes in blood smears (Figure 32B) did show an increase after HFD as compared to SFD feeding, but no difference between WT and *Adamts13*$^{-/-}$ mice (Figure 32A). Taken together, these data indicate that obesity is a risk factor for development of TTP in genetically predisposed *Adamts13*$^{-/-}$ mice, induced by the additional injection of rVWF.

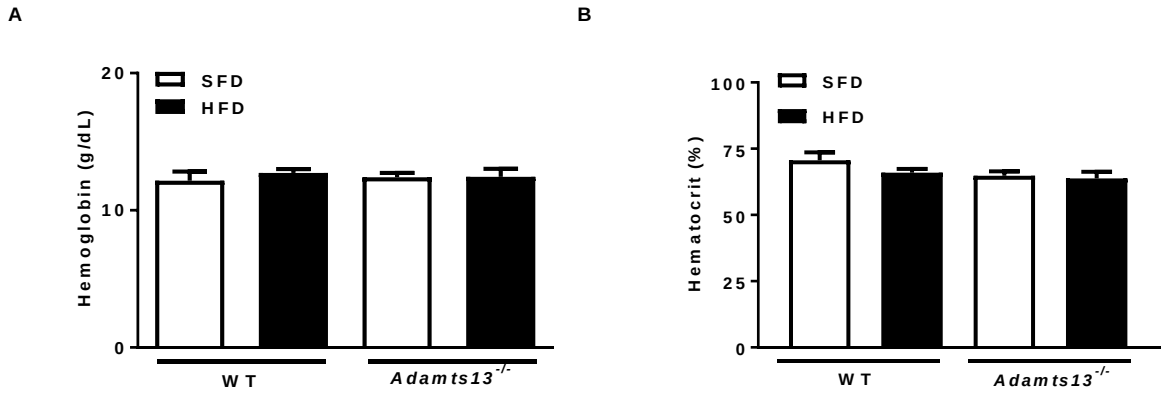

Figure 31: Hemoglobin and hematocrit levels after injection of rVWF in lean and obese WT or *Adamts13*$^{-/-}$ mice.

(A) hemoglobin levels, and (B) hematocrit levels for WT and *Adamts13*$^{-/-}$ mice on SFD or HFD. Data are means ± SEM of 9-11 experiments. No significant differences were observed (Mann-Whitney U test).

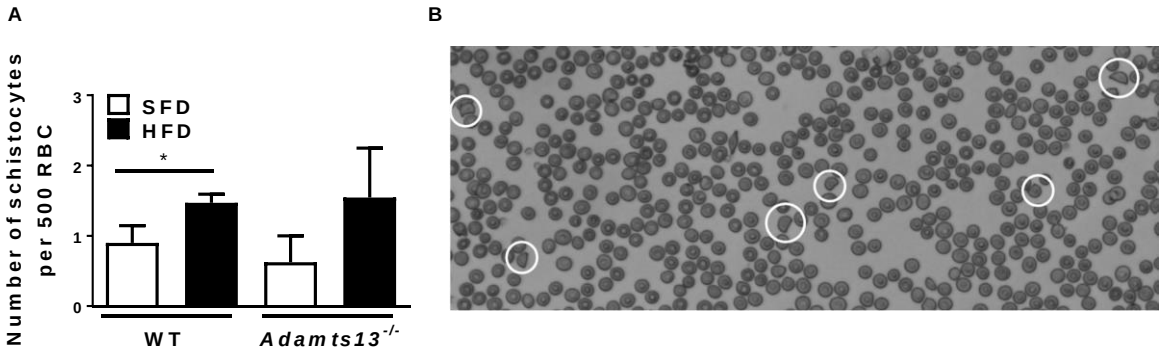

Figure 32: Schistocytes in blood smears after injection of rVWF in lean and obese WT or *Adamts13*$^{-/-}$ mice.

(A) Quantitation of schistocytes (number per 500 red blood cells) in lean and obese WT and *Adamts13*$^{-/-}$ mice. (B) Blood smear (40x magnification) from an obese *Adamts13*$^{-/-}$ mouse after rVWF injection. Schistocytes, visualized by May-Grühnwald Giemsa staining, are indicated by white circles. Data are means ± SEM of 9-11 experiments with * $p < 0.05$ (Mann-Whitney U test).

Hepatic macrophages contribute to severe thrombocytopenia

HFD feeding was associated with enhanced hepatic macrophage content (Figure 29C), which may contribute to enhanced clearance of platelets and platelet/VWF complexes. Therefore, we have depleted macrophages in the liver and spleen of lean

and obese WT and *Adamts13*$^{-/-}$ mice by i.v. clodronate treatment before rVWF injection. Reduction of macrophage populations in livers of all treated mice was confirmed by reduced staining and expression of F4/80 as compared to PBS treatment (Figure 33A, C). This was further supported by reduced expression of macrophage markers IL-1β, MRC-1 and TNF-α (Figure 33B).

A

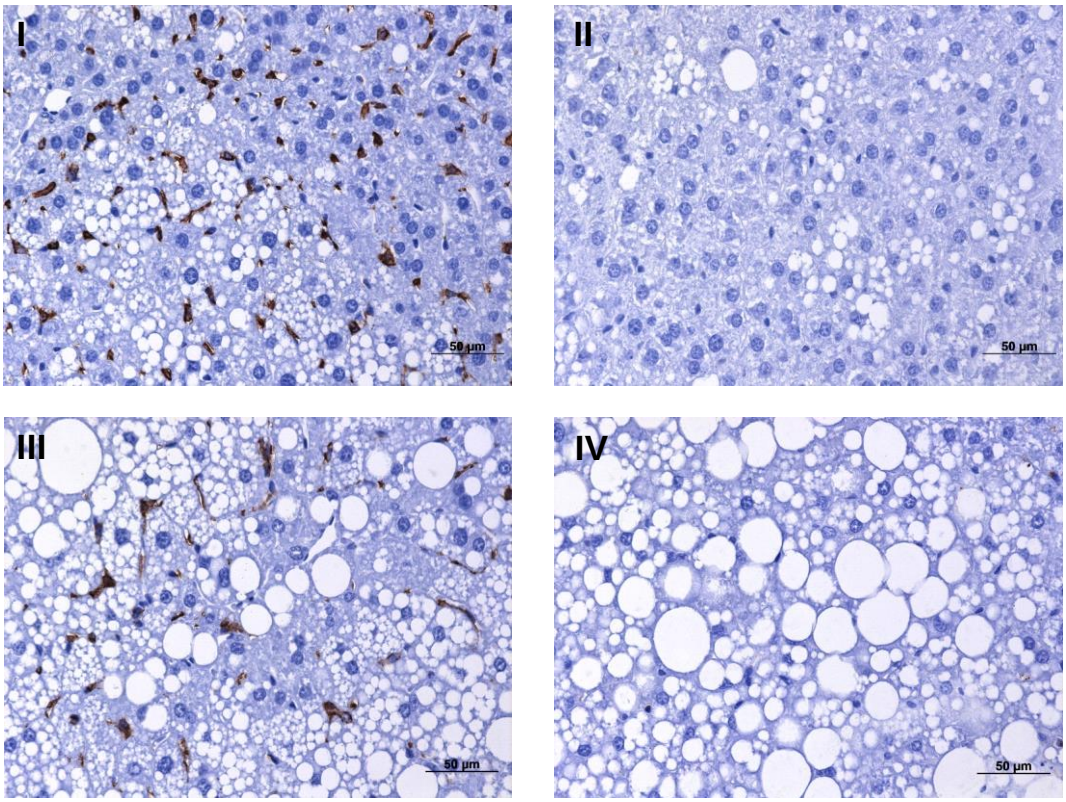

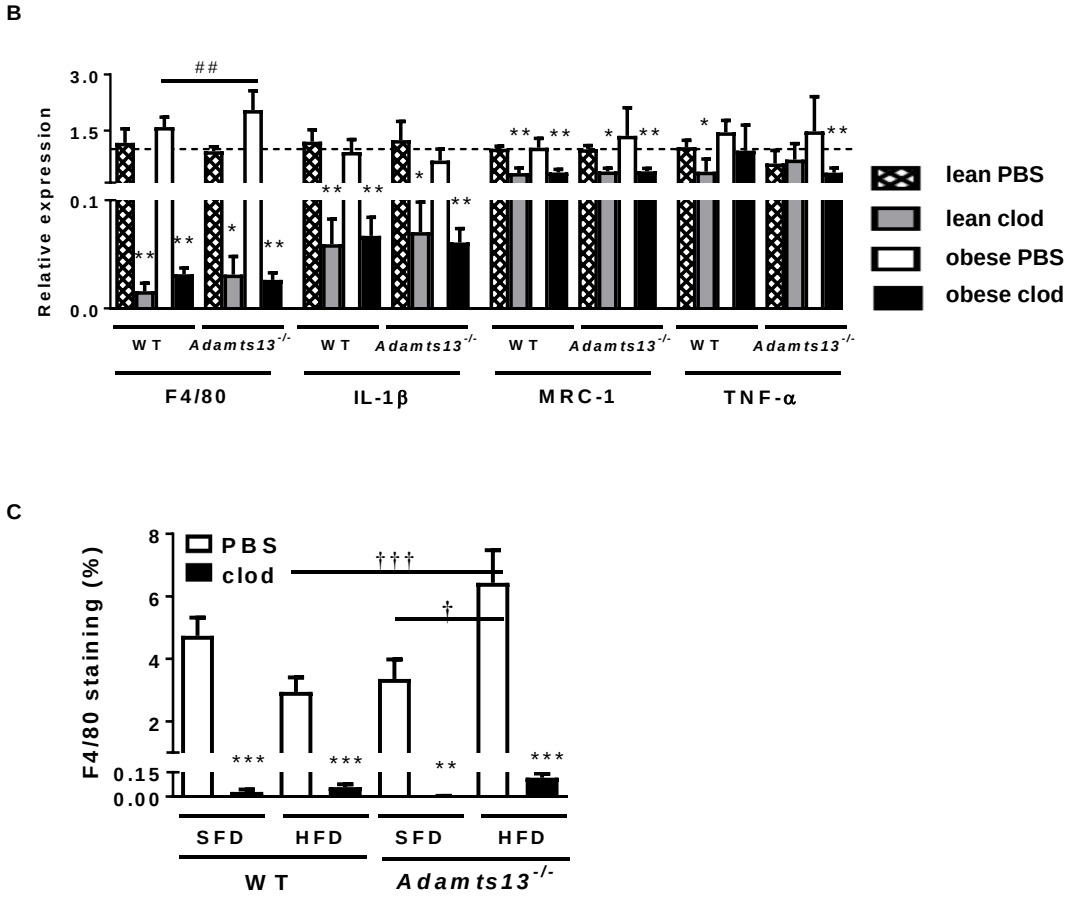

Figure 33: Effect of clodronate treatment 48h before injection of rVWF on hepatic macrophage populations in WT and *Adamts13*$^{-/-}$ mice.

(A) F4/80 staining of liver sections of obese WT (panels III and IV) and *Adamts13*$^{-/-}$ (panels I and II) mice treated with PBS (left panels) or clodronate (right panels). Scale bars represent 50 µm. (B) mRNA expression of macrophage markers F4/80, IL-1β, MRC-1 and TNF-α in the liver of lean and obese WT and *Adamts13*$^{-/-}$ mice injected with PBS or clodronate normalized to lean WT mice injected with PBS liposomes. (C) Quantitation of macrophages from F4/80 staining for injection of PBS (white bars) or clodronate (black bars). *, ** $p < 0.05$, $p < 0.01$ as compared to mice of the same genotype on the same diet injected with PBS; ## $p < 0.01$ as compared to obese WT mice injected with PBS; † $p < 0.05$ and ††† $p < 0.001$ (Mann Whitney U test). Data are means ± SEM of 5 experiments.

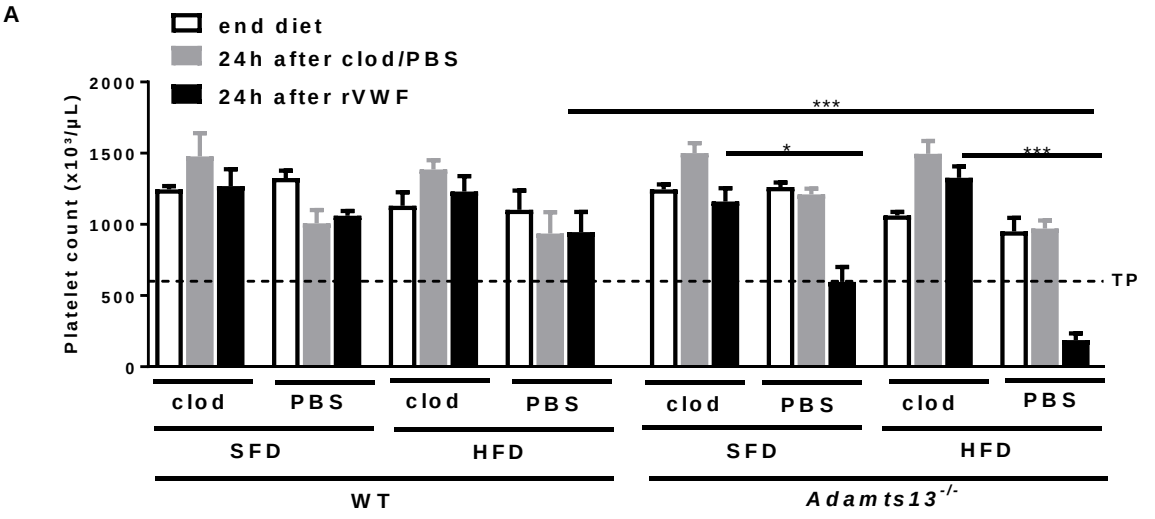
A
end diet
24h after clod/PBS
24h after rVWF
Platelet count (x10³/µL)
2000
1500
1000
500
0
***
*
***
TP
clod
PBS
clod
PBS
clod
PBS
clod
PBS
SFD
HFD
SFD
HFD
WT
Adamts13-/-

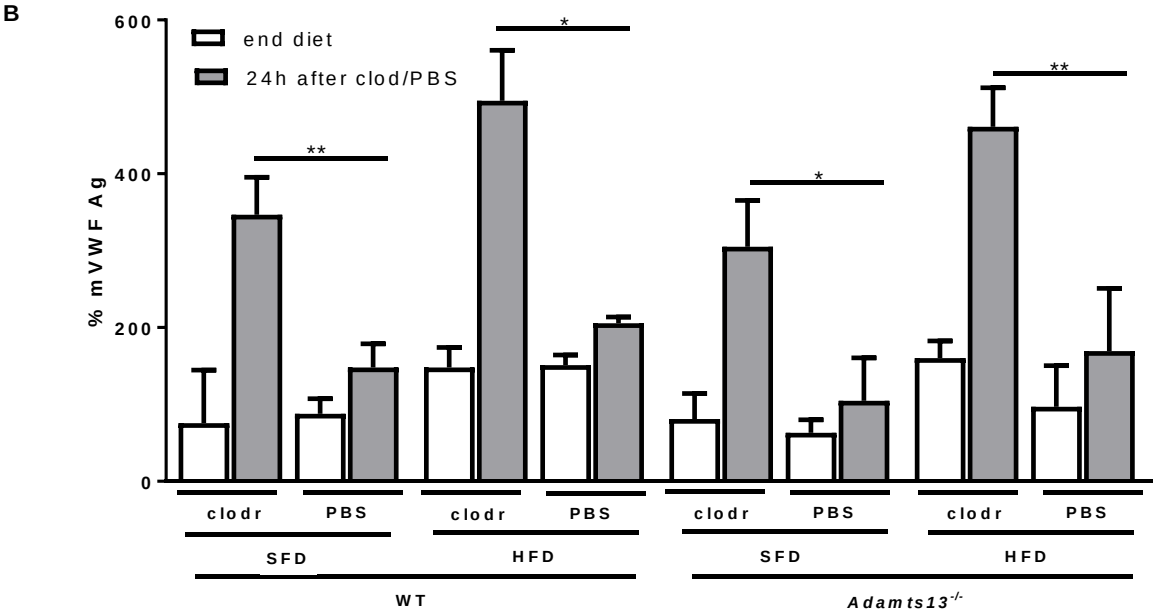
B
600
400
200
0
% mVWF Ag
end diet
24h after clod/PBS
*
**
*
**
clodr
PBS
clodr
PBS
clodr
PBS
clodr
PBS
SFD
HFD
SFD
HFD
WT
Adamts13-/-

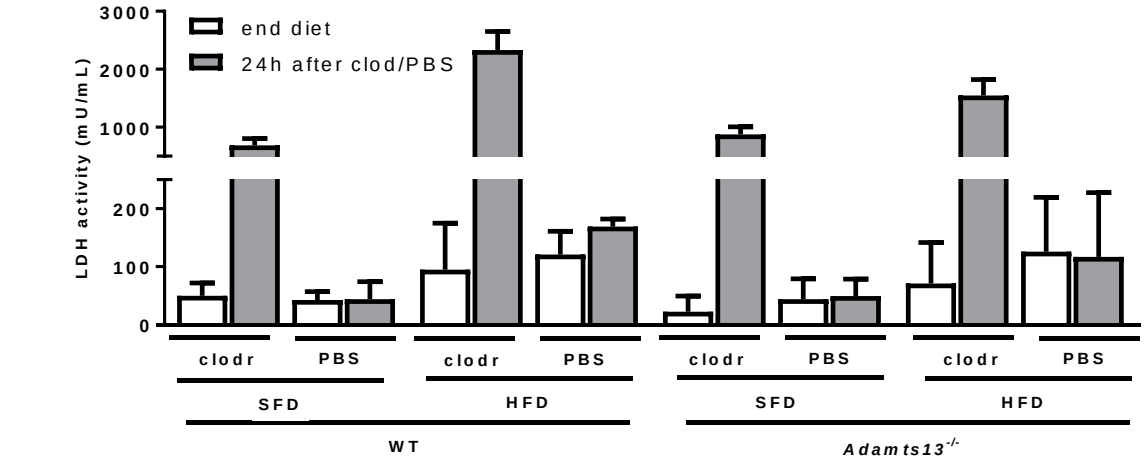
C
3000
2000
1000
200
100
0
LDH activity (mU/mL)
end diet
24h after clod/PBS
clodr
PBS
clodr
PBS
clodr
PBS
clodr
PBS
SFD
HFD
SFD
HFD
WT
Adamts13-/-

Figure 34: Effect of macrophage depletion on TTP characteristics of lean and obese WT or *Adamts13*$^{-/-}$ mice.

(A) Platelet count, (B) endogenous VWF antigen levels and (C) LDH activity at the end of the diet (white bars) and 24h after injection of clodronate or PBS (grey bars) and rVWF (only in panel A) (black bars). Data are means ± SEM of 5 determinations. * p < 0.05, ** p < 0.01, *** p < 0.001. (Mann-Whitney U test or Wilcoxon Rank test). Abbreviation: TP: thrombocytopenia.

Platelet counts at the end of the diet were not significantly affected by treatment with either clodronate or PBS (Figure 34A). However, platelet counts 24h after injection of rVWF (250 U/kg) remained significantly higher in lean and obese *Adamts13*$^{-/-}$ mice when macrophages were depleted as compared to PBS controls. These differences were not observed for lean or obese WT mice. Thus without macrophage depletion (PBS), platelet counts of obese *Adamts13*$^{-/-}$ mice were significantly lower than for obese WT mice (Figure 34A). Treatment with clodronate caused a significant rise of endogenous VWF levels in lean as well as obese WT and *Adamts13*$^{-/-}$ mice as compared to PBS injected mice (Figure 34B). Hemoglobin and hematocrit levels were comparable for all mice (data not shown). LDH activity was not affected by diet only, but increased after depletion of the macrophages in all mice (Figure 34C). The prevalence of schistocytes in fresh blood smears of *Adamts13*$^{-/-}$ mice tended to be (non-significantly) higher upon clodronate versus PBS treatment for both lean (1.5 ± 0.4/500 RBC versus 0.7 ± 0.1/500 RBC) and obese (0.7 ± 0.2/500 RBC versus 0.4 ± 0.4/500 RBC) mice.

rVWF enhances platelet phagocytosis by macrophages

When fluorescently labeled platelets were added *in vitro* to fluorescently labeled macrophages in the presence of rVWF and botrocetin, phagocytosis of platelets was observed (Figure 35A). The total amount of macrophages that phagocytosed platelets was not affected by rVWF (Figure 35B), whereas the proportion of phagocytosed platelets increased with rising concentrations of rVWF (Figure 35C, D).

Subsequently, we isolated and fluorescently marked platelets from obese WT donor mice and injected them in obese *Adamts13*$^{-/-}$ mice before injection of rVWF. Twenty-four hours later, liver and spleen were harvested to track the administered platelets. In mice with normal functioning macrophages, single platelets as well as platelet aggregates could be visualized particularly in the liver (Figure 36, I). Macrophage depletion strongly reduces platelet aggregate accumulation in the liver (Figure 36, II). Injection of rVWF triggered little platelet aggregate accumulation in the spleen (Figure 36, III), unless mice were treated with clodronate in which more platelet aggregates accumulated in the spleen (Figure 36, IV).

These preliminary data need to be confirmed by histological stainings and/or western blot analysis.

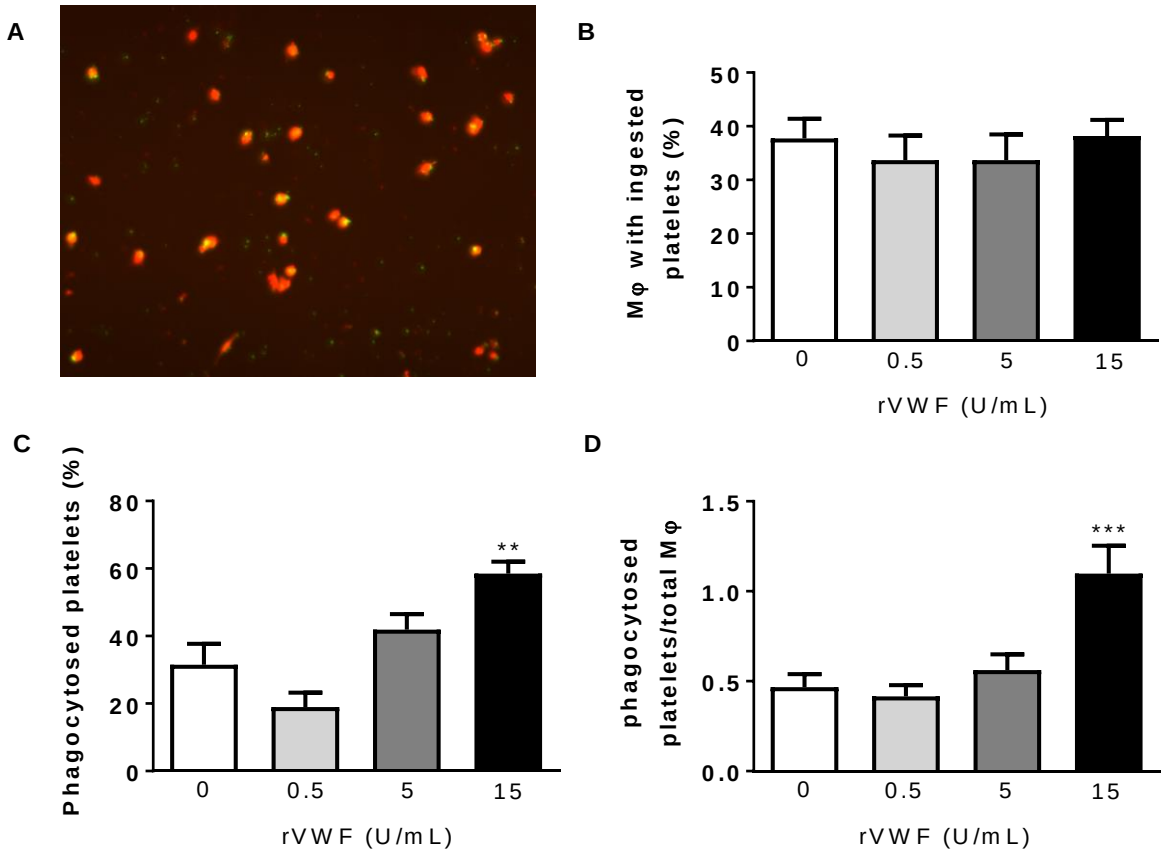

Figure 35: Phagocytosis of platelets by macrophages in the presence of rVWF.

(A) Representative image of phagocytosis of platelets (green/yellow) by macrophages (red) (magnification 20x). (B) The proportion of macrophages (Mφ) that phagocytosed platelets. (C) The proportion of phagocytosed platelets. (D) The ratio of phagocytosed platelets to the total macrophage content in the presence of increasing concentrations of rVWF. Data are means ± SEM of 15 experiments. ** $p < 0.01$, *** $p < 0.001$ as compared to the absence of rVWF (Mann-Whitney U test).

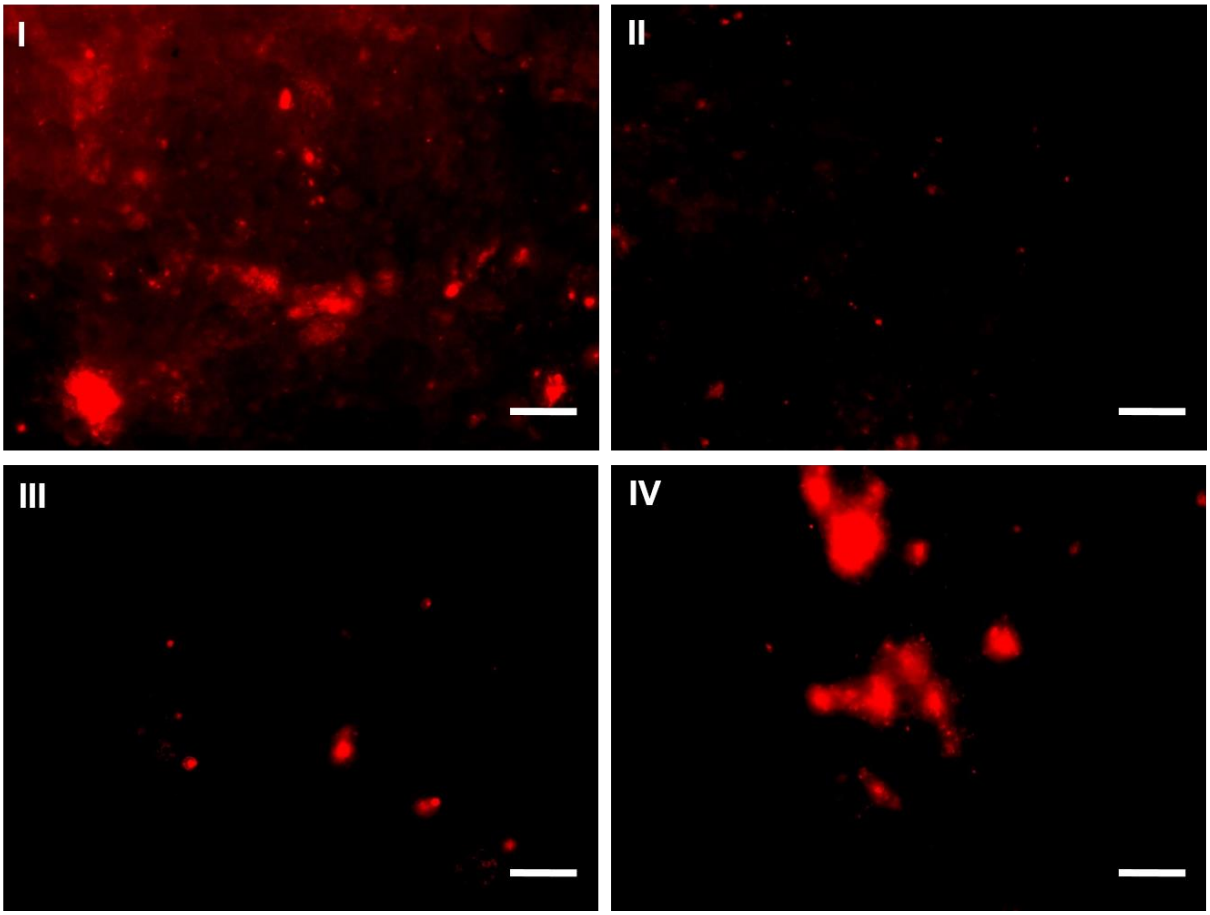

Figure 36: Effect of macrophage depletion on *in vivo* platelet distribution in obese *Adamts13*$^{-/-}$ mice.

Washed platelets isolated from obese WT mice were fluorescently labeled by CMTMR-Orange and injected i.v. in obese *Adamts13*$^{-/-}$ mice 24h after clodronate injection (II and IV) or without macrophage depletion (I and III), followed by rVWF injection 24h later. Liver (I and II) and spleen (III and IV) were removed 24h after rVWF injection to track fluorescent platelets. Scale bars represent 50 µm.

DISCUSSION

TTP is an extremely rare, but life-threatening disease caused by the absence of ADAMTS13 activity, the VWF cleaving proteinase, whereby microthrombi are formed in the microcirculation causing tissue damage and ultimately death (2). TTP patients may have a genetic predisposition, but an additional triggering factor is needed to evoke an acute TTP episode. Known triggers include pregnancy, HIV infection and alcohol abuse. However, in many cases the trigger remains unknown, and therefore the exact etiology of TTP remains unclear (1). Interestingly, obesity, which is a state of chronic inflammation, was found to be associated with higher ADAMTS13 levels in mice and man (6, 11). Nonetheless, obesity was suggested to be a possible risk factor for TTP (9). Although apparently contradictory, there are indications that obesity is indeed a risk factor for TTP. In the Oklahoma TTP cohort study, morbid obesity had a significantly higher prevalence in TTP patients (10), and ADAMTS13 levels were lower in obese TTP patients as compared to patients with a healthy BMI (16, 17). In contrast, in 21% of obese patients undergoing bariatric surgery non-inhibitory ADAMTS13 autoantibodies were detected, whereas ADAMTS13 antigen and activity levels were comparable to lean subjects (18). Weight loss after bariatric surgery was associated with a reduction of anti-ADAMTS13 autoantibodies (19).

Studies on TTP are hampered by the lack of suitable animal models; indeed mice deficient in ADAMTS13 do not spontaneously develop TTP. Furthermore, obese WT mice have enhanced ADAMTS13 levels. We previously reported that obese *Adamts13*$^{-/-}$ mice had a slightly lower platelet count and more hepatic microthrombi than obese WT or lean *Adamts13*$^{-/-}$ mice (20). However, because obese *Adamts13*$^{-/-}$ mice did not suffer from severe thrombocytopenia and did not show marked organ damage or blood schistocytes, they did not represent an improved model of TTP.

In this study, we show that obesity is indeed a risk factor for TTP in *Adamts13*$^{-/-}$ mice, as injection of a threshold dose of rVWF (250 U/kg) resulted in severe thrombocytopenia and more organ damage. Thus, when both risk factors, obesity and deficiency of ADAMTS13, are present, mice are more susceptible for TTP development upon triggering by rVWF.

The human body produces and removes up to 10^{11} platelets daily in order to maintain a normal steady state platelet count. Multiple mechanisms may contribute to platelet production and clearance (reviewed in (21)). It was shown that macrophages play a crucial role in clearance of platelets and platelet/VWF complexes (22, 23). Indeed, increased clearance of platelet/VWF complexes by macrophages in liver and spleen contributes to the thrombocytopenia associated with von Willebrand disease type 2B, which is characterized by enhanced affinity of VWF for platelets (12).

Due to the inflammatory state, obesity is especially associated with an increase in pro-inflammatory M1 macrophages in both the adipose tissue (24) and the liver (25). Thus, whereas obesity is associated with enhanced ADAMTS13 levels in mice (5), it also causes more abundant macrophage populations. The expected protective effect of enhanced ADAMTS13 levels on TTP development by reducing microthrombi formation may therefore be blunted by higher macrophage content that may lead to enhanced platelet clearance. In order to further investigate a potential causative relation between enhanced macrophage content and reduced platelet counts in TTP, we have depleted hepatic as well as splenic macrophages by i.v. clodronate treatment. Clodronate treatment by itself had no effect on platelet counts in either lean or obese WT or *Adamts13*$^{-/-}$ mice. Reduced macrophage populations (clodronate) in lean and obese *Adamts13*$^{-/-}$ mice were indeed associated with higher platelet counts after triggering with rVWF as compared to PBS treatment. A causal relationship between both

observations is further suggested by a significant negative correlation between hepatic macrophage content and platelet counts ($p = 0.001$, $r = -0.7$ for *Adamts13*$^{-/-}$ mice). Taken together, these observations indicate that enhanced platelet clearance in control PBS-treated lean and obese *Adamts13*$^{-/-}$ mice involves interaction with injected VWF. This is not observed in WT mice possibly because of cleavage of UL-VWF by ADAMTS13. Endogenous VWF levels were significantly elevated after clodronate treatment of lean and obese mice, possibly reflecting reduced clearance after macrophage depletion.

By both *in vitro* and in *vivo* approaches, we showed that addition of rVWF causes enhanced phagocytosis of platelets by macrophages. Increasing concentrations of rVWF induced significantly more platelet phagocytosis by the same number of macrophages *in vitro*. Thus, in the presence of high concentrations of VWF, each macrophage phagocytizes a higher number of platelets. This observation should be further confirmed by histological stainings for platelet and macrophage markers on liver and spleen sections from mice injected with rVWF and clodronate or control liposomes.

Thus, in addition to microthrombi formation (26), enhanced platelet clearance by upregulated macrophage populations may also contribute significantly to severe thrombocytopenia in obese subjects with TTP. The stimulating role of VWF on platelet phagocytosis by macrophages may also be relevant in other pathologies with associated thrombocytopenia. In such pathologies, VWF-targeting treatment such as Caplacizumab (27) could be beneficial.

The animal model for TTP used in this study (a nutritionally induced obese *Adamts13*$^{-/-}$ mouse injected with rVWF), albeit complex and time consuming, could be useful in studies to evaluate new pharmacological approaches.

In conclusion, our data indicate that obesity is a risk factor for TTP development in genetically predisposed mice, and that hepatic macrophages play an active role in platelet clearance leading to severe thrombocytopenia.

REFERENCES

1. Murrin RJ, Murray JA. Thrombotic thrombocytopenic purpura: aetiology, pathophysiology and treatment. Blood Rev. 2006;20(1):51-60.
2. Coppo P, Veyradier A. Current management and therapeutical perspectives in thrombotic thrombocytopenic purpura. Presse Med. 2012;41(3 Pt 2):e163-76.
3. Schiviz A, Wuersch K, Piskernik C, Dietrich B, Hoellriegl W, Rottensteiner H, et al. A new mouse model mimicking thrombotic thrombocytopenic purpura: correction of symptoms by recombinant human ADAMTS13. Blood. 2012;119(25):6128-35.
4. Motto DG, Chauhan AK, Zhu G, Homeister J, Lamb CB, Desch KC, et al. Shigatoxin triggers thrombotic thrombocytopenic purpura in genetically susceptible ADAMTS13-deficient mice. J Clin Invest. 2005;115(10):2752-61.
5. Geys L, Scroyen I, Roose E, Vanhoorelbeke K, Lijnen HR. ADAMTS13 deficiency in mice does not affect adipose tissue development. Biochim Biophys Acta. 2015;1850(7):1368-74.
6. Liu MY, Zhou Z, Ma R, Tao Z, Choi H, Bergeron AL, et al. Gender-dependent up-regulation of ADAMTS-13 in mice with obesity and hypercholesterolemia. Thromb Res. 2012;129(4):536-9.
7. Chauhan AK, Kisucka J, Brill A, Walsh MT, Scheiflinger F, Wagner DD. ADAMTS13: a new link between thrombosis and inflammation. J Exp Med. 2008;205(9):2065-74.
8. Sutherland JP, McKinley B, Eckel RH. The metabolic syndrome and inflammation. Metab Syndr Relat Disord. 2004;2(2):82-104.
9. Nicol KK, Shelton BJ, Knovich MA, Owen J. Overweight individuals are at increased risk for thrombotic thrombocytopenic purpura. Am J Hematol. 2003;74(3):170-4.
10. Deford CC, Reese JA, Schwartz LH, Perdue JJ, Kremer Hovinga JA, Lammle B, et al. Multiple major morbidities and increased mortality during long-term follow-up after recovery from thrombotic thrombocytopenic purpura. Blood. 2013;122(12):2023-9; quiz 142.
11. Crawley JT, Lane DA, Woodward M, Rumley A, Lowe GD. Evidence that high von Willebrand factor and low ADAMTS-13 levels independently increase the risk of a non-fatal heart attack. J Thromb Haemost. 2008;6(4):583-8.
12. Casari C, Du V, Wu YP, Kauskot A, de Groot PG, Christophe OD, et al. Accelerated uptake of VWF/platelet complexes in macrophages contributes to VWD type 2B-associated thrombocytopenia. Blood. 2013;122(16):2893-902.
13. Akyol O, Akyol S, Chen CH. Update on ADAMTS13 and VWF in cardiovascular and hematological disorders. Clin Chim Acta. 2016;463:109-18.
14. Grozovsky R, Hoffmeister KM, Falet H. Novel clearance mechanisms of platelets. Curr Opin Hematol. 2010;17(6):585-9.
15. Vanhoorelbeke K, Cauwenberghs N, Vauterin S, Schlammadinger A, Mazurier C, Deckmyn H. A reliable and reproducible ELISA method to measure ristocetin cofactor activity of von Willebrand factor. Thromb Haemost. 2000;83(1):107-13.
16. Vesely SK, George JN, Lammle B, Studt JD, Alberio L, El-Harake MA, et al. ADAMTS13 activity in thrombotic thrombocytopenic purpura-hemolytic uremic syndrome: relation to presenting features and clinical outcomes in a prospective cohort of 142 patients. Blood. 2003;102(1):60-8.
17. Kremer Hovinga JA, Vesely SK, Terrell DR, Lammle B, George JN. Survival and relapse in patients with thrombotic thrombocytopenic purpura. Blood. 2010;115(8):1500-11; quiz 662.
18. Lombardi AM, Fabris R, Scarda A, Zanato V, Dal Pra C, Scarparo P, et al. Presence of anti-ADAMTS13 antibodies in obesity. Eur J Clin Invest. 2012;42(11):1197-204.
19. Zanato V, Lombardi AM, Busetto L, Pra CD, Foletto M, Prevedello L, et al. Weight loss reduces anti-ADAMTS13 autoantibodies and improves inflammatory and coagulative parameters in obese patients. Endocrine. 2016.
20. Geys L, Bauters D, Roose E, Tersteeg C, Vanhoorelbeke K, Hoylaerts MF, et al. ADAMTS13 deficiency promotes microthrombosis in a murine model of diet-induced liver steatosis. Thromb Haemost. 2016;116(6).
21. Grozovsky R, Giannini S, Falet H, Hoffmeister KM. Regulating billions of blood platelets: glycans and beyond. Blood. 2015;126(16):1877-84.
22. van Schooten CJ, Shahbazi S, Groot E, Oortwijn BD, van den Berg HM, Denis CV, et al. Macrophages contribute to the cellular uptake of von Willebrand factor and factor VIII in vivo. Blood. 2008;112(5):1704-12.
23. Schlepper-Schafer J, Hulsmann D, Djovkar A, Meyer HE, Herbertz L, Kolb H, et al. Endocytosis via galactose receptors in vivo. Ligand size directs uptake by hepatocytes and/or liver macrophages. Exp Cell Res. 1986;165(2):494-506.

24. Weisberg SP, McCann D, Desai M, Rosenbaum M, Leibel RL, Ferrante AW, Jr. Obesity is associated with macrophage accumulation in adipose tissue. J Clin Invest. 2003;112(12):1796-808.
25. Morinaga H, Mayoral R, Heinrichsdorff J, Osborn O, Franck N, Hah N, et al. Characterization of distinct subpopulations of hepatic macrophages in HFD/obese mice. Diabetes. 2015;64(4):1120-30.
26. Tsai HM. Pathophysiology of thrombotic thrombocytopenic purpura. Int J Hematol. 2010;91(1):1-19.
27. Peyvandi F, Scully M, Kremer Hovinga JA, Cataland S, Knobl P, Wu H, et al. Caplacizumab for Acquired Thrombotic Thrombocytopenic Purpura. N Engl J Med. 2016;374(6):511-22.

Chapter 7

General Discussion

Second hit theory in TTP: a role for obesity?

TTP is a life-threatening disease of which the most distinct characteristics are severe thrombocytopenia and formation of microthrombi in the microcirculation where the shear stress is high. The main cause of TTP is a deficiency or absence of ADAMTS13 (activity < 5%), the VWF cleaving proteinase, leading to persistence of uncleaved ultra-large hyperactive VWF multimers. These will bind to platelets, resulting in platelet/VWF-rich thrombi and thrombocytopenia due to the high platelet consumption (2, 56). It is thought that ADAMTS13 deficiency as such is insufficient to develop a TTP episode, since patients with congenital TTP only sporadically develop TTP attacks alternated with periods of remission. Therefore, it is postulated that a second hit, driving endothelial damage or activation, is needed to develop an acute TTP episode (130). Despite known triggers as pregnancy, HIV, several anti-platelet drugs such as ticlopidine and clopidogrel, and alcohol abuse, the triggering factor to induce endothelial damage/activation is still largely unknown. Hence, the exact pathophysiology remains unexplained, hampering prevention of TTP attacks in high-risk subjects and development of specific treatments. Nowadays, acquired or congenital TTP is treated mainly by plasma exchange or infusion therapy, respectively, complemented or not by immunosuppressive therapy. Further research is needed to unravel the exact etiology of TTP. Since the prevalence of TTP is low, an experimental animal model would be useful. However, the existing TTP mouse models have major limitations, including complexity and lack of reproducibility.

Although several studies, both in mice and men, proposed obesity as a potential risk factor for TTP (128, 131), this is associated with increased ADAMTS13 levels (124, 125, 131). This is somewhat paradoxical, since higher ADAMTS13 levels should be protective instead of harmful for TTP development. Moreover, obesity is a state of low-

grade chronic inflammation (110), whereas ADAMTS13 has anti-inflammatory capacities (75) (Figure 37).

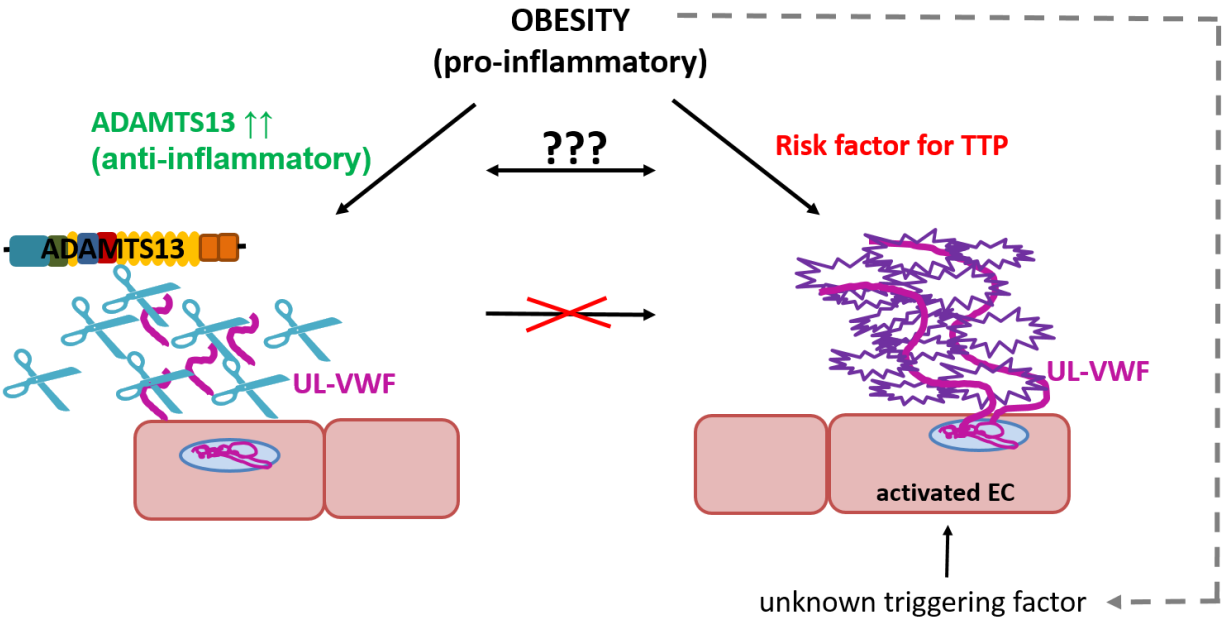

Figure 37: Paradoxical setting of obesity as risk factor for TTP.
Whereas obesity is a state of low-grade chronic inflammation, it is associated with increased levels of the anti-inflammatory proteinase ADAMTS13. Although ADAMTS13 is shown to be protective against TTP development, obesity has been proposed as risk factor for TTP.
Abbreviations: ADAMTS13: a disintegrin and metalloproteinase with thrombospondin-1 repeat, member 13; UL-VWF: ultra-large von Willebrand Factor; TTP: thrombotic thrombocytopenic purpura; EC: endothelial cell.

To resolve a potential role of ADAMTS13 in obesity and TTP, we have addressed the following research questions:

- Does ADAMTS13 play a role in adipose tissue development/expansion?
- Does ADAMTS13 in an obese context promote microthrombosis?
- Does ADAMTS13 play a role in NASH?
- Does obesity represent a risk factor for TTP?
- Do macrophages play a role in TTP-related thrombocytopenia?

These issues were addressed mainly with the use of diet-induced obese ADAMTS13 deficient mice.

ADAMTS13 in adiposity

Since ADAMTS13 levels are positively correlated with BMI (124) and it was proposed as a potential player in angiogenesis (78, 79) and oxidative stress/inflammation (75, 76), we investigated a potential role of ADAMTS13 in adipose tissue expansion. We did not find any relevant differences between WT and *Adamts13*$^{-/-}$ mice kept on SFD or HFD concerning body weight, weight of different fat depots, adipocyte size and density, inflammation, oxidative stress or angiogenesis related to obesity. Thus, despite its role in several obesity-related processes, we concluded that ADAMTS13 has no functional role in adiposity in mice. This may be in agreement with the fact that ADAMTS13 is not expressed in adipose tissue or adipocytes (data not shown). Surprisingly, ADAMTS13 expression in the liver, the main organ of secretion, was not enhanced with obesity, whereas plasma ADAMTS13 antigen and activity levels were markedly elevated after a HFD. Furthermore, increased hepatic ADAMTS13 expression in obese WT and *ApoE*$^{-/-}$ mice was described before (125).

Interestingly, adiponectin levels were not decreased upon a HFD in *Adamts13*$^{-/-}$ mice, which is puzzling, because adiponectin has metabolically protective characteristics; its levels are generally negatively correlated with fat mass and ADAMTS13 has anti-inflammatory properties (75). Therefore, it would be expected that adiponectin levels would decrease upon a HFD in *Adamts13*$^{-/-}$ mice and would be even lower than in obese WT mice. Adiponectin forms complexes with serum proteins such as TSP-1. Since obese subjects have lower levels of adiponectin, free TSP-1 levels may be increased, probably due to reduced complex formation (132). Since we did not measure TSP-1 levels in plasma of our mice, we cannot determine whether TSP-1

levels were lower in obese *Adamts13*$^{-/-}$ mice as compared to obese WT mice. Because ADAMTS13 contains TSP-1 domains (TSR), it is conceivable that adiponectin forms complexes with ADAMTS13. Moreover, we found a negative correlation between ADAMTS13 and adiponectin levels in WT mice ($r = -0.6$; $p = 0.01$).Thus, on the condition that complexes are cleared from the body, reduced complex formation of adiponectin with ADAMTS13 may in part explain the increase of ADAMTS13 in obese WT mice.

In human subjects, obesity is associated with production of non-inhibitory antibodies directed against ADAMTS13, but Lombardi *et al.* (129) did not observe differences in ADAMTS13 antigen and activity between lean and obese human subjects. This is in contrast to our own and other peer-reviewed data (124, 125). Lombardi *et al.* suggested that increased TSP-1 levels, because of decreased complex formation with adiponectin, would be responsible for the antibody production, since TSP-1 has structural homology with ADAMTS13. Moreover, a negative correlation between TSP-1 and ADAMTS13 was observed, whereas adiponectin and ADAMTS13 were not correlated, which is in contrast to our findings in mice.

Hence, both adiponectin and TSP-1 may influence ADAMTS13 levels, but this remains enigmatic. The increased adiponectin levels in obese *Adamts13*$^{-/-}$ mice remain unexplained.

Similarly as adiponectin levels, total cholesterol levels were increased in obese *Adamts13*$^{-/-}$ mice as compared to WT mice. Atherosclerosis is a consequence of hypercholesterolemia, which is frequently accompanied by obesity. Uptake of LDL by macrophages in the arterial wall leads to foam cell and plaque formation combined with secretion of inflammatory mediators. Atherosclerosis is a common comorbidity of obesity, which is also known as a state of low-grade systemic chronic inflammation in

which macrophages play an important role. The role of the ADAMTS13/VWF axis was previously described in systemic inflammation (75, 133). Additionally, Gandhi *et al.* reported that macrophage infiltration in the aortic sinus of *ApoE*$^{-/-}$/*Adamts13*$^{-/-}$ mice was increased as compared to *ApoE*$^{-/-}$ mice. Interestingly, this effect was reversed in *Adamts13*$^{-/-}$/*VWF*$^{-/-}$/*ApoE*$^{-/-}$ mice. Besides infiltration of macrophages, also neutrophil infiltration was higher in the absence of ADAMTS13, whereas deficiency of VWF had opposite effects in *ApoE*$^{-/-}$ mice. Therefore, it was suggested that ADAMTS13 reduced macrophage and neutrophil infiltration by cleavage of UL-VWF, thereby affecting atherosclerotic lesions. Whereas Ghandi *et al.* did not report an effect of ADAMTS13 on cholesterol levels in *ApoE*$^{-/-}$ mice (134), others observed positive correlations between ADAMTS13 and cholesterol levels, in both mice (135) and men (124). We did, however, not find a clear functional association between ADAMTS13 and cholesterol in our study, as total cholesterol levels were higher in obese *Adamts13*$^{-/-}$ than WT mice. Interestingly, a diet rich in cholesterol increases VWF levels (136). Therefore, increased ADAMTS13 levels after a HFD may be explained as reaction to increased VWF related to higher cholesterol levels. Indeed, both cholesterol as well as VWF levels were increased in obese WT mice as compared to lean WT mice ($p < 0.0001$ and $p = 0.003$, respectively; pooled data from two diet studies, $n = 40$). Consequently, VWF and cholesterol levels in both lean and obese WT mice correlated positively ($r = 0.3$; $p = 0.056$). Hence, ADAMTS13 elevation could possibly be regarded as a protective mechanism against atherosclerosis and possibly also against TTP (Figure 38). Thus, obese subjects deficient in ADAMTS13 could be at higher risk for TTP development, since the increased VWF levels (as result of both elevated cholesterol levels and ADAMTS13 deficiency) are not counteracted by ADAMTS13.

To summarize, although we did not find a significant role of ADAMTS13 in adipose tissue expansion, this proteinase may be relevant in protection against obesity-related disorders such as atherosclerosis. The increased ADAMTS13 levels after a HFD in WT mice may probably be explained as a protective reaction mechanism to enhanced cholesterol and increased VWF levels.

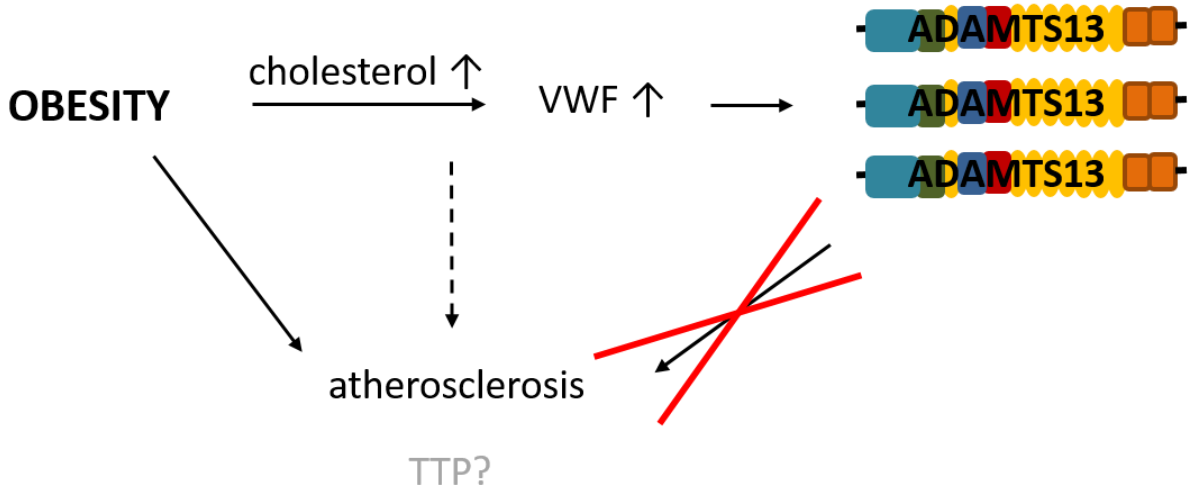

Figure 38: Increased ADAMTS13 in the obese context as protection mechanism against elevated VWF.
High cholesterol leads to increased VWF levels. As reaction, ADAMTS13 levels are enhanced, which is protective against atherosclerosis, but also against TTP. Hence, obesity could be a risk factor for TTP in obese subjects deficient for ADAMTS13.
Abbreviations: VWF: von Willebrand Factor; ADAMTS13: a disintegrin and metalloproteinase with thrombospondin-1 repeat, member 13.

Role of the fibrinolytic system in hepatic microthrombosis in obese *Adamts13*$^{-/-}$ mice?

Deficiency of ADAMTS13 in combination with obesity caused enhanced formation of thrombi in the liver. We measured TAT complex levels reflecting thrombin generation and representing a marker for a pro-coagulant state. We found a slight increase of TAT levels in plasma and in liver extracts upon HFD as compared to SFD feeding. In liver extracts, TAT levels were slightly, but significantly higher for lean WT than *Adamts13*$^{-/-}$ mice, whereas in plasma no significant differences were found between

the genotypes. However, thrombin generation causes fibrin-rich thrombi, whereas hepatic microthrombi in the obese *Adamts13*$^{-/-}$ mice are rich in VWF and platelets. In addition, fluorescent platelet-rich aggregates were observed in livers of obese *Adamts13*$^{-/-}$ mice injected with fluorescently labeled platelets (preliminary data of *in vivo* study). Noteworthy, these latter mice were triggered for TTP, in contrast to the mice of the diet-induced obesity experiment. Higher prevalence of hepatic platelet-rich thrombi in obese *Adamts13*$^{-/-}$ mice could possibly be explained by higher levels of leptin ($p < 0.05$) in obese mice, promoting platelet aggregation (137), combined with the absence of the antithrombotic proteinase ADAMTS13.

In addition, we measured PAP complex levels in both plasma and liver extracts, but we did not find evidence of an increased activity of plasmin in our study. This is not in agreement with a compensatory role of plasmin in ADAMTS13 deficiency, as described by Tersteeg *et al.* (81). Nonetheless, the conditions in our study were different, as our mice did not suffer from TTP. In the study of Tersteeg *et al.*, *Adamts13*$^{-/-}$ mice were injected with high dose rVWF to induce TTP, simultaneous with plasminogen and streptokinase administration. Hence, it may be that more extensive endothelial damage is required for activation of the fibrinolytic system, and subsequent degradation of UL-VWF multimers. Therefore, increased PAP complex levels would be expected after induction of endothelial damage by injection of rVWF in obese *Adamts13*$^{-/-}$ mice, but this was not investigated. Tersteeg *et al.* hypothesized that plasminogen is activated during TTP attacks and that plasmin degrades VWF in recently formed microthrombi when α2-AP is depleted. Thereafter, plasmin can further degrade the remaining VWF (Figure 39).

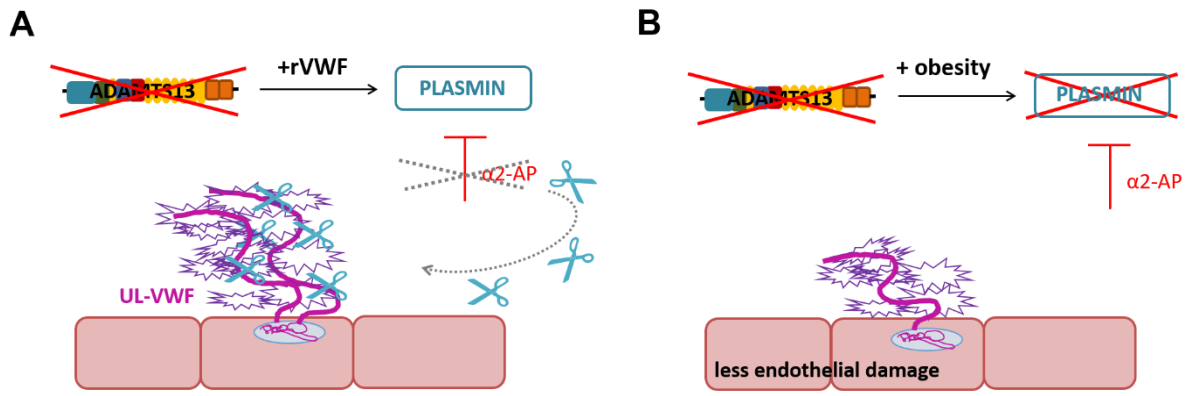

Figure 39: Plasmin as compensatory proteinase for ADAMTS13?
Plasmin can act as bypass for ADAMTS13 in case of deficiency during TTP attacks when α2-AP is depleted (A). In obese *Adamts13*$^{-/-}$ mice, platelet-rich hepatic thrombi were detected, but without marked activation of the fibrinolytic system. Probably because of less pronounced endothelial damage (B).
Abbreviations: ADAMTS13: a disintegrin and metalloproteinase with thrombospondin-1 repeat, member 13; rVWF: recombinant von Willebrand Factor; α2-AP: α2-antiplasmin; UL-VWF: ultra-large von Willebrand Factor multimers.

ADAMTS13 does not affect development of liver steatosis

Since ADAMTS13 is produced by the liver, its role in liver diseases was studied extensively, but data are somewhat controversial (138). We could not find a role of ADAMTS13 in liver steatosis using two different mouse models. The first model, a diet-induced obese mouse, represents liver steatosis as a consequence of obesity, the most common form of NAFLD (139, 140). It shows typical signs of human NASH as hypertriglyceridemia, hyperlipidemia and insulin resistance. The MCD diet, on the other hand, is not related to obesity, but induces weight loss. Despite that liver injury and steatosis are histologically similar to humans, the MCD diet fed mice do not present with insulin resistance, a typical NASH characteristic (141-143). These mice actually showed improved peripheral insulin sensitivity. We observed a somewhat decreased platelet count after MCD as compared to MCC diet in *Adamts13*$^{-/-}$ mice, but VWF levels were unchanged. Additionally, LDH activity was comparable for *Adamts13*$^{-/-}$ mice on

either diet and clear TTP symptoms could not be identified in *Adamts13*$^{-/-}$ mice fed the MCD diet. Thus, these data do not support a role for steatosis in TTP development in this model. Nonetheless, Lombardi *et al.* suggested that since hepatic stellate cells are the main producers of ADAMTS13, NAFLD/NASH could affect ADAMTS13 levels. This hypothesis was based on a clinical case of TTP not induced by inhibitory antibodies nor by a genetic ablation of ADAMTS13, in a morbid obese subject suffering from NASH (144). However, we did not find differences in ADAMTS13 antigen levels between WT mice fed the MCC or MCD diet.

Animal models to the rescue

Since TTP is a very rare disease, databases and registries are scarce and patients are spread around the world, hampering clinical research.

In the Oklahoma TTP cohort study, it was observed that the prevalence of morbid obesity was significantly higher in TTP patients (126) and that ADAMTS13 levels were lower when patients were obese (127, 145). This is in contrast with the higher ADAMTS13 levels we found in obese WT mice. Therefore, the increase in ADAMTS13 antigen and activity in obese WT mice could be a potential protection mechanism against TTP (see Figure 38). Probably, this mechanism fails in genetically predisposed subjects resulting in a higher risk for TTP development. From a few observational studies, obesity was suggested as a risk factor for TTP. We investigated this by using lean and obese *Adamts13*$^{-/-}$ mice. Animal models are indeed valuable to gain insight in the cause, clinical course and outcome of TTP. However, *Adamts13*$^{-/-}$ mice do not show signs of TTP without extra triggering factors as Stx (61) or high dose human rVWF (64). Therefore, we attempted to develop an improved model using obese *Adamts13*$^{-/-}$ mice. Although the obese *Adamts13*$^{-/-}$ mice showed a lower platelet count and more hepatic microthrombi in comparison with lean *Adamts13*$^{-/-}$ or obese WT mice,

these findings did not allow to conclude that obesity is indeed a risk factor for TTP, nor to use the obese *Adamts13*$^{-/-}$ mouse as a new model for TTP. However, after injection of a threshold dose of rVWF in obese genetically predisposed mice, severe thrombocytopenia and organ damage were observed (Figure 40). Since this was not seen in lean mice, obesity may indeed be a risk factor for TTP development in *Adamts13*$^{-/-}$ mice. The injection of a threshold dose represents an improvement towards the previously used injection of high dose rVWF as this causes thrombocytopenia also in WT mice. Unfortunately, despite the severe thrombocytopenia and increased LDH activity levels, none of our obese mice developed end-stage TTP.

Because of the 15 weeks diet, our model is quite time-consuming. Alternatively to diet-induced obese, genetically obese mice (*ob/ob*) could be used. These are deficient in leptin, the satiety hormone, leading to uncontrolled food intake. Leptin stimulates energy expenditure by stimulating brown adipose tissue (146, 147) and modulating glucose and fat metabolism (148). It is unclear whether our results in the nutritionally induced obesity model would be the same in *ob/ob* mice. As it has been described that leptin promotes platelet aggregation, absence of leptin may delay thrombi formation and lead to decreased stability of the thrombus (137). The exact mechanisms of the effect of leptin on platelet aggregation and thrombus formation are still unclear, but since leptin-deficiency in obese subjects is very rare, a nutritionally induced obese mouse model is probably more representative.

Because of the ADAMTS13 deficiency, the model is more representative for the hereditary form of TTP. Congenital TTP represents only 5% of all TTP cases (56), and therefore a model for acquired TTP could be more interesting. Lean WT mice injected with antibodies against ADAMTS13 before high dose rVWF injection were previously

used as model for acquired TTP (149). Possibly, similar approaches could be used in obese WT mice, but instead of high dose rVWF, the threshold dose should be injected. However, the injection of antibodies in addition to the diet and rVWF injection would further complicate the model.

Rodents are the most used animals to study obesity and related comorbidities. Mouse models show several important similarities with humans concerning adipose tissue (150). Unlike murine obesity models, mouse models for TTP are difficult to acquire and to work with. Baboons, on the other hand, develop acute acquired TTP by injection of ADAMTS13 neutralizing antibodies without further triggering (65). Baboons are more closely related to humans and are therefore very useful as non-human primates. Lean baboons do not develop end-stage TTP after administration of ADAMTS13 antibodies, but induction of obesity could possibly aggravate the TTP symptoms. Obesity has not yet been induced in baboons in TTP research, but has already been applied in pregnancy studies (151, 152) or studies investigating complex genetic diseases like the metabolic syndrome and cardiovascular diseases (153). Therefore, it could be of interest to use obese baboons injected with ADAMTS13 neutralizing antibodies as animal model for acquired TTP. However, expensive housing requirements and ethical considerations will hamper the widespread use of such model.

In conclusion, obese *Adamts13*$^{-/-}$ mice injected with a threshold dose of rVWF represent an improved TTP model, suffering from severe thrombocytopenia and organ damage. Despite the time-consuming diet, absence of several other TTP symptoms, non-clinical setting and genetic basis origin, this model has significant advantages as compared to existing mouse models or larger animal models.

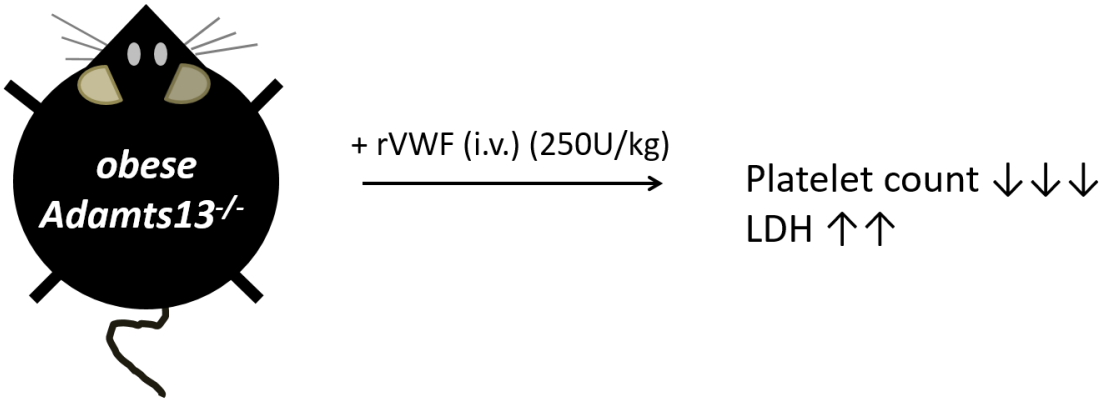

advantages	disadvantages
severe thrombocytopenia	time-consuming (15 weeks diet)
organ damage	several manipulations (obese, injection)
improved mouse model	congenital TTP model
easier accessible than baboon or human	no end-stage TTP
	non-clinical model

Figure 40: Newly developed mouse model for TTP and its (dis)advantages.
Obese *Adamts13*$^{-/-}$ mice injected with a threshold dose of rVWF present with TTP symptoms. Abbreviations: *Adamts13*$^{-/-}$: ADAMTS13 deficient; rVWF: recombinant von Willebrand Factor; i.v.: intravenously; LDH: lactate dehydrogenase activity; TTP: thrombotic thrombocytopenic purpura.

Macrophages: important in TTP pathophysiology?

Obesity is a pro-inflammatory state characterized by an increase in pro-inflammatory macrophages in the adipose tissue (154), but also in the liver (155). These hepatic macrophages (Kupffer cells) are involved in clearance of both platelets and VWF (23, 49). In our study, depletion of hepatic and splenic macrophages by clodronate resulted in normal platelet counts after injection of rVWF in obese *Adamts13*$^{-/-}$ mice, suggesting that macrophages may play a causative role in severe thrombocytopenia by clearance of platelet/VWF complexes. Thus, in addition to what is generally accepted (156), TTP related thrombocytopenia may be a consequence of platelet clearance by

macrophages combined with microthrombosis. It was, however, not possible to determine the quantitative contribution of either process to thrombocytopenia.

To investigate a potential role of macrophages in TTP related thrombocytopenia, we used *Adamts13*$^{-/-}$ mice injected with clodronate liposomes followed by rVWF. Clodronate is delivered intracellularly by liposomes that will become phagocytosed by macrophages in the sinusoids. Phospholipases in the macrophages disrupt the liposomal phospholipid bilayers resulting in clodronate release specifically inside the macrophages (157) (Figure 41).

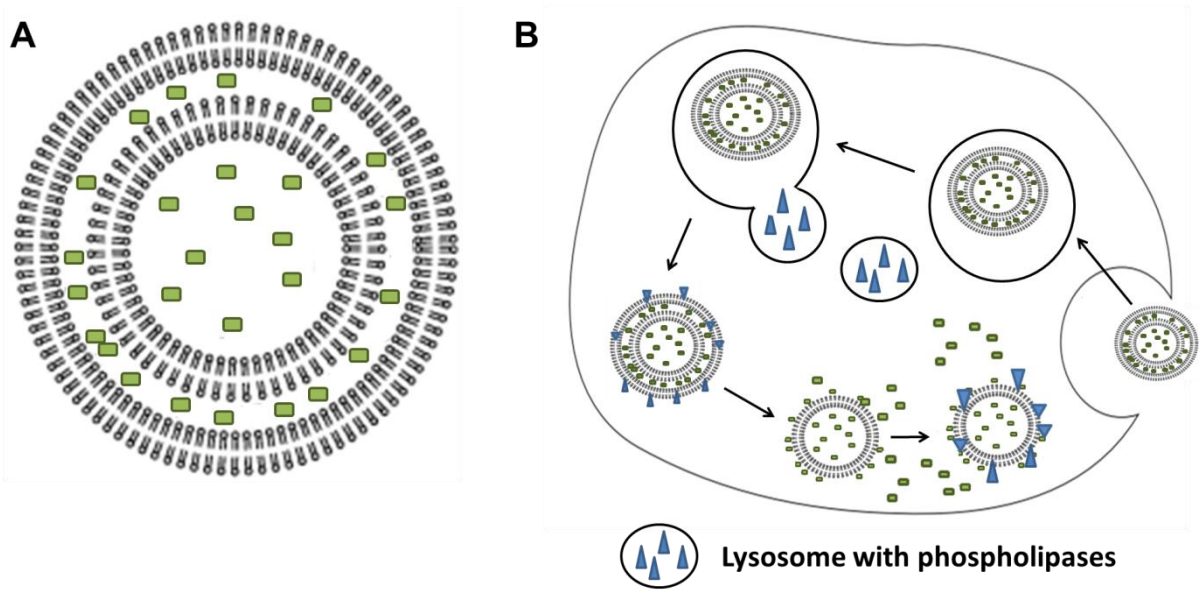

Figure 41: Mechanism of macrophage apoptosis by clodronate.
Clodronate liposomes consist of phospholipid bilayers separated by hydrophilic compartments containing clodronate (green) (A). Liposomes filled with clodronate are endocytosed by macrophages. Fusion of lysosomes (filled with phospholipases (blue)) with clodronate liposomes causes disruption of the bilayers resulting in clodronate release and apoptosis of the macrophage (B).
Figure based on (157).

It should be kept in mind that clodronate liposomes may have several limitations:

1) Whereas in our study i.v. clodronate injection resulted in a small, but not significant increase of platelet counts after 24h, it is possible that without VWF

injection, clodronate treatment could affect platelet counts after 48h or 72h (158-160). Macrophages in the spleen and bone marrow may be important in the regulation of megakaryopoiesis and thrombopoiesis, processes stimulated by clodronate (161). Therefore, it is conceivable that in our study, clodronate also stimulates platelet production, leading to very high platelet numbers that will decrease after rVWF treatment. Hence, the normal platelet counts in obese *Adamts13*$^{-/-}$ mice after clodronate and rVWF injection could be misleading. This should be further investigated in separate experiments.

2) Phagocytic uptake of liposomes has been ascribed to platelets as well. Male *et al.* showed that platelets are able to phagocytose liposomes with a diameter of 74 nm (162). Since clodronate liposomes have a diameter between 150 nm and 3 µm (163) they are unlikely to be encapsulated by platelets. Furthermore, because clodronate liposomes were injected intravenously, hepatic and splenic macrophages were effectively killed without affecting other organs, since clodronate does not cross the cell membrane of macrophages (157, 164). Additionally, free clodronate in circulation from dead macrophages has an extremely short half-life (157). Therefore, it can be assumed that clodronate did not affect platelets directly.
3) Potential uptake of clodronate by phagocytic dendritic cells (165, 166) has not been evaluated in our study.

Theoretically, the higher abundance of macrophages in the obese phenotype could be protective against microthrombi formation in obese *Adamts13*$^{-/-}$ mice, because macrophages clear VWF, particularly in the activated state. Hence, after macrophage depletion, both platelets and VWF are not efficiently cleared. In an ADAMTS13 deficient setting, UL-VWF (unfolded due to the high shear forces in the arterioles and

capillaries) will remain uncleaved and hyperactively bind to platelets, resulting in microthrombosis. Therefore, since the macrophages phagocytose VWF in its active state (bound to platelets), they might play a protective role against microthrombi formation and consequently organ ischemia. However, this also results in severe thrombocytopenia due to platelet clearance by macrophages. Generally, the effect of platelet clearance by macrophages seems more explicit in mice of an *Adamts13*$^{-/-}$ background, particularly when injected with rVWF. Our *in vitro* data also indicated that platelet clearance by macrophages is enhanced by VWF.

Nonetheless, the preliminary data of our *in vivo* study indicate that rVWF injection resulted in formation of platelet aggregates and presence of single platelets in the liver when macrophages were not depleted (Figure 42A). Therefore, this observation does not allow to propose a protective role of macrophages against microthrombi formation. Moreover, after clodronate injection in comparison with control mice, fewer hepatic, but more splenic platelet aggregates were found (Figure 42B). This platelet consumption in splenic microaggregates could probably explain the slight decrease of platelets we observed after rVWF injection in mice treated with clodronate.

Noteworthy, in ITP patients, most platelets are accumulated in the spleen, whereas in mice the accumulation of sensitized platelets is primarily observed in the liver (159). Hence, our findings may not be entirely representative for humans due to species differences.

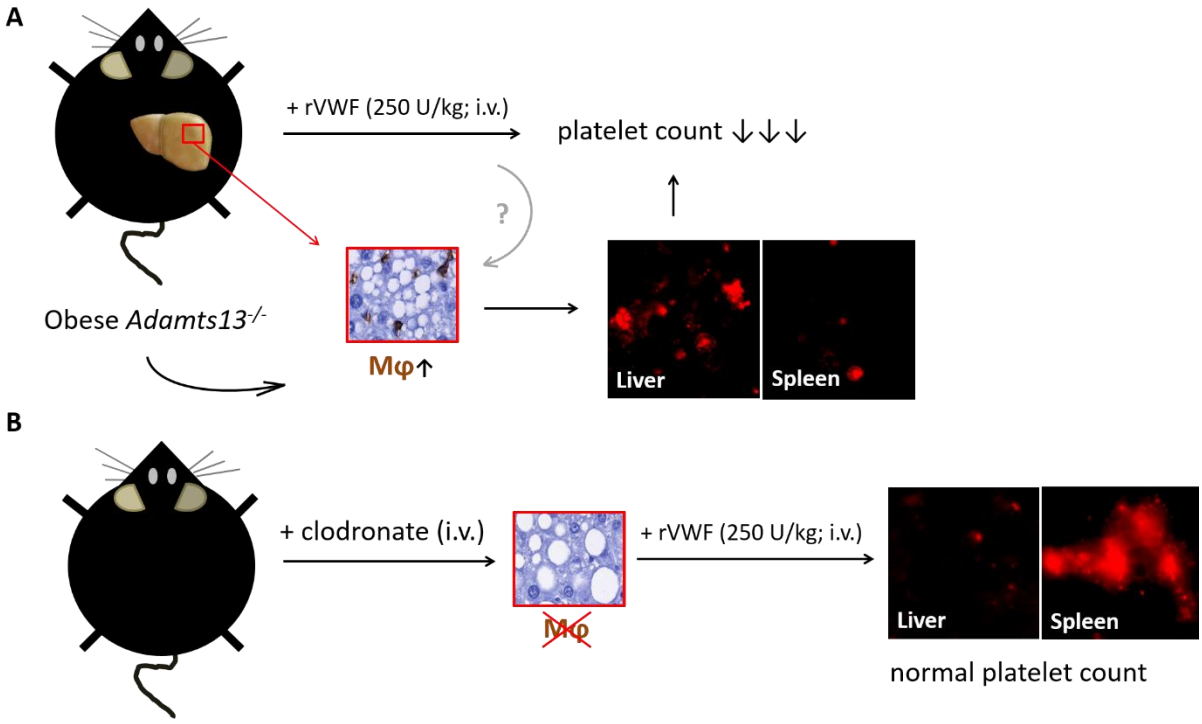

Figure 42: Role of macrophages in TTP.
After injection of rVWF in obese *Adamts13*$^{-/-}$ mice, platelet counts were extremely low, probably due to microaggregation and platelet clearance in the liver by hepatic macrophages (A). Macrophage depletion prevented thrombocytopenia after rVWF injection. The limited platelet drop induced by rVWF could probably be explained by microaggregate formation in the spleen (B). Abbreviations: rVWF: recombinant von Willebrand Factor; *Adamts13*$^{-/-}$: ADAMTS13 (a disintegrin and metalloproteinase with thrombospondin-1 repeat, member 13) deficient; i.v.: intravenously; Mφ: macrophages.

Novel TTP treatments to prevent platelet-VWF interactions, such as the nanobody Caplacizumab (58), aptamers (167) or anfibatide (168) are very promising (55). These agents prevent the first step in platelet adhesion to the vessel wall, resulting in improved endothelial function (169) and decreased thrombi formation, hence less organ damage (58, 168). Although the most important effect of these drugs is inhibition of microthrombosis, platelet clearance by macrophages will probably also be affected, because platelets will not bind to VWF in the presence of these agents. Combined with decreased formation of platelet-rich thrombi, reduced platelet clearance will result in normal platelet counts.

Future perspectives

The preliminary *in vivo* data showing hepatic or splenic microaggregates of fluorescent platelets and single platelets in obese *Adamts13*$^{-/-}$ mice should be investigated more extensively and quantitatively. Therefore, histological stainings and/or western blot analysis of platelet markers on liver and spleen tissue of obese mice injected with clodronate or PBS, followed by rVWF, should be performed. Preferably, these analyses should be carried out on tissues acquired from mice that were not injected with fluorescently labeled platelets obtained from donor mice. Furthermore, the effects of clodronate treatment on megakario-/thrombopoiesis in *Adamts13*$^{-/-}$ mice should be investigated.

Finally, it will be important to demonstrate the validity of the newly developed mouse model. This could be done by treatment with inhibitors of the interaction between VWF and platelets. Furthermore, since this mouse model shows high rates of platelet clearance, it could also be useful for platelet clearance studies in other diseases.

General conclusions

1. Despite the increased levels of ADAMTS13 in obesity and its reported role in angiogenesis and inflammation, it does not affect adipose tissue expansion in a diet-induced obese mouse model.
2. Obesity in combination with ADAMTS13 deficiency results in a slightly decreased platelet count accompanied by formation of platelet-rich hepatic thrombi.
3. Although ADAMTS13 has been implicated in several liver diseases, it does not play a role in development of steatosis in our mouse models.
4. Obesity is a risk factor for TTP in mice. Despite the absence of some TTP related symptoms and a disease onset different from human subjects, obese

Adamts13$^{-/-}$ mice injected with a threshold dose of rVWF can be useful as new model for TTP.

5. After triggering for TTP, macrophages, particularly in the liver, are involved in platelet clearance, resulting, in combination with formation of platelet-rich hepatic microthrombi, in severe thrombocytopenia.

Thesis abstract

TTP is a life-threatening disease characterized by severe thrombocytopenia and formation of platelet-rich thrombi in the microcirculation. It is caused by deficiency of ADAMTS13 activity, the VWF cleaving proteinase, in combination with an additional triggering factor. Altough it is associated with higher ADAMTS13 levels, obesity has been proposed as potential risk factor for TTP development. Using *Adamts13*$^{-/-}$ mice, we did not find evidence for a role of ADAMTS13 in adipose tissue development or liver steatosis. However, we found that obesity combined with deficiency of ADAMTS13 leads to enhanced hepatic thrombosis. Since *Adamts13*$^{-/-}$ mice do not develop TTP spontaneously, we injected a threshold dose of rVWF to trigger it and observed that obese mice are more sensitive, indicating that obesity indeed may be a risk factor for TTP. Obesity is a state of low-grade chronic inflammation associated with an increase of macrophage content in adipose tissues and liver. Since hepatic macrophages are important in platelet and VWF clearance, we depleted these cells, and observed that platelet counts were normalized in obese *Adamts13*$^{-/-}$ mice despite TTP triggering. Thus, the severe thrombocytopenia in TTP appears to be due to consumption of platelets in microthrombi as well as to platelet clearance by macrophages. These findings could be relevant for the development of new strategies for prevention or treatment of TTP.

References

1. Terrell DR, Williams LA, Vesely SK, Lammle B, Hovinga JA, George JN. The incidence of thrombotic thrombocytopenic purpura-hemolytic uremic syndrome: all patients, idiopathic patients, and patients with severe ADAMTS-13 deficiency. J Thromb Haemost. 2005;3(7):1432-6.
2. Murrin RJ, Murray JA. Thrombotic thrombocytopenic purpura: aetiology, pathophysiology and treatment. Blood Rev. 2006;20(1):51-60.
3. Raven P, Johnson, G, Losos, J., Singer, S. "Biology", eighth, international edietion/Ed. Boston: McGraw-Hill2008.
4. Johnson-Wimbley TD, Graham DY. Diagnosis and management of iron deficiency anemia in the 21st century. Therap Adv Gastroenterol. 2011;4(3):177-84.
5. Kindt T, Goldsby RA, Osborne BA, Kuby J. Kuby Immunology 6th ed. Freeman NYWH, editor2007.
6. Garraud O, Cognasse F. Are Platelets Cells? And if Yes, are They Immune Cells? Front Immunol. 2015;6:70.
7. Grozovsky R, Giannini S, Falet H, Hoffmeister KM. Regulating billions of blood platelets: glycans and beyond. Blood. 2015;126(16):1877-84.
8. Italiano JE, Jr. Unraveling mechanisms that control platelet production. Semin Thromb Hemost. 2013;39(1):15-24.
9. Heemskerk JW, Bevers EM, Lindhout T. Platelet activation and blood coagulation. Thromb Haemost. 2002;88(2):186-93.
10. Kauskot A, Hoylaerts MF. Platelet receptors. Handb Exp Pharmacol. 2012(210):23-57.
11. Blair P, Flaumenhaft R. Platelet alpha-granules: basic biology and clinical correlates. Blood Rev. 2009;23(4):177-89.
12. Flaumenhaft R. Molecular basis of platelet granule secretion. Arterioscler Thromb Vasc Biol. 2003;23(7):1152-60.
13. Chen Y, Corey SJ, Kim OV, Alber MS. Systems biology of platelet-vessel wall interactions. Adv Exp Med Biol. 2014;844:85-98.
14. Schmitt A, Guichard J, Masse JM, Debili N, Cramer EM. Of mice and men: comparison of the ultrastructure of megakaryocytes and platelets. Exp Hematol. 2001;29(11):1295-302.
15. C57BL/6 Mouse Hematology [http://www.criver.com/files/pdfs/rms/c57bl6/rm_rm_r_c57bl6_mouse_clinical_pathology_data.aspx.
16. The Complete Blood Count 2010 [http://sinoemedicalassociation.org/AP4/CompleteBloodCount.pdf.
17. Junt T, Schulze H, Chen Z, Massberg S, Goerge T, Krueger A, et al. Dynamic visualization of thrombopoiesis within bone marrow. Science. 2007;317(5845):1767-70.
18. Kile BT. The role of the intrinsic apoptosis pathway in platelet life and death. J Thromb Haemost. 2009;7 Suppl 1:214-7.
19. Zhang H, Nimmer PM, Tahir SK, Chen J, Fryer RM, Hahn KR, et al. Bcl-2 family proteins are essential for platelet survival. Cell Death Differ. 2007;14(5):943-51.
20. Mason KD, Carpinelli MR, Fletcher JI, Collinge JE, Hilton AA, Ellis S, et al. Programmed anuclear cell death delimits platelet life span. Cell. 2007;128(6):1173-86.
21. Kuwana M, Okazaki Y, Kaburaki J, Kawakami Y, Ikeda Y. Spleen is a primary site for activation of platelet-reactive T and B cells in patients with immune thrombocytopenic purpura. J Immunol. 2002;168(7):3675-82.
22. McMillan R. The pathogenesis of chronic immune thrombocytopenic purpura. Semin Hematol. 2007;44(4 Suppl 5):S3-S11.
23. Grozovsky R, Hoffmeister KM, Falet H. Novel clearance mechanisms of platelets. Curr Opin Hematol. 2010;17(6):585-9.
24. Hoffmeister KM. The role of lectins and glycans in platelet clearance. J Thromb Haemost. 2011;9 Suppl 1:35-43.
25. Grozovsky R, Begonja AJ, Liu K, Visner G, Hartwig JH, Falet H, et al. The Ashwell-Morell receptor regulates hepatic thrombopoietin production via JAK2-STAT3 signaling. Nat Med. 2015;21(1):47-54.

26. Josefsson EC, Gebhard HH, Stossel TP, Hartwig JH, Hoffmeister KM. The macrophage alphaMbeta2 integrin alphaM lectin domain mediates the phagocytosis of chilled platelets. J Biol Chem. 2005;280(18):18025-32.
27. Gitz E, Koekman CA, van den Heuvel DJ, Deckmyn H, Akkerman JW, Gerritsen HC, et al. Improved platelet survival after cold storage by prevention of glycoprotein Ibalpha clustering in lipid rafts. Haematologica. 2012;97(12):1873-81.
28. Hanson SR, Sakariassen KS. Blood flow and antithrombotic drug effects. Am Heart J. 1998;135(5 Pt 2 Su):S132-45.
29. Jones EA, le Noble F, Eichmann A. What determines blood vessel structure? Genetic prespecification vs. hemodynamics. Physiology (Bethesda). 2006;21:388-95.
30. Gogia S, Neelamegham S. Role of fluid shear stress in regulating VWF structure, function and related blood disorders. Biorheology. 2015;52(5-6):319-35.
31. Broos K, Feys HB, De Meyer SF, Vanhoorelbeke K, Deckmyn H. Platelets at work in primary hemostasis. Blood Rev. 2011;25(4):155-67.
32. Gale AJ. Continuing education course #2: current understanding of hemostasis. Toxicol Pathol. 2011;39(1):273-80.
33. Jurk K, Kehrel BE. Platelets: physiology and biochemistry. Semin Thromb Hemost. 2005;31(4):381-92.
34. Siljander PR, Munnix IC, Smethurst PA, Deckmyn H, Lindhout T, Ouwehand WH, et al. Platelet receptor interplay regulates collagen-induced thrombus formation in flowing human blood. Blood. 2004;103(4):1333-41.
35. de Groot PG, Urbanus RT, Roest M. Platelet interaction with the vessel wall. Handb Exp Pharmacol. 2012(210):87-110.
36. Polgar J, Matuskova J, Wagner DD. The P-selectin, tissue factor, coagulation triad. J Thromb Haemost. 2005;3(8):1590-6.
37. Furie B, Furie BC. Role of platelet P-selectin and microparticle PSGL-1 in thrombus formation. Trends Mol Med. 2004;10(4):171-8.
38. Bevers EM, Comfurius P, van Rijn JL, Hemker HC, Zwaal RF. Generation of prothrombin-converting activity and the exposure of phosphatidylserine at the outer surface of platelets. Eur J Biochem. 1982;122(2):429-36.
39. Palta S, Saroa R, Palta A. Overview of the coagulation system. Indian J Anaesth. 2014;58(5):515-23.
40. Rijken DC, Lijnen HR. New insights into the molecular mechanisms of the fibrinolytic system. J Thromb Haemost. 2009;7(1):4-13.
41. Chapin JC, Hajjar KA. Fibrinolysis and the control of blood coagulation. Blood Rev. 2015;29(1):17-24.
42. Lijnen HR. Role of fibrinolysis in obesity and thrombosis. Thromb Res. 2009;123 Suppl 4:S46-9.
43. Sadler JE. Biochemistry and genetics of von Willebrand factor. Annu Rev Biochem. 1998;67:395-424.
44. De Meyer SF, Deckmyn H, Vanhoorelbeke K. von Willebrand factor to the rescue. Blood. 2009;113(21):5049-57.
45. Crawley JT, de Groot R, Xiang Y, Luken BM, Lane DA. Unraveling the scissile bond: how ADAMTS13 recognizes and cleaves von Willebrand factor. Blood. 2011;118(12):3212-21.
46. Bryckaert M, Rosa JP, Denis CV, Lenting PJ. Of von Willebrand factor and platelets. Cell Mol Life Sci. 2015;72(2):307-26.
47. De Ceunynck K, De Meyer SF, Vanhoorelbeke K. Unwinding the von Willebrand factor strings puzzle. Blood. 2013;121(2):270-7.
48. Luo GP, Ni B, Yang X, Wu YZ. von Willebrand factor: more than a regulator of hemostasis and thrombosis. Acta Haematol. 2012;128(3):158-69.
49. van Schooten CJ, Shahbazi S, Groot E, Oortwijn BD, van den Berg HM, Denis CV, et al. Macrophages contribute to the cellular uptake of von Willebrand factor and factor VIII in vivo. Blood. 2008;112(5):1704-12.
50. Lenting PJ, Christophe OD, Denis CV. von Willebrand factor biosynthesis, secretion, and clearance: connecting the far ends. Blood. 2015;125(13):2019-28.
51. Zhou YF, Eng ET, Zhu J, Lu C, Walz T, Springer TA. Sequence and structure relationships within von Willebrand factor. Blood. 2012;120(2):449-58.
52. Hoylaerts MF, Yamamoto H, Nuyts K, Vreys I, Deckmyn H, Vermylen J. von Willebrand factor binds to native collagen VI primarily via its A1 domain. Biochem J. 1997;324 (Pt 1):185-91.

53. Siedlecki CA, Lestini BJ, Kottke-Marchant KK, Eppell SJ, Wilson DL, Marchant RE. Shear-dependent changes in the three-dimensional structure of human von Willebrand factor. Blood. 1996;88(8):2939-50.
54. Tersteeg C, Fijnheer R, Pasterkamp G, de Groot PG, Vanhoorelbeke K, de Maat S, et al. Keeping von Willebrand Factor under Control: Alternatives for ADAMTS13. Semin Thromb Hemost. 2016;42(1):9-17.
55. Knobl P. Inherited and acquired thrombotic thrombocytopenic purpura (TTP) in adults. Semin Thromb Hemost. 2014;40(4):493-502.
56. Coppo P, Veyradier A. Current management and therapeutical perspectives in thrombotic thrombocytopenic purpura. Presse Med. 2012;41(3 Pt 2):e163-76.
57. Coppo P, French Reference Center for Thrombotic M. Treatment of autoimmune thrombotic thrombocytopenic purpura in the more severe forms. Transfus Apher Sci. 2016.
58. Peyvandi F, Scully M, Kremer Hovinga JA, Cataland S, Knobl P, Wu H, et al. Caplacizumab for Acquired Thrombotic Thrombocytopenic Purpura. N Engl J Med. 2016;374(6):511-22.
59. Knobl P. New treatment options for thrombotic thrombocytopenic purpura. Hamostaseologie. 2016.
60. Vanhoorelbeke K, De Meyer SF. Animal models for thrombotic thrombocytopenic purpura. J Thromb Haemost. 2013;11 Suppl 1:2-10.
61. Motto DG, Chauhan AK, Zhu G, Homeister J, Lamb CB, Desch KC, et al. Shigatoxin triggers thrombotic thrombocytopenic purpura in genetically susceptible ADAMTS13-deficient mice. J Clin Invest. 2005;115(10):2752-61.
62. Banno F, Kokame K, Okuda T, Honda S, Miyata S, Kato H, et al. Complete deficiency in ADAMTS13 is prothrombotic, but it alone is not sufficient to cause thrombotic thrombocytopenic purpura. Blood. 2006;107(8):3161-6.
63. Mohlke KL, Purkayastha AA, Westrick RJ, Smith PL, Petryniak B, Lowe JB, et al. Mvwf, a dominant modifier of murine von Willebrand factor, results from altered lineage-specific expression of a glycosyltransferase. Cell. 1999;96(1):111-20.
64. Schiviz A, Wuersch K, Piskernik C, Dietrich B, Hoellriegl W, Rottensteiner H, et al. A new mouse model mimicking thrombotic thrombocytopenic purpura: correction of symptoms by recombinant human ADAMTS13. Blood. 2012;119(25):6128-35.
65. Feys HB, Roodt J, Vandeputte N, Pareyn I, Lamprecht S, van Rensburg WJ, et al. Thrombotic thrombocytopenic purpura directly linked with ADAMTS13 inhibition in the baboon (Papio ursinus). Blood. 2010;116(12):2005-10.
66. Tsai HM. Physiologic cleavage of von Willebrand factor by a plasma protease is dependent on its conformation and requires calcium ion. Blood. 1996;87(10):4235-44.
67. Uemura M, Tatsumi K, Matsumoto M, Fujimoto M, Matsuyama T, Ishikawa M, et al. Localization of ADAMTS13 to the stellate cells of human liver. Blood. 2005;106(3):922-4.
68. Turner N, Nolasco L, Tao Z, Dong JF, Moake J. Human endothelial cells synthesize and release ADAMTS-13. J Thromb Haemost. 2006;4(6):1396-404.
69. Sadler JE. Von Willebrand factor, ADAMTS13, and thrombotic thrombocytopenic purpura. Blood. 2008;112(1):11-8.
70. De Maeyer B, De Meyer SF, Feys HB, Pareyn I, Vandeputte N, Deckmyn H, et al. The distal carboxyterminal domains of murine ADAMTS13 influence proteolysis of platelet-decorated VWF strings in vivo. J Thromb Haemost. 2010;8(10):2305-12.
71. Muia J, Zhu J, Gupta G, Haberichter SL, Friedman KD, Feys HB, et al. Allosteric activation of ADAMTS13 by von Willebrand factor. Proc Natl Acad Sci U S A. 2014;111(52):18584-9.
72. Zanardelli S, Crawley JT, Chion CK, Lam JK, Preston RJ, Lane DA. ADAMTS13 substrate recognition of von Willebrand factor A2 domain. J Biol Chem. 2006;281(3):1555-63.
73. Zhang X, Halvorsen K, Zhang CZ, Wong WP, Springer TA. Mechanoenzymatic cleavage of the ultralarge vascular protein von Willebrand factor. Science. 2009;324(5932):1330-4.
74. Denorme F, Langhauser F, Desender L, Vandenbulcke A, Rottensteiner H, Plaimauer B, et al. ADAMTS13-mediated thrombolysis of tPA-resistant occlusions in ischemic stroke in mice. Blood. 2016;127(19):2337-45.
75. Chauhan AK, Kisucka J, Brill A, Walsh MT, Scheiflinger F, Wagner DD. ADAMTS13: a new link between thrombosis and inflammation. J Exp Med. 2008;205(9):2065-74.
76. Feng Y, Li X, Xiao J, Li W, Liu J, Zeng X, et al. ADAMTS13: more than a regulator of thrombosis. Int J Hematol. 2016;104(5):534-9.
77. Rodriguez-Manzaneque JC, Fernandez-Rodriguez R, Rodriguez-Baena FJ, Iruela-Arispe ML. ADAMTS proteases in vascular biology. Matrix Biol. 2015;44-46:38-45.

78. Lee M, Rodansky ES, Smith JK, Rodgers GM. ADAMTS13 promotes angiogenesis and modulates VEGF-induced angiogenesis. Microvasc Res. 2012;84(2):109-15.
79. Lee M, Keener J, Xiao J, Long Zheng X, Rodgers GM. ADAMTS13 and its variants promote angiogenesis via upregulation of VEGF and VEGFR2. Cell Mol Life Sci. 2015;72(2):349-56.
80. Groot E, Fijnheer R, Sebastian SA, de Groot PG, Lenting PJ. The active conformation of von Willebrand factor in patients with thrombotic thrombocytopenic purpura in remission. J Thromb Haemost. 2009;7(6):962-9.
81. Tersteeg C, de Maat S, De Meyer SF, Smeets MW, Barendrecht AD, Roest M, et al. Plasmin cleavage of von Willebrand factor as an emergency bypass for ADAMTS13 deficiency in thrombotic microangiopathy. Circulation. 2014;129(12):1320-31.
82. World Health Organization. Obesity and overweight Fact Sheet N°311 2016 [http://www.who.int/mediacentre/factsheets/fs311/en/.
83. Knowler WC, Garrow J. Obesity indices derived from weight and height. Int J Obes (Lond). 1982;6(3):241-3.
84. Wang JW, Hu DY, Sun YH, Wang JH, Wang GL, Xie J, et al. Obesity criteria for identifying metabolic risks. Asia Pac J Clin Nutr. 2009;18(1):105-13.
85. Hsieh SD, Muto T. Metabolic syndrome in Japanese men and women with special reference to the anthropometric criteria for the assessment of obesity: Proposal to use the waist-to-height ratio. Prev Med. 2006;42(2):135-9.
86. Vazquez G, Duval S, Jacobs DR, Jr., Silventoinen K. Comparison of body mass index, waist circumference, and waist/hip ratio in predicting incident diabetes: a meta-analysis. Epidemiol Rev. 2007;29:115-28.
87. Welborn TA, Dhaliwal SS. Preferred clinical measures of central obesity for predicting mortality. Eur J Clin Nutr. 2007;61(12):1373-9.
88. Misra A, Chowbey P, Makkar BM, Vikram NK, Wasir JS, Chadha D, et al. Consensus statement for diagnosis of obesity, abdominal obesity and the metabolic syndrome for Asian Indians and recommendations for physical activity, medical and surgical management. J Assoc Physicians India. 2009;57:163-70.
89. Grundy SM, Cleeman JI, Daniels SR, Donato KA, Eckel RH, Franklin BA, et al. Diagnosis and management of the metabolic syndrome: an American Heart Association/National Heart, Lung, and Blood Institute Scientific Statement. Circulation. 2005;112(17):2735-52.
90. Lijnen HR. Murine models of obesity and hormonal therapy. Thromb Res. 2011;127 Suppl 3:S17-20.
91. Kopelman PG. Obesity as a medical problem. Nature. 2000;404(6778):635-43.
92. Hult M, Tornhammar P, Ueda P, Chima C, Bonamy AK, Ozumba B, et al. Hypertension, diabetes and overweight: looming legacies of the Biafran famine. PLoS One. 2010;5(10):e13582.
93. Brug J, van Stralen MM, Te Velde SJ, Chinapaw MJ, De Bourdeaudhuij I, Lien N, et al. Differences in weight status and energy-balance related behaviors among schoolchildren across Europe: the ENERGY-project. PLoS One. 2012;7(4):e34742.
94. Mehta NK, Chang VW. Mortality attributable to obesity among middle-aged adults in the United States. Demography. 2009;46(4):851-72.
95. Chan RS, Woo J. Prevention of overweight and obesity: how effective is the current public health approach. Int J Environ Res Public Health. 2010;7(3):765-83.
96. Crawford D, Oxford University Press. Obesity epidemiology from aetiology to public health. Oxford: Oxford University Press,; 2010. Available from: http://dx.doi.org/10.1093/acprof:oso/9780199571512.001.0001.
97. Birmingham CL, Muller JL, Palepu A, Spinelli JJ, Anis AH. The cost of obesity in Canada. Cmaj. 1999;160(4):483-8.
98. Katzmarzyk PT, Janssen I. The economic costs associated with physical inactivity and obesity in Canada: an update. Can J Appl Physiol. 2004;29(1):90-115.
99. Swinburn B, Ashton T, Gillespie J, Cox B, Menon A, Simmons D, et al. Health care costs of obesity in New Zealand. Int J Obes Relat Metab Disord. 1997;21(10):891-6.
100. Luo L, Liu M. Adipose tissue in control of metabolism. J Endocrinol. 2016;231(3):R77-R99.
101. Rosen ED, Spiegelman BM. What we talk about when we talk about fat. Cell. 2014;156(1-2):20-44.
102. Bouloumie A, Lolmede K, Sengenes C, Galitzky J, Lafontan M. Angiogenesis in adipose tissue. Ann Endocrinol (Paris). 2002;63(2 Pt 1):91-5.

103. Lundgren M, Svensson M, Lindmark S, Renstrom F, Ruge T, Eriksson JW. Fat cell enlargement is an independent marker of insulin resistance and 'hyperleptinaemia'. Diabetologia. 2007;50(3):625-33.
104. O'Connell J, Lynch L, Cawood TJ, Kwasnik A, Nolan N, Geoghegan J, et al. The relationship of omental and subcutaneous adipocyte size to metabolic disease in severe obesity. PLoS One. 2010;5(4):e9997.
105. Ahima RS. Adipose tissue as an endocrine organ. Obesity (Silver Spring). 2006;14 Suppl 5:242S-9S.
106. Arita Y, Kihara S, Ouchi N, Takahashi M, Maeda K, Miyagawa J, et al. Paradoxical decrease of an adipose-specific protein, adiponectin, in obesity. Biochem Biophys Res Commun. 1999;257(1):79-83.
107. Yadav A, Kataria MA, Saini V, Yadav A. Role of leptin and adiponectin in insulin resistance. Clin Chim Acta. 2013;417:80-4.
108. Lumeng CN, Bodzin JL, Saltiel AR. Obesity induces a phenotypic switch in adipose tissue macrophage polarization. J Clin Invest. 2007;117(1):175-84.
109. Fessler MB, Rudel LL, Brown JM. Toll-like receptor signaling links dietary fatty acids to the metabolic syndrome. Curr Opin Lipidol. 2009;20(5):379-85.
110. Hummasti S, Hotamisligil GS. Endoplasmic reticulum stress and inflammation in obesity and diabetes. Circ Res. 2010;107(5):579-91.
111. Murano I, Barbatelli G, Parisani V, Latini C, Muzzonigro G, Castellucci M, et al. Dead adipocytes, detected as crown-like structures, are prevalent in visceral fat depots of genetically obese mice. J Lipid Res. 2008;49(7):1562-8.
112. Perez de Heredia F, Wood IS, Trayhurn P. Hypoxia stimulates lactate release and modulates monocarboxylate transporter (MCT1, MCT2, and MCT4) expression in human adipocytes. Pflugers Arch. 2010;459(3):509-18.
113. Alkhouri N, Gornicka A, Berk MP, Thapaliya S, Dixon LJ, Kashyap S, et al. Adipocyte apoptosis, a link between obesity, insulin resistance, and hepatic steatosis. J Biol Chem. 2010;285(5):3428-38.
114. Lee MJ, Wu Y, Fried SK. Adipose tissue heterogeneity: implication of depot differences in adipose tissue for obesity complications. Mol Aspects Med. 2013;34(1):1-11.
115. Tchkonia T, Thomou T, Zhu Y, Karagiannides I, Pothoulakis C, Jensen MD, et al. Mechanisms and metabolic implications of regional differences among fat depots. Cell Metab. 2013;17(5):644-56.
116. Tran TT, Kahn CR. Transplantation of adipose tissue and stem cells: role in metabolism and disease. Nat Rev Endocrinol. 2010;6(4):195-213.
117. Day CP, Saksena S. Non-alcoholic steatohepatitis: definitions and pathogenesis. J Gastroenterol Hepatol. 2002;17 Suppl 3:S377-84.
118. Bellentani S. The epidemiology of non-alcoholic fatty liver disease. Liver Int. 2017;37 Suppl 1:81-4.
119. Kahn SE, Hull RL, Utzschneider KM. Mechanisms linking obesity to insulin resistance and type 2 diabetes. Nature. 2006;444(7121):840-6.
120. Kraegen EW, Cooney GJ, Ye JM, Thompson AL, Furler SM. The role of lipids in the pathogenesis of muscle insulin resistance and beta cell failure in type II diabetes and obesity. Exp Clin Endocrinol Diabetes. 2001;109 Suppl 2:S189-201.
121. Van Gaal LF, Mertens IL, De Block CE. Mechanisms linking obesity with cardiovascular disease. Nature. 2006;444(7121):875-80.
122. Anfossi G, Russo I, Trovati M. Platelet dysfunction in central obesity. Nutr Metab Cardiovasc Dis. 2009;19(6):440-9.
123. King RJ, Ajjan RA. Vascular risk in obesity: Facts, misconceptions and the unknown. Diab Vasc Dis Res. 2017;14(1):2-13.
124. Crawley JT, Lane DA, Woodward M, Rumley A, Lowe GD. Evidence that high von Willebrand factor and low ADAMTS-13 levels independently increase the risk of a non-fatal heart attack. J Thromb Haemost. 2008;6(4):583-8.
125. Liu MY, Zhou Z, Ma R, Tao Z, Choi H, Bergeron AL, et al. Gender-dependent up-regulation of ADAMTS-13 in mice with obesity and hypercholesterolemia. Thromb Res. 2012;129(4):536-9.
126. Deford CC, Reese JA, Schwartz LH, Perdue JJ, Kremer Hovinga JA, Lammle B, et al. Multiple major morbidities and increased mortality during long-term follow-up after recovery from thrombotic thrombocytopenic purpura. Blood. 2013;122(12):2023-9; quiz 142.

127. Vesely SK, George JN, Lammle B, Studt JD, Alberio L, El-Harake MA, et al. ADAMTS13 activity in thrombotic thrombocytopenic purpura-hemolytic uremic syndrome: relation to presenting features and clinical outcomes in a prospective cohort of 142 patients. Blood. 2003;102(1):60-8.
128. Nicol KK, Shelton BJ, Knovich MA, Owen J. Overweight individuals are at increased risk for thrombotic thrombocytopenic purpura. Am J Hematol. 2003;74(3):170-4.
129. Lombardi AM, Fabris R, Scarda A, Zanato V, Dal Pra C, Scarparo P, et al. Presence of anti-ADAMTS13 antibodies in obesity. Eur J Clin Invest. 2012;42(11):1197-204.
130. Diaz-Cremades J, Fernandez-Fuertes F, Ruano JA, Tapia M, Soler S, Bosch JM, et al. Concurrent thrombotic thrombocytopenic purpura and antiphospholipid syndrome: a rare and severe clinical combination. Br J Haematol. 2009;147(4):584-5.
131. George JN, Vesely SK, Terrell DR, Deford CC, Reese JA, Al-Nouri ZL, et al. The Oklahoma Thrombotic Thrombocytopenic Purpura-haemolytic Uraemic Syndrome Registry. A model for clinical research, education and patient care. Hamostaseologie. 2013;33(2):105-12.
132. Wang Y, Xu LY, Lam KS, Lu G, Cooper GJ, Xu A. Proteomic characterization of human serum proteins associated with the fat-derived hormone adiponectin. Proteomics. 2006;6(13):3862-70.
133. De Meyer SF, Savchenko AS, Haas MS, Schatzberg D, Carroll MC, Schiviz A, et al. Protective anti-inflammatory effect of ADAMTS13 on myocardial ischemia/reperfusion injury in mice. Blood. 2012;120(26):5217-23.
134. Gandhi C, Ahmad A, Wilson KM, Chauhan AK. ADAMTS13 modulates atherosclerotic plaque progression in mice via a VWF-dependent mechanism. J Thromb Haemost. 2014;12(2):255-60.
135. Geys L, Scroyen I, Roose E, Vanhoorelbeke K, Lijnen HR. ADAMTS13 deficiency in mice does not affect adipose tissue development. Biochim Biophys Acta. 2015;1850(7):1368-74.
136. Ghayour-Mobarhan M, Lamb DJ, Tavallaie S, Ferns GA. Relationship between plasma cholesterol, von Willebrand factor concentrations, extent of atherosclerosis and antibody titres to heat shock proteins-60, -65 and -70 in cholesterol-fed rabbits. Int J Exp Pathol. 2007;88(4):249-55.
137. Konstantinides S, Schafer K, Koschnick S, Loskutoff DJ. Leptin-dependent platelet aggregation and arterial thrombosis suggests a mechanism for atherothrombotic disease in obesity. J Clin Invest. 2001;108(10):1533-40.
138. Uemura M, Fujimura Y, Ko S, Matsumoto M, Nakajima Y, Fukui H. Pivotal role of ADAMTS13 function in liver diseases. Int J Hematol. 2010;91(1):20-9.
139. Bedogni G, Miglioli L, Masutti F, Tiribelli C, Marchesini G, Bellentani S. Prevalence of and risk factors for nonalcoholic fatty liver disease: the Dionysos nutrition and liver study. Hepatology. 2005;42(1):44-52.
140. Blachier M, Leleu H, Peck-Radosavljevic M, Valla DC, Roudot-Thoraval F. The burden of liver disease in Europe: a review of available epidemiological data. J Hepatol. 2013;58(3):593-608.
141. Weltman MD, Farrell GC, Liddle C. Increased hepatocyte CYP2E1 expression in a rat nutritional model of hepatic steatosis with inflammation. Gastroenterology. 1996;111(6):1645-53.
142. Weltman MD, Farrell GC, Hall P, Ingelman-Sundberg M, Liddle C. Hepatic cytochrome P450 2E1 is increased in patients with nonalcoholic steatohepatitis. Hepatology. 1998;27(1):128-33.
143. Rinella ME, Green RM. The methionine-choline deficient dietary model of steatohepatitis does not exhibit insulin resistance. J Hepatol. 2004;40(1):47-51.
144. Lombardi AM, Fabris R, Berti de Marinis G, Marson P, Navaglia F, Plebani M, et al. Defective ADAMTS13 synthesis as a possible consequence of NASH in an obese patient with recurrent thrombotic thrombocytopenic purpura. Eur J Haematol. 2014;92(6):497-501.
145. Kremer Hovinga JA, Vesely SK, Terrell DR, Lammle B, George JN. Survival and relapse in patients with thrombotic thrombocytopenic purpura. Blood. 2010;115(8):1500-11; quiz 662.
146. Dubuc PU, Wilden NJ, Carlisle HJ. Fed and fasting thermoregulation in ob/ob mice. Ann Nutr Metab. 1985;29(6):358-65.
147. Pandit R, Beerens S, Adan RA. The role of leptin in energy expenditure: The hypothalamic perspective. Am J Physiol Regul Integr Comp Physiol. 2017:ajpregu 00045 2016.
148. Friedman JM, Halaas JL. Leptin and the regulation of body weight in mammals. Nature. 1998;395(6704):763-70.
149. Deforche L, Tersteeg C, Roose E, Vandenbulcke A, Vandeputte N, Pareyn I, et al. Generation of Anti-Murine ADAMTS13 Antibodies and Their Application in a Mouse Model for Acquired Thrombotic Thrombocytopenic Purpura. PLoS One. 2016;11(8):e0160388.

150. Scroyen I, Hemmeryckx B, Lijnen HR. From mice to men--mouse models in obesity research: what can we learn? Thromb Haemost. 2013;110(4):634-40.
151. Nathanielsz PW, Yan J, Green R, Nijland M, Miller JW, Wu G, et al. Maternal obesity disrupts the methionine cycle in baboon pregnancy. Physiol Rep. 2015;3(11).
152. Schlabritz-Loutsevitch N, Apostolakis-Kyrus K, Krutilina R, Hubbard G, Kocak M, Janjetovic Z, et al. Pregnancy-driven cardiovascular maternal miR-29 plasticity in obesity. J Med Primatol. 2016.
153. Cox LA, Comuzzie AG, Havill LM, Karere GM, Spradling KD, Mahaney MC, et al. Baboons as a model to study genetics and epigenetics of human disease. ILAR J. 2013;54(2):106-21.
154. Weisberg SP, McCann D, Desai M, Rosenbaum M, Leibel RL, Ferrante AW, Jr. Obesity is associated with macrophage accumulation in adipose tissue. J Clin Invest. 2003;112(12):1796-808.
155. Morinaga H, Mayoral R, Heinrichsdorff J, Osborn O, Franck N, Hah N, et al. Characterization of distinct subpopulations of hepatic macrophages in HFD/obese mice. Diabetes. 2015;64(4):1120-30.
156. Tsai HM. Pathophysiology of thrombotic thrombocytopenic purpura. Int J Hematol. 2010;91(1):1-19.
157. Van Rooijen N, Sanders A. Liposome mediated depletion of macrophages: mechanism of action, preparation of liposomes and applications. J Immunol Methods. 1994;174(1-2):83-93.
158. Casari C, Du V, Wu YP, Kauskot A, de Groot PG, Christophe OD, et al. Accelerated uptake of VWF/platelet complexes in macrophages contributes to VWD type 2B-associated thrombocytopenia. Blood. 2013;122(16):2893-902.
159. Alves-Rosa F, Stanganelli C, Cabrera J, van Rooijen N, Palermo MS, Isturiz MA. Treatment with liposome-encapsulated clodronate as a new strategic approach in the management of immune thrombocytopenic purpura in a mouse model. Blood. 2000;96(8):2834-40.
160. Alves-Rosa F, Stanganelli C, Cabrera J, Cymberknop D, Rubel C, Vanzulli S, et al. Rapid recovery of platelet count following administration of liposome-encapsulated clodronate in a mouse model of immune thrombocytopenia. Br J Haematol. 2002;116(2):357-66.
161. Alves-Rosa F, Vermeulen M, Cabrera J, Stanganelli C, Capozzo A, Narbaitz M, et al. Macrophage depletion following liposomal-encapsulated clodronate (LIP-CLOD) injection enhances megakaryocytopoietic and thrombopoietic activities in mice. Br J Haematol. 2003;121(1):130-8.
162. Male R, Vannier WE, Baldeschwieler JD. Phagocytosis of liposomes by human platelets. Proc Natl Acad Sci U S A. 1992;89(19):9191-5.
163. Preparation of liposomes and materials used [http://www.clodronateliposomes.org/ashwindigital.asp?docname=preparation.
164. Van Rooijen N. The liposome-mediated macrophage 'suicide' technique. J Immunol Methods. 1989;124(1):1-6.
165. Leenen PJ, Radosevic K, Voerman JS, Salomon B, van Rooijen N, Klatzmann D, et al. Heterogeneity of mouse spleen dendritic cells: in vivo phagocytic activity, expression of macrophage markers, and subpopulation turnover. J Immunol. 1998;160(5):2166-73.
166. van Blijswijk J, Schraml BU, Rogers NC, Whitney PG, Zelenay S, Acton SE, et al. Altered lymph node composition in diphtheria toxin receptor-based mouse models to ablate dendritic cells. J Immunol. 2015;194(1):307-15.
167. Cataland SR, Peyvandi F, Mannucci PM, Lammle B, Kremer Hovinga JA, Machin SJ, et al. Initial experience from a double-blind, placebo-controlled, clinical outcome study of ARC1779 in patients with thrombotic thrombocytopenic purpura. Am J Hematol. 2012;87(4):430-2.
168. Zheng L, Mao Y, Abdelgawwad MS, Kocher NK, Li M, Dai X, et al. Therapeutic efficacy of the platelet glycoprotein Ib antagonist anfibatide in murine models of thrombotic thrombocytopenic purpura. Blood Adv. 2016;1:75-83.
169. Muller O, Bartunek J, Hamilos M, Berza CT, Mangiacapra F, Ntalianis A, et al. von Willebrand factor inhibition improves endothelial function in patients with stable angina. J Cardiovasc Transl Res. 2013;6(3):364-70.

Summary

Thrombotic thrombocytopenic purpura (TTP) is a very rare, but life-threatening disease characterized by severe thrombocytopenia, micro-angiopathic hemolytic anemia (formation of microthrombi, schistocytes, low hematocrit) and less common by fever, neurological damage and kidney failure. TTP is caused by a deficiency or total absence of the proteinase ADAMTS13 (a disintegrin and metalloproteinase with thrombospondin-1 repeat, member 13) that can cleave hyperactive ultra-large von Willebrand Factor (UL-VWF) multimers thereby preventing thrombus formation. In addition to an ADAMTS13 activity of less than 5%, a secondary risk factor appears to be needed to evoke endothelial damage resulting in an acute TTP attack. Known triggers are pregnancy and inflammatory diseases, but in most cases the triggering factor remains unknown. Therefore, the precise etiology of TTP is still a matter of debate, hampering prevention of TTP episodes and adapted treatments.

Obesity has been proposed as a potential risk factor for TTP development. However, the obese state is associated with increased systemic ADAMTS13 antigen and activity levels, which would be expected to protect against TTP. Moreover, obesity is a pro-inflammatory state, whereas ADAMTS13 has anti-inflammatory potential.

Because of the enhanced ADAMTS13 levels after a high fat diet (HFD) in mice, we proposed that ADAMTS13 could play a functional role in adipose tissue expansion. Therefore, both *Adamts13*$^{-/-}$ and WT mice were kept on a HFD or standard fat diet (SFD). Body weight gain and food intake, as well as weight of gonadal (GN) and subcutaneous (SC) fat depots, expression of inflammatory or oxidative stress markers in the adipose tissues, and obesity-related angiogenesis were not different between

WT and *Adamts13*$^{-/-}$ mice. Therefore, we concluded that ADAMTS13 does not play a functional role in adiposity and adipose tissue expansion in mice.

Besides adipose tissues, we examined the liver (the major organ of ADAMTS13 secretion) of lean and obese *Adamts13*$^{-/-}$ and WT mice. Histological staining for VWF, TSP-1 and fibrinogen revealed a higher prevalence of platelet-rich microthrombi in liver tissue of obese *Adamts13*$^{-/-}$ as compared to WT mice. Moreover, platelet counts in the obese *Adamts13*$^{-/-}$ mice were significantly lower than in their lean or WT counterparts, and the plasma contained higher levels of ultra-large VWF multimers (UL-VWF). Thus, ADAMTS13 deficiency in mice in combination with obesity acts synergistically in development of hepatic microthrombi and some symptoms of TTP (lower platelet count, more UL-VWF). This does, however, not represent a complete TTP phenotype.

Adamts13$^{-/-}$ mice are healthy and do not present with clear TTP-related symptoms. Administration of Shiga toxin (Stx) or high dose recombinant VWF (rVWF) induces a TTP-like phenotype. However, such TTP mouse models are difficult to handle and not very reproducible. Therefore, we tried to develop a new TTP mouse model using obese *Adamts13*$^{-/-}$ mice, since these were likely to be more sensitive to TTP development. After injection of a threshold dose of recombinant VWF (rVWF) (250 U/kg) (the highest dose not causing thrombocytopenia in lean *Adamts13*$^{-/-}$ mice), we observed a platelet drop of 96% in obese *Adamts13*$^{-/-}$ mice. Moreover, these obese mice showed signs of organ damage, likely as a consequence of microthrombosis. Since these symptoms of TTP were not seen in lean *Adamts13*$^{-/-}$ or in obese WT mice, we conclude that obesity is a risk factor for TTP development in genetically predisposed (*Adamts13*$^{-/-}$) mice. However, obese *Adamts13*$^{-/-}$ mice injected with a threshold dose of rVWF still have limitations as animal model for TTP, as they do not show schistocytosis or a decrease in hematocrit.

Obesity is a state of low-grade chronic inflammation primarily caused by an increase of pro-inflammatory macrophages in the adipose tissue, but also in the liver. Since macrophages in the liver and the spleen are involved in clearance of both platelets and VWF, we depleted these macrophages in obese *Adamts13*$^{-/-}$ mice before injection of rVWF, and observed that platelet counts were normalized. Moreover, a higher number of platelets was phagocytosed by macrophages *in vitro* after addition of rVWF. Hence, the severe thrombocytopenia in TTP may be the result of both platelet consumption in microthrombi and platelet clearance by macrophages.

Future studies should further unravel the mechanism of platelet clearance by macrophages in TTP models. Our findings could be relevant for the development of new strategies for prevention or treatment of TTP.

Nederlandse samenvatting

Trombotische trombocytopenische purpura (TTP) is een zeer zeldzame, maar levensbedreigende ziekte gekenmerkt door ernstige trombocytopenie, micro-angiopathische hemolytische anemie (vorming van microtrombi, schistocyten, laag hematocriet) en minder vaak door koorts, neurologische schade en nierfalen. TTP wordt veroorzaakt door een tekort of totale afwezigheid van het protease ADAMTS13 (*a disintegrin and metalloproteinase with thrombospondin-1 repeat, member 13*) die hyperactieve ultralange von Willebrand Factor (UL-VWF) multimeren kan splitsen en daardoor trombusvorming kan voorkomen. Naast een ADAMTS13 activiteit onder 5%, wordt gedacht dat een secundaire risicofactor nodig is om endotheliale schade of activatie uit te lokken met een acute TTP-aanval als gevolg. Gekende triggers zijn onder meer zwangerschap en ontstekingsziekten, maar in de meeste gevallen is de oorzaak onduidelijk. Daarom is de exacte etiologie van TTP niet uitgeklaard, wat het voorkomen van TTP-aanvallen en gerichte behandelingen bemoeilijkt.

Obesitas werd voorgesteld als een mogelijke risicofactor voor de ontwikkeling van TTP. Vreemd genoeg zien we bij obesitas verhoogde systemische ADAMTS13 antigen- en activiteitniveaus, waardoor men een bescherming tegen TTP zou verwachten. Daarenboven is obesitas een pro-inflammatoire toestand terwijl ADAMTS13 anti-inflammatoire eigenschappen heeft.

De verhoogde ADAMTS13-niveaus na een vetrijk dieet (HFD) bij muizen wijzen op een mogelijke functionele rol van ADAMTS13 in vetweefselexpansie. Om dit te onderzoeken hebben we zowel *Adamts13*$^{-/-}$ als WT muizen op een HFD of standaard vet dieet (SFD) gezet voor 15 weken en de toename in lichaamsgewicht en voedselinname gemeten; we vonden geen verschillen tussen de genotypes. Verder

waren er geen relevante verschillen tussen WT en *Adamts13*$^{-/-}$ muizen wat betreft gewicht van gonadale (GN) en subcutane (SC) vetdepots, expressie van inflammatoire en oxidatieve stressmerkers in het vetweefsel, of obesitasgerelateerde angiogenese. Daarom besloten we dat ADAMTS13 geen functionele rol speelt in vetweefselexpansie bij muizen.

Naast vetweefsel, onderzochten we de lever (het belangrijkste orgaan voor secretie van ADAMTS13) van magere en obese *Adamts13*$^{-/-}$ en WT muizen. Histologische kleuringen voor VWF, TSP-1 en fibrinogeen toonden een groter aantal microtrombi rijk in plaatjes/VWF in leverweefsel van obese *Adamts13*$^{-/-}$ in vergelijking met WT muizen. Bovendien was het bloedplaatjesaantal is deze *Adamts13*$^{-/-}$ muizen significant verlaagd in vergelijking met de magere of WT tegenhangers. De plasmawaarden van ultralange VWF multimeren (UL-VWF) waren daarenboven ook hoger. ADAMTS13-deficiëntie in combinatie met obesitas bij muizen werkt dus synergistisch in het ontwikkelen van hepatische microtrombi. Alhoewel deze muizen daarbij tekenen van TTP (lager aantal bloedplaatjes, meer UL-VWF) vertoonden, waren de resultaten niet overtuigend genoeg om dit fenotype als TTP te definiëren.

Adamts13$^{-/-}$ muizen zijn gezond en vertonen geen TTP-gerelateerde symptomen. Toediening van Shigatoxine (Stx) of hoge dosis recombinant VWF (rVWF) kunnen een TTP-gelijkend fenotype induceren in *Adamts13*$^{-/-}$ muizen. Deze bestaande TTP-muismodellen zijn moeilijk in gebruik en niet altijd reproduceerbaar. Daarom hebben we getracht een nieuw TTP-muismodel te ontwikkelen, vertrekkende van obese *Adamts13*$^{-/-}$ muizen, gezien deze gevoeliger leken te zijn voor TTP-ontwikkeling. Hiervoor bepaalden we een *threshold* dosis van rVWF (250 U/kg) (de hoogste dosis die net geen thrombocytopenie veroorzaakt in magere *Adamts13*$^{-/-}$ muizen) om te injecteren in de obese muizen. Na injectie namen de bloedplaatjesaantallen in obese

genetisch voorbeschikte muizen af met maar liefst 96%. Bovendien vertoonden deze obese *Adamts13*$^{-/-}$ muizen tekenen van orgaanschade, waarschijnlijk als gevolg van microtrombose. Aangezien deze TTP-indicaties niet werden teruggevonden in magere *Adamts13*$^{-/-}$ of obese WT muizen, besluiten we dat obesitas een risicofactor is voor de ontwikkeling van TTP in muizen met een genetische aanleg (*Adamts13*$^{-/-}$). De obese *Adamts13*$^{-/-}$ muizen geïnjecteerd met een drempeldosis van VWF zijn echter nog niet optimaal als diermodel voor TTP omdat deze muizen geen duidelijke schistocytose of een verlaagd hematocriet vertonen.

Obesitas is gekend als een pro-inflammatoire toestand voornamelijk veroorzaakt door een toename van pro-inflammatoire macrofagen in het vetweefsel, maar ook in de lever. Aangezien macrofagen in de lever en de milt betrokken zijn bij de klaring van zowel bloedplaatjes als VWF, hebben we de macrofagen in obese *Adamts13*$^{-/-}$ muizen gedood vóór injectie van rVWF en merkten we op dat het bloedplaatjesaantal normaliseerde. Bovendien werd een groter aantal bloedplaatjes *in vitro* gefagocyteerd door macrofagen na toevoeging van rVWF. Het lijkt er dus op dat de ernstige trombocytopenie bij TTP een gevolg is van zowel bloedplaatjesconsumptie in microtrombi als van klaring van bloedplaatjes door macrofagen.

Het zou zinvol zijn toekomstige studies uit te voeren om het onderliggend mechanisme van plaatjesklaring door macrofagen in TTP te ontrafelen. Dergelijke kennis zou nuttig kunnen zijn om TTP-aanvallen te voorkomen of te behandelen.

Curriculum Vitae

Lotte Geys
July 3rd 1990 (Lommel, Belgium)
Willem de Croylaan 49/21, 3001 Heverlee
lottegeys@gmail.com
0496/46 69 39
Belgian

Education

2013-2017	PhD student at Department of Cardiovascular Sciences Center for Molecular and Vascular Biology KU Leuven, Leuven, Belgium Doctoral School program: Emerging Concepts in Cardiovascular Medicine
2011-2013	Master Biomedical Sciences KU Leuven, Leuven, Belgium Major: Research
2008-2011	Bachelor Biomedical Sciences KU Leuven, Leuven, Belgium
2002-2008	ASO: Science-Mathematics WICO Campus Sint-Jozef, Lommel

Additional courses and workshops

Certificate of Laboratory Animals (Felasa B) and Expert Laboratory Animal Leader (Felasa C)
Writing courses: Writing for Biomedical Journals
Writing for a General Audience
Writing Biomedical Research papers
Creating effective posters
Interpersonal skills
Roche Continents – Youth, Arts, Science (Austria, Salzburg, 2013)

List of Publications

Publications as a part of this thesis

Geys L, Roose E, Scroyen I, Rottensteiner H, Tersteeg C, Hoylaerts M, Vanhoorelbeke K, Lijnen HR. ADAMTS13 deficiency and obesity as risk factors for thrombotic thrombocytopenic purpura. (Manuscript in preparation).

Geys L, Roose E, Vanhoorelbeke K, Bedossa P, Scroyen I, Lijnen HR. Role of ADAMTS13 in diet-induced liver steatosis. Molecular Medicine Reports. 2017 (in press).

Geys L, Bauters D, Roose E, Tersteeg C, Vanhoorelbeke K, Hoylaerts MF, Lijnen HR, Scroyen I. ADAMTS13 deficiency promotes microthrombosis in a murine model of diet-induced liver steatosis. Thromb Haemost. 2017; 117(1):19-26.

Geys L, Scroyen I, Roose E, Vanhoorelbeke K, Lijnen HR. ADAMTS13 deficiency in mice does not affect adipose tissue development. Biochim Biophys Acta. 2015; 1850(7):1368-1374.

Other publications

Bauters D, Cobbaut M, **Geys L**, Van Lint J, Hemmeryckx B, Lijnen HR. Loss of ADAMTS5 enhances brown adipose tissue mass and promotes browning of white adipose tissue via CREB signaling. Molecular Metabolism. 2017. Published online (DOI: 10.1016/j.molmet.2017.05.004).

Bauters D, Spincemaille P, **Geys L**, Cassiman D, Vermeersch P, Bedossa P, Scroyen I, Lijnen HR. ADAMTS5 deficiency protects against non-alcoholic steatohepatitis in obesity. Liver Int. 2016; 36(12):1848-1859.

Geys L, Vranckx C, Lijnen HR, Scroyen I. CD36 deficiency blunts effects of diet on regulatory T cells in murine gonadal adipose tissue and mesenteric lymph nodes. Cell Immunol. 2015; 298(1-2):33-36

Active participations at (inter)national congresses

Geys L, Roose E, Scroyen I, Lijnen HR, Vanhoorelbeke K. (2016). Obesity as a risk factor for the development of thrombotic thrombocytopenic purpura in ADAMTS1313 deficient mice. European Obesity Summit. Gothenburg, Sweden, 1-4 June 2016, Abstract No. P02.037.

Geys L, Roose E, Vanhoorelbeke K, Hoylaerts MF, Lijnen HR, Scroyen I. (2015). ADAMTS13 deficiency in mice does not aggravate diet-induced liver steatosis. BSTH annual conference. Mechelen, 19-20 November 2015.

Geys L, Lijnen HR, Scroyen I. (2015). Effect of diet and CD36 deficiency on murine mesenteric lymph nodes. 22nd European Congress on Obesity (ECO2015). Prague, Czech Republic, 6-9 May 2015, Abstract No. T1:PO.048.

Geys L, Scroyen I, Roose E, Vanhoorelbeke K, Lijnen HR. (2014). No functional role of ADAMTS13 in adipose tissue development. 22nd International Congress on Fibrinolysis and Proteolysis. Marseille, France, 6-9 July 2014, Abstract No. P25.